DEVELOPMENT OF AN ELECTROCHEMICAL IMMUNOSENSOR FOR DIRECT DETECTION OF ACRYLAMIDE IN FOOD SAMPLES

LAU PEI YING

FACULTY OF SCIENCE
UNIVERSITI MALAYA
KUALA LUMPUR

2020

DEVELOPMENT OF AN ELECTROCHEMICAL IMMUNOSENSOR FOR DIRECT DETECTION OF ACRYLAMIDE IN FOOD SAMPLES

LAU PEI YING

DISSERTATION SUBMITTED IN FULFILMENT OF THE REQUIREMENTS FOR THE DEGREE OF MASTER OF SCIENCE

DEPARTMENT OF CHEMISTRY
FACULTY OF SCIENCE
UNIVERSITI MALAYA
KUALA LUMPUR

2020

UNIVERSITY OF MALAYA

ORIGINAL LITERARY WORK DECLARATION

Name of Candidate: **LAU PEI YING**

Matric No: **SGR 160007**

Name of Degree: **MASTER OF SCIENCE (EXCEPT MATHEMATICS & SCIENCE PHILOSOPHY)**

Title of Project Paper/Research Report/Dissertation/Thesis ("this Work"):

DEVELOPMENT OF AN ELECTROCHEMICAL IMMUNOSENSOR FOR DIRECT DETECTION OF ACRYLAMIDE IN FOOD SAMPLES

Field of Study:

ANALYTICAL CHEMISTRY

I do solemnly and sincerely declare that:

(1) I am the sole author/writer of this Work;
(2) This Work is original;
(3) Any use of any work in which copyright exists was done by way of fair dealing and for permitted purposes and any excerpt or extract from, or reference to or reproduction of any copyright work has been disclosed expressly and sufficiently and the title of the Work and its authorship have been acknowledged in this Work;
(4) I do not have any actual knowledge nor do I ought reasonably to know that the making of this work constitutes an infringement of any copyright work;
(5) I hereby assign all and every rights in the copyright to this Work to the University of Malaya ("UM"), who henceforth shall be owner of the copyright in this Work and that any reproduction or use in any form or by any means whatsoever is prohibited without the written consent of UM having been first had and obtained;
(6) I am fully aware that if in the course of making this Work I have infringed any copyright whether intentionally or otherwise, I may be subject to legal action or any other action as may be determined by UM.

Candidate's Signature Date:

Subscribed and solemnly declared before,

Witness's Signature Date:

Name:

Designation:

DEVELOPMENT OF AN ELECTROCHEMICAL IMMUNOSENSOR FOR DIRECT DETECTION OF ACRYLAMIDE IN FOOD SAMPLES

ABSTRACT

Acrylamide, a potential carcinogen which is mainly found in plant-based food such as potato chips, French fries, bread, biscuit, coffee and coco, after undergoing heating process at temperature above 120°C. The permissible maximum intake of acrylamide is 2.6 μg kg^{-1} of body weight per day to prevent cancer risk. Due to its neurotoxicity and carcinogenicity, a rapid detection method for acrylamide is strongly needed in food safety concern. Herein, a sample pre-treatment free electrochemical immunosensor was developed based on a displacement assay. In a displacement assay format, an antibody is initially bound to the surface immobilized hapten (analyte analogue) and upon adding of analyte (which is acrylamide in this study), antibody would exhibit a higher affinity towards its target analyte compared to hapten. This phenomenon leads to the dissociation of antibody from hapten where a displacement assay occurs. The dissociation of anti-acrylamide antibody from the electrode surface bound hapten is the predominant factor for an effective displacement assay to take place. Therefore, the objective of this study is to investigate the effect of introducing electro-pulsion to enhance the dissociation of antibody from the surface bound hapten. The displacement assay was then being analysed in a series of electro-pulsion with positive and negative charge. Other than that, pulsing potential and pulsion duration are also factors that affecting the displacement of antibody. Consequently, the optimal conditions for a displacement assay were identified via actual experimental set-up. The findings showed the dissociation rate of antibody from the surface bound hapten could be enhanced by applying a negative electro-pulsion to the working electrode surface. In addition, a three-level three-factorial Box-Behnken experimental design was employed as theoretical statistical method to confirm the optimal displacement conditions required based on a minimal experiment number (17

trials) without involving all possible experimental combinations. By pulsing the electrode with -800 mV for 10 minutes (the optimal displacement conditions), a linear dynamic range from 0.01 μg mL^{-1} to 35.00 μg mL^{-1} was obtained, with limit of detection (LOD) of 3.84 ng mL^{-1}. The evidences of high reproducibility and repeatability of developed immunosensor by performing a satisfied relative standard deviation (RSD) of 3.13% in reproducibility test and RSD of 5.49% to 8.22% for repeatability (intra-day and inter-day) assessments. The immunosensor could retain its detection ability for 90.69% even after 28 days storage and showed high specificity toward acrylamide. The accuracy of developed immunosensor was validated by using standard method, GC−MS. Moreover, the recoveries obtained of spiked sample were ranged between 90.33% to 99.23%. As a conclusion, the developed immunosensor showed a high reproducibility, repeatability, selectivity, sensitivity, and stability for the determination of acrylamide typically in liquid food samples (coffee, coco, and prune juice). Due to its simplicity of use which exclude sample pre-treatment steps, this developed immunosensor is believed to have potential to provide a direct and quantitative approach for the detection of acrylamide.

Keywords: Acrylamide, displacement assay, electrochemical immunosensor, negative electro-pulsion, sample pre-treatment free.

PEMBANGUNAN IMUNOSENSOR ELECTROKIMIA UNTUK PENGESANAN AKRILAMIDA SECARA TERUS DAN KUANTITATIF DALAM SAMPEL MAKANAN

ABSTRAK

Akrilamida adalah berpotensi karsinogen yang biasanya ditemui dalam makanan berasaskan tumbuhan seperti kerepek kentang, kentang goreng, roti, biskut, kopi dan koko selepas proses pemanasan melebihi suhu 120°C. Pengambilan akrilamida yang dibenarkan adalah 2.6 μg kg^{-1} berat badan sehari untuk mengelak risiko kanser. Disebabkan oleh kandungan keneurotoksikan dan kekarsinogenan, kaedah pengesanan pantas akrilamide adalah sangat diperlukan dalam keselamatan makanan yang berkesan. Di sinilah imunosensor elektrokimia yang tidak melibatkan sampel pra-merawat telah dibangunkan berdasarkan pengalihan assai. Dalam format pengalihan assai, antibodi pada mulanya terikat dengan hapten (analog analit) yang diubah suai pada permukaan electrod dan apabila penambahan analit (iaitu akrilamida dalam kajian ini) berlaku, antibodi akan menunjukkan pertalian yang lebih tinggi ke arah analit berbanding dengan hapten. Fenomena ini akan menyebabkan disosiasi antibodi dari hapten, di mana pengalihan assai akan berlaku. Disosiasi antibodi anti-akrilamida dari elektrod permukaan terikat hapten adalah faktor utama bagi keberkesaan pengalihan assai untuk berlaku dengan berkesan. Oleh itu, objektif kajian ini adalah untuk mengkaji kesan pengenalan elektro-*pulsion* untuk meningkatkan disosiasi antibodi daripada permukaan terikat hapten. Pengalihan assai kemudian dianalisis dalam satu siri electro-*pulsion* yang mengandungi caj positif dan negatif. Selain itu, keupayaan *pulsion* dan tempoh masa *pulsion* juga merupakan faktor yang memberi kesan kepada pengalihan antibodi. Akibatnya, keadaan optimum untuk pengalihan assai akan dikenal pasti melalui penyediaan eksperimen sebenar. Dapatan telah menunjukkan kadar disosiasi antibodi dari permukaan terikat hapten dapat ditingkatkan ketika caj negatif electro-*pulsion* digunakan di permukaan elektrod bekerja.

Tambahan pula, tiga tahap tiga factor reka bentuk eksperimen Box-Behnken digunakan sebagai kaedah teori statistik untuk mengesahkan keadaan optimum pengalihan assai yang diperlukan, berdasarkan bilangan eksperimen yang minimum (17 percubaan) yang tidak melibatkan semua kemungkinan kombinasi eksperimen. Dengan *pulsion* electrod pada -800 mV selama 10 minit (keadaan pengalihan yang optimum), dinamik linear dari 0.01 μg mL^{-1} hingga 35.00 μg mL^{-1} diperoleh dengan had pengesanan (LOD) iaitu 3.84 ng mL^{-1}. Bukti keberhasilan yang tinggi dan kebolehulangan imunsensor yang dibangunkan dengan bukti sisihan piawai relatif (RSD) sebanyak 3.13% dalam ujian keberhasilan dan RSD 5.49% hingga 8.22% untuk penilaian kebolehulangan (dalam sehari dan antara hari). Immunosensor yang dibangunkan dapat mengekalkan keupayaan pengesanannya sebanyak 90.69% walaupun setelah penyimpanan selama 28 hari, dan juga menunjukkan ketepatan yang tinggi terhadap akrilamida. Ketepatan keputusan yang diperoleh daripada immunosensor yang dibangunkan telah disahkan dengan menggunakan kaedah standard GC-MS. Tambahan lagi, pemulihan yang diperolehi daripada sampel (dengan tambahan kepekatan akrilamida yang diketahui) adalah antara 90.33% hingga 99.23%. Kesimpulannya, imunosensor yang dibanguankan didapati menunjukkan keberhasilan, kebolehulangan, kepilihan, kepekaan, dan kestabilan yang tinggi untuk pengesanan akrilamida, terutamanya dalam sampel makanan bentuk cecair (seperti kopi, coco, dan jus *prune*). Dengan cara penggunaan ringkas yang tidak melibatkan langkah pra-merawat sampel, imunosensor yang dibangunkan ini dipercayai berpotensi untuk memberi pengesanan secara terus dan kuantitatif untuk mengesan akrilamida.

Kata kunci: Akrilamida, pangalihan assai, imunosensor electrokimia, negatif electro-*pulsion*, tanpa sampel pra-merawat.

ACKNOWLEDGEMENTS

I would like to take this opportunity to express my heartfelt thanks to people who helped and supported me throughout my M.Sc. study. I would first like to thank my supervisor, Dr. Khor Sook Mei, who has provided her support at all time and has given me invaluable guidance, inspiration and suggestions along my study. Without her able guidance, this dissertation would not have been possible and I shall eternally be grateful to her for her assistance. Besides, I would like to thank my other supervisor, Prof. Dr. Yatimah binti Alias, who has given me her useful advice, supported and trusted me throughout the study. In addition, I would like to thank the chemistry teammates for their willingness to help with the arrangements and the reservation of the equipment and facilities necessary to complete the research.

I would like to thank my family, lab mates at FD-L5-19 and friends for their continuous support and encouragement all along the way. Finally, I would like to thank my parents for their wise counsel as well as sympathetic ear and always be there for me. Their love has driven me to move forward even at low tides and has given me the encourage to complete what I have started.

TABLE OF CONTENTS

LIST OF FIGURES

LIST OF TABLES

LIST OF SYMBOLS AND ABBREVIATIONS

x_1, x_2 and x_3	:	Variables
β_1, β_2 and β_3	:	Coefficient of the linear parameters
β_{11}, β_{22} and β_{33}	:	Coefficient of the quadratic parameters
β_{12}, β_{13} and β_{23}	:	Coefficient of the interaction parameters
C_{dl}	:	Capacitance of the double layer
n	:	Exponent of constant phase element
Q	:	Pre-factor of constant phase element
R_{ct}	:	Charge-transfer resistance
R_s	:	Resistance of the solution
Y	:	Predicted response
2FI	:	Interaction of two factors
3-MBA	:	3-mercaptobenzoic acid
4-MPA	:	4 mercaptophenylacetic acid
ANOVA	:	Analysis of variance
AuNPs	:	Gold nanoparticles
BSA	:	Bovine serum albumin
CNTs	:	Carbon nanotubes
CPE	:	Constant phase element
CuNPs	:	Copper nanoparticles
CV	:	Cyclic voltammetry
DEL	:	Double electric layer
DNA	:	Deoxyribonucleic acid
EDX	:	Energy dispersive X-ray
EIS	:	Electrochemical impedance spectroscopy
ELISA	:	Enzyme-linked immunosorbent assay

EtOH	:	Ethyl alcohol
FE-SEM	:	Field Scanning Electron Microscope
FT-IR	:	Fourier Transform Infrared
GC-MS	:	Gas chromatography mass spectrometry
GCP	:	Glassy carbon plate
Hb	:	Haemoglobin
HbNPs	:	Nanoparticles of Hb
HPLC-MS	:	High-performance liquid chromatography mass spectrometry
IARC	:	International Agency for Research on Cancer
IgG	:	Immunoglobin G
IgY	:	Immunoglobin Y
ISE	:	Ion selective electrode
ITO	:	Indium tin oxide
IUPAC	:	International Union of Pure and Applied Chemistry
LC-MS	:	Liquid chromatography mass spectrometry
LOB	:	Limit of blank
LOD	:	Limit of detection
LOQ	:	Limit of quantification
NAS	:	N-acryloxysuccinimide
NHS	:	N-hydroxysuccinimide
OVA	:	Ovalbumin conjugate
PBS	:	Phosphate buffer saline
pI	:	Isoelectric point
QDs	:	Quantum dots
R^2	:	Square of correlation coefficient

RCF	:	Rotational centrifugation force
RSD	:	Relative standard deviation
RSD	:	Relative standard deviation
SD	:	Standard deviation
SRA	:	Specific respiratory activity
SWCNT	:	Single walled carbon nanotubes
UPLC	:	Ultra-performance liquid chromatography
Z'	:	Real impedance component
Z''	:	Imaginary impedance component

LIST OF APPENDICES

CHAPTER 1: INTRODUCTION

1.1 Introduction

In 2002, Swedish National Food Agency and researchers from Stockholm University were first reported on the presence of unexpected high concentration of acrylamide found in thermal by processed food (Tareke et al., 2002), where the amount of acrylamide detected was far more than the guideline value (0.5 μg L^{-1}) suggested in drinking water (WHO, 2017). This finding has attracted the attention of scientific communities as acrylamide has been classified by the International Agency for Research on Cancer (IARC) as a potential carcinogen to humans (Group 2A) based on its carcinogenicity in rodents (IARC, 1994). Acrylamide is the product between asparagine and reducing sugar under Millard's reaction and normally formed in plant-based food, for example potato chips, fried potatoes, coffee, cereal, bread, biscuits, after heated to temperature higher than 120 °C during roasting, baking and frying processes (Mottram et al., 2002). Acrylamide can be absorbed into humans after ingestion and distributed in several vital organs (heart, brain, thymus, kidney and liver), and also will cause various toxic disorders (Capuano & Fogliano, 2011). Due to its carcinogenicity, genotoxicity and neurotoxicity, a rapid, sensitive and specific detection method for the determination of acrylamide in food is a crucial concern in food safety and health security.

Standard methods for acrylamide detection including gas chromatography mass spectrometry (GC-MS), liquid chromatography mass spectrometry (LC-MS) and high-performance liquid chromatography mass spectrometry (HPLC-MS) (Fernandes & Soares, 2007; Liu et al., 2008; Qin et al., 2017) showed advantages such as high sensitivity, selectivity and accuracy, but these methods involved time consuming sample pre-treatment steps and required expensive experiment equipment. Alternatively, analytical techniques such as enzyme-linked immunosorbent assay (ELISA) (Wu et al., 2014), fluorescent sensing method (Asnaashari et al., 2018; Hu et al., 2014) and

electrochemical biosensor (Batra et al., 2013; Krajewska et al., 2008; Stobiecka et al., 2007) were developed. Electrochemical biosensing detection methods for acrylamide are growing in the past few years as they combine advantages of simplicity, stability, sensitivity, selectivity, fast in response and require small amount of sample (Asnaashari et al., 2019; Huang et al., 2016; Silva et al., 2011). Haemoglobin (Hb) was one of the commonly used bioactive receptors for detection of acrylamide. The reaction between acrylamide molecule with α-NH_2 group of N-terminal valine of Hb resulted the formation of adduct (Garabagiu & Mihailescu, 2011; Stobiecka et al., 2007). The formation of Hb-acrylamide adduct could change the electrical characteristic of Hb redox centre and this had caused a decrease in the current peak. However, Hb shows a higher reactivity towards acrylamide's epoxide, glycidamide (Bjellaas et al., 2007) and thus the specificity of Hb towards acrylamide itself cannot be assured.

Furthermore, direct detection of acrylamide is another challenging part due to the complexity of food matrixes in food sample. For the existing electrochemical detection of acrylamide in food sample, pre-treatment steps involving defatting with hexane and Carrez solution clarification are commonly practiced (Asnaashari et al., 2019; Batra et al., 2013; Huang et al., 2016; Krajewska et al., 2008; Stobiecka et al., 2007; Varmira et al., 2018). This is due to the presence of matrix effect in food samples could hinder the electron transfer rate of redox species $[Fe(CN)_6]^{3-/4-}$ to electrode surface during the electrochemical detection, thus a direct detection by using electrochemical method for acrylamide is still a difficult task. In order to simplify the complicated preparation procedure for electrochemically detection of acrylamide, a direct or on-side detection format should be applied. Interestingly, a uncomplicated sample preparation step as simple as using phosphate buffered saline to extract acrylamide in solid food sample was proposed by Quan et al. (2011) by using ELISA (Quan et al., 2011). Inspired by the fact that by utilizing specific binding affinity between antibody and antigen, direct detection

of acrylamide in food sample without purification step is possible, and at the same time it could overcome the limitations faced in Hb bioreceptor biosensor. More importantly, the use of antibody could increase the specificity of a newly developed sensor.

Therefore, an electrochemical immunosensor for direct detection of acrylamide has been developed in this study. In this electrochemical immunosensor, an antibody is selected as a bioreceptor with electrochemical as a transducer with electric signal output to detect target analyte acrylamide. Electrochemical immunosensor has a wide range of applications including in medical diagnostics (Darwish et al., 2016), agriculture residues (Ionescu et al., 2010) and food analysis (Čadková et al., 2015), due to the rapidity and simplicity used. Since the target analyte (acrylamide) is small in size with only 71.09 g mol^{-1} molecular weight, hence it has limited epitopes to bind with two antibodies simultaneously (for sandwich assay) and electrical signal of direct binding of acrylamide to its antibody was hardly generated (for direct assay) (Hu et al., 2015). Hence a displacement assay was employed in my M.Sc. study to overcome this drawback. In a displacement assay, the biorecognition molecule (an antibody) is initially bound to an analyte analogue (a hapten) that has been covalently immobilized on the surface of an electrode. Upon exposure of free acrylamide in sample solution, the displacement assay would take place when the surface bound antibody been dissociated from the hapten. Most importantly, no additional derivatization step of analyte is needed. In an effective displacement assay, the binding affinity strength between antibody with hapten has to be relatively lower as compared to antibody-antigen for the antibody to be successfully dissociated from the surface bound hapten when free antigen is present (Khor et al., 2013).

Apart from the effect of affinity strength, an addition of electrical pulsing potential can be incorporated and such pulsing electric field can hinder the affinity interaction between the antibody with the hapten on the immunosensor interface. There are few studies were reported on an application of electrical pulsing to cause the dissociation of antibodies

(Asanov et al., 1998; Brod et al., 2008). The studies implied that when an electrode to be applied with a more negative potential, the antibody molecules showed less interactions towards the electrode surface. The extension of this concept has been applied in an immunosensor developed for biotin detection. The application of a negative electrode polarization resulted an enhancement in the dissociation of antibody (Khoo et al., 2016; Khor et al., 2011). This is the good evidence to elucidate that when at the neutral pH, IgG antibody is an anion that carries negatively charges and caused dissociation from a negatively charged transducer surface (Gooding et al., 2004).

The main approach of this study is to investigate the effect of electrical pulsing on the dissociation of surface bound antibody. A displacement assay will be performed within a series of electro-pulsion involving positive or negative charges. Besides, by varying the pulsing conditions (with different pulsing potential and pulsing duration) could influence the dissociation of surface bound antibody. For that reason, optimization on the conditions of the displacement assay in this M.Sc. project was conducted experimentally and also using a statistical technique. Response surface methodology is a valuable statistical approach for determining the interaction between several factors with responses and also to optimize the optimal condition of various factors, especially for studies that involve numerous factors that influencing responses (Ferreira et al., 2007). Box-Behnken experimental design (one of the respond surface methodologies) was applied in current study to determine the factors that significantly affect the displacement assay, to investigate the correlating effect between factors, and to validate the optimal displacement conditions as compared to experimental result. Box-Behnken was selected with the benefit of efficiency which only involved 17 trials experimental sets as described in this thesis.

An impedimetric immunosensor interface based on a displacement assay format was constructed in this study. With application of an optimized displacement assay conditions,

this immunosensor was used for the direct detection of acrylamide in coffee, cocoa and prune juice, where sample pre-treatment step can be totally excluded. The platform of immunosensor was initially modified with surface bound hapten and then incubated in an antibody solution. A negative electrochemical pulsion was applied on the modified electrode in standard/sample solution with presence of free acrylamide small molecule. Relative to the higher binding affinity of surface bound antibody to free acrylamide, thereby resulting a displacement assay upon antibody dissociation from the surface bound hapten. The dissociation of antibody will induce a resistivity decrease where this resistivity change can be determined by electrochemical impedance spectroscopy method (EIS). The resulted of decrease in resistivity was utilized for quantification determination of acrylamide present. To demonstrate the practicality and usefulness of developed immunosensor, the amount of acrylamide was detected in real liquid food samples. As reported, other than potato chips and fried potatoes, other plant-based foods such as coffee, cocoa and prune juice also grouped as the main source of acrylamide exposure in diet (Andrzejewski et al., 2004; Authority, 2012). Subsequently, the obtained results from my developed immunosensor was validated with a standard method, GC-MS to confirm the accuracy of developed immunosensor. The developed electrochemical immunosensor is believe to be a possible rapid approach for direct quantitative detection of acrylamide (food carcinogen).

1.2 Motivations and Objectives

The objectives of the research work presented in this thesis are

1. To evaluate the effect of positive and negative electro-pulsion on the dissociation of surface bound antibody from the surface bound hapten.
2. To develop an electrochemical immunosensor for specific and selective detection of acrylamide.

3. To perform a direct, rapid and quantitative detection of acrylamide in liquid food samples without sample pre-treatment steps.
4. To determine the linear range, limit of detection, repeatability, reproducibility, selectivity and stability of newly developed immunosensor.

CHAPTER 2: LITERATURE REVIEW

2.1 Why acrylamide?

2.1.1 Background

Acrylamide is a colourless and odourless crystalline solid with an IUPAC name of 2-propenamide. It is a low molecular weight compound with only 71.08 g mol^{-1}. The small size of acrylamide containing a reactive electrophilic double bond and amide group, also defined as a difunctional monomer. Acrylamide can be easily polymerized to form polyacrylamide and has wide ranges of industrial usage, such as manufacturing of plastics, waste water treatment, construction of dam and tunnels, pulp binder and manufacturing of cosmetics product.

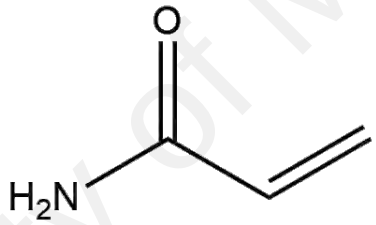

Figure 2.1: Acrylamide structure.

After the incident of acrylamide leakage occurred in a tunnel construction happened in Sweden, dead fish in fish-culture downstream of the brook, paralyzed of cows in a herd after grazing around the brook and neurotoxicity symptoms on the construction workers were reported (Weideborg et al., 2001). Then, a considerable level of Hb-acrylamide adducts found in blood of control population of non-smoker and these findings led to the hypothesis that acrylamide exposure might due to dietary source (Bergmark, 1997; Tareke et al., 2000). The demonstration of animal study on the relation between acrylamide intake in fried food with the formation of Hb adduct, followed by the reported high concentration of acrylamide in heated processed food (Tareke et al., 2002). The presence of acrylamide in food has gained the attention of researchers since acrylamide

has been classified as "potential carcinogen to human" by the International Agency for Research on Cancer (IARC, 1994).

2.1.2 Toxicity of acrylamide

The genotoxicity and carcinogenicity of acrylamide are mainly due to two reasons. First, acrylamide can be bio-transformed *in vivo* by cytochrome P450 2E1 (CYP2E1) to its metabolite glycidamide, an epoxide derivative, which is more reactive toward DNA and protein than acrylamide (Watzek et al., 2012; Zeiger et al., 2008). Formation of glycidamide considered as the critical step for genotoxic effect of acrylamide, and later can be induced to point mutation (genetic mutation). Secondly, acrylamide can act as a Michael acceptor and reactive to thiol, hydroxyl or amino groups in DNA to form adducts and consequently cause DNA damage (Erkekoğlu & Baydar, 2010). Furthermore, the binding of acrylamide to sulfhydryl groups on proteins in the nervous system can cause damages in regeneration activity of nerves and axons, significantly contributes to the neurotoxic effect of acrylamide (Friedman, 2003). The tolerable daily intakes for acrylamide was suggested to be 2.6 μg kg^{-1} of body weight per day to avoid cancer risk and 40 μg kg^{-1} per day for neurotoxicity (Tardiff et al., 2010).

2.2 Introduction to biosensor

A biosensor is a chemical sensing device used to detect an analyte where a biologically derived recognition (bioreceptor) is coupled with a physicochemical detector (transducer) (Monošíka, 2012). In a simple word, a biosensor is a device used to measure biological or chemical reactions by generating signals proportional to the concentration of substance of interest (analyte). Biosensors are classified according to type of transducer or bioreceptor (Thévenot et al., 2001). Bioreceptor is a molecule that specifically recognises

the analyte (termed as bio–recognition) and produces signal. Examples of bioreceptors including enzymes, antibody and antigen, nucleic acids, cellular structures or whole cells. On the other hand, the role of transducer is to convert the bio–recognition event into a measurable signal. The main type of transducer can be divided into four groups, which are optical, electrochemical, piezoelectric and thermometric.

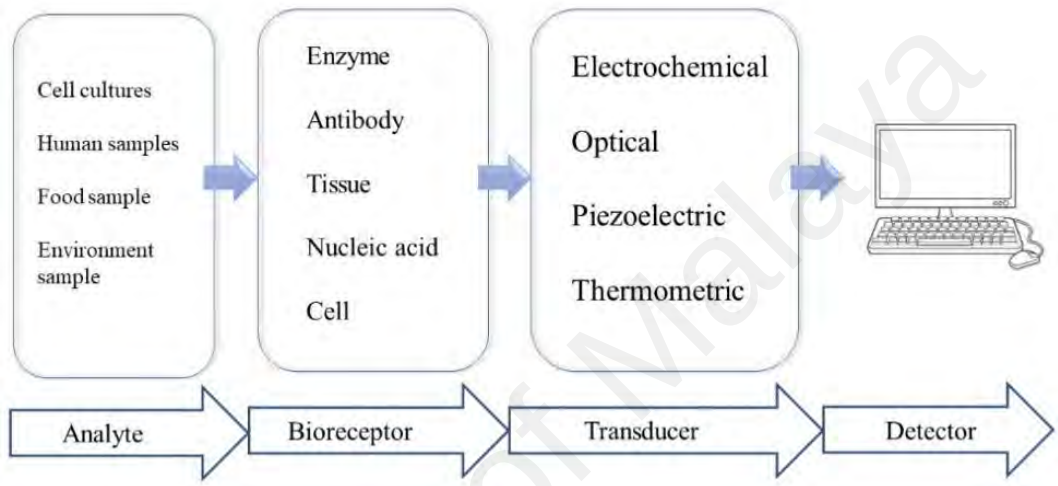

Figure 2.2: Components of biosensor.

Optical biosensors utilize the principle of optical measurement based on fluorescence, luminescence or refractive index (Leung et al., 2007; Velasco-Garcia, 2009). The mass-sensitive sensors, piezoelectric biosensors are based on the changes of mass. Upon addition of the sample, specific binding occurs between the bioreceptor molecules being immobilized onto the transducer surface with the analyte in the sample solution and consequently changes in mass occurs. This lead to a subsequent change in the oscillation frequency and production of an electric signal that is detected (Kovář et al., 2014). Besides, several biological reactions are associated with the production of heat and this forms the basis of thermometric biosensors. They are more commonly referred as thermal biosensors or calorimetric biosensors by measuring the amount of heat with a sensitive thermistor to determine the analyte concentration (Senesac et al., 2009). An

electrochemical biosensor's basic principle is chemical reaction occurs between immobilized biomolecules and target analytes, which affects measurable electrical properties (Muhammad-Tahir & Alocilja, 2003; Trivedi et al., 2009). Electrochemical biosensors have approach advantages of being economic, allow application in a wide number of samples and present a fast response.

2.3 Electrochemical immunosensor

Immunosensor is an analytical device used to detect the binding event between antibody and antigen with the formation of a stable complex (Lin & Ju, 2005). Either the antibody or the antigen can be immobilized on the surface of different transducers (Holford et al., 2012). Antibodies, also called immunoglobulins, are a large family of glycoproteins capable of recognizing antigens with high specificity. Due to the specific relationship between antibody and antigen, immunosensor has received major attention. The antibody can be characterized into two types, monoclonal and polyclonal, depending on the epitope (region of an antigen and antibody interacts). Monoclonal antibody is more specific or recognise a single epitope, while polyclonal antibody can bind to multiple epitopes (Lipman et al., 2005). The choice of antibody will be determined by its analytical application. Both of the antibodies approach their own advantages which make them useful for different applications. Monoclonal antibody is mainly based on its high recognizing ability to the same epitope of an antigen and resulting a high specificity among experiments. For polyclonal antibody, it helps to amplify the signal of target analyte even with a low concentration level as polyclonal antibody binds more than one epitope.

The combination of immunosensor and electrochemical transducer is generally inexpensive, has fast response times, high sensitivity and selectivity, requires a small

volume of analyte and widely applicable in many fields (Belkhamssa et al., 2016; Marín-Barroso et al., 2019; Wang & Ma, 2018). In electrochemical immunosensor, the immunoreaction of antibody-antigen serves as bioreceptor which produces result in electrical signal by varying the potential, current, ion concentration, conductance, capacitance or impedance (Felix & Angnes, 2018). Electrochemical immunosensor can be further classified into conductimetric, potentiometric, amperometric, and impedimetric transducers.

Conductometric transducer measures the changes of conductivity in a system due to the presence of analyte. When the biorecognition reaction occurs, the changes in ionic species concentration could later cause changes in electrical conductivity of solution and current flow (Bhardwaj et al., 2017; Liu et al., 2006). For potentiometric transducer, the analytical signal obtained is based on the potential between working and reference electrode. The electrical potential changes as the antibody-antigen complex is formed (Silva et al., 2019; Sun, 2018). While amperometric transducer involves measuring the current generated by electrochemical oxidation or reduction of electroactive species at a constant applied potential (Wang & Ma, 2018; Yan et al., 2019).

In impedimetric electrochemical transducer, EIS is the tool to detect the bio–affinity reactions between the target analytes and the immobilized antibody, by monitoring the electron transfer reaction of redox species on the electrode surface. When antibody and antigen bound together, the formation of the immunocomplex caused a blocking effect and as a result, electron transfer resistivity/impedance increases. Impedance is usually expressed as a complex number, where the ohmic resistance is the real component and the capacitive reactance is the imaginary one (Prodromidis, 2010). The most popular format for evaluating electrochemical impedance data is the Nyquist plot. In the Nyquist plot, the imaginary impedance component (Z'') is plotted against the real impedance component (Z') at each excitation frequency (Prodromidis, 2010). The Nyquist plot can

be analysed with fitted to an equivalent circuit and the information on the electrical parameters response to the impedance changes can be extracted (Lisdat & Schäfer, 2008). Impedimetric immunosensor is a sensitive technique for label-free detection, and has attracted great interest in recent years due to its promising application of various areas (Hleli et al., 2006; Jin et al., 2011; Sharma et al., 2018).

2.4 Immunosensor detection mechanisms

Immunosensors are mainly depend on measuring the fractional occupancy of recognition sites, either from measuring of occupied site (direct format) or rely on the assessment of unoccupied site (indirect format) (Wen et al., 2017). In addition, some mechanisms involved labelling (enzyme/electroactive) which produce a signal and indirectly allow determination of the amount of antibody-antigen complex. The recognition elements, either antibodies or antigen can be immobilized on the transducer surface.

Competitive and sandwich assay are the popular detection mechanism in immunosensor detection. Sandwich assay (Figure 2.3 b), also known as non-competitive assay, requires the sample antigen binds to the immobilized antibody/primary antibody on the transducer surface (Pang et al., 2018; Serafín et al., 2018). Then, when an excess of labelled secondary antibodies exposed to the transducer, the secondary antibody only binds to antigen-primary antibody complex. The antigen is "sandwiched" by two antibodies and the signal produced is directly proportional to the sample analyte present. The sandwich format is generally used for macromolecules antigen but not suitable for micromolecules with molecular weight lower than 1000 Da, since micromolecules have limited epitope to bind two antibodies simultaneously.

In a competitive assay, the sample antigen competes with labelled/immobilized antigen to bind with limited antibody binding sides and more suitable for micromolecule detection (Liu et al., 2013; Zhang et al., 2018). This assay can be divided into direct competitive format and indirect competitive format. While direct competitive assay can also be divided into two approaches, i.) labelled antigen competes with sample antigen to form complex with immobilized antibody (Figure 2.3 c); ii.) sample antigen competing with immobilized antigen for limited free antibody (Figure 2.3 f). Indirect competitive format is applied when primary antibody is not suitable for labelling or labelling could affect antibody binding affinity, and thus the labelled secondary antibody is introduced (Figure 2.3 g) (Goud et al., 2019). Due to the competition between sample antigen and immobilized/labelled antigen, an inversely proportional relationship between signal produced and the concentration of antigen is expected.

Direct assay is the simplest detection mechanism, mainly based on binding of antigen and antibody (Figure 2.3 a and 2.3 e), and labelling of antibody or antigen is not necessary (Darwish et al., 2016). Direct assay is only suitable for macromolecules since the presence of micromolecule could not exhibit a significant signal changes. Conversely, a displacement assay is depending on the displacement of labelled antigen or antibody due to the presence of sample antigen (Figure 2.3 d and 2.3 h). The antibody should show a relatively high binding affinity to sample antigen in order for a displacement assay to occur. This detection mechanism with immobilized antigen/hapten exhibited an advantage of rapid detection on small molecule, this is because labelling of antigen is not required to perform the immunosensing (Khor et al., 2011; Liu et al., 2012). The differences between each detection mechanism as listed in Table 2.1.

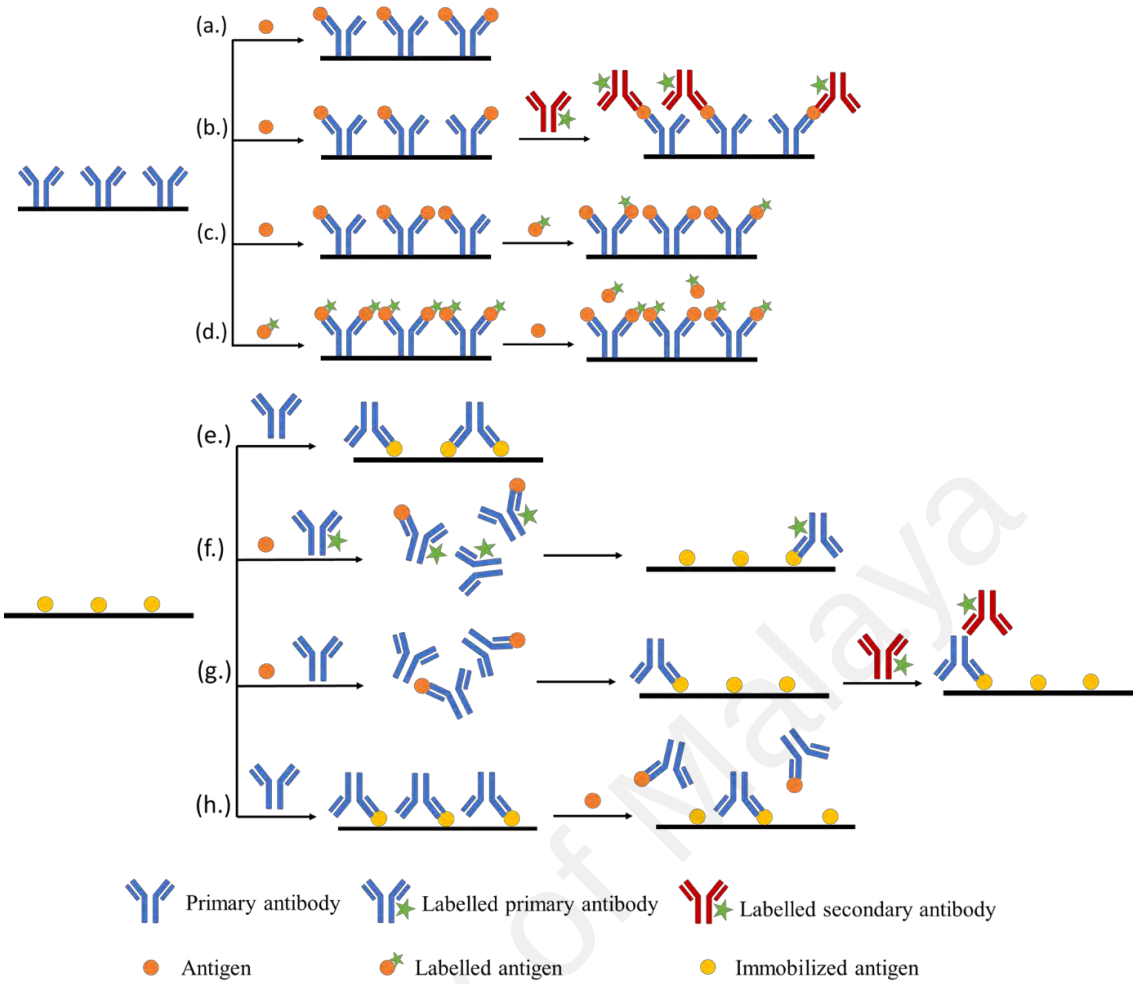

Figure 2.3: (a) A direct assay with immobilized antibody, (b) a sandwich assay, (c) a direct competitive assay with immobilized antibody, (d) a displacement assay with immobilized antibody, (e) a direct assay with immobilized antigen, (f) a direct competitive assay with immobilized antigen, (g) an indirect competitive assay, and (h) a displacement assay with immobilized antigen. (Ricci et al., 2007) (adapted with copyright permission from Elsevier)

Table 2.1: Differences between each immunosensor detection mechanisms.

Detection mechanism	Sandwich	Competitive	Direct	Displacement
Labelling	✓	✓	×	✓ Immobilized antibody format × Immobilized antigen format
Requirement of secondary antibody	✓	✓ Indirect × Direct	×	×
Detection of macromolecule	✓	✓	✓	✓ Immobilized antibody format
Detection of micromolecule	×	✓	×	✓ Immobilized antigen format
Preferable applications	• Optical	• Optical	• Electrochemical • Piezoelectric	• Electrochemical • Piezoelectric

2.5 Acrylamide detection methods

The detection methods for acrylamide can be classified into standard and rapid methods, the advantages and disadvantages of both detection methods are summarized in Table 2.2.

2.5.1 Standard detection methods

The standard analysis techniques for detection of acrylamide commonly used are chromatography methods such as LC, GC and HPLC coupled with mass spectrometry (Kim et al., 2007; Ono et al., 2003; Qin et al., 2017; Surma et al., 2017). Acrylamide can be detected using LC-MS is due to its solubility in water and at the same time can be detected by using GC-MS because of its improved volatility properties after derivatization. The ultra-performance liquid chromatography (UPLC) is the alternative to LC which enable to perform a better acrylamide separation from samples in a shorter time (Galuch et al., 2019). The high specificity and selectivity of the chromatography methods ensure the measurement sensitivity for quantitative detection of acrylamide. However, these standard analysis methods exhibit limitation such as time-consuming sample preparation, require expensive equipment and professional operating skill; hence enforce the development of rapid detection analysis.

2.5.2 Rapid detection methods

To overcome the drawbacks of standard methods, rapid detection method shows advantages such as shorter detection time, independent of costly experiment instruments, simpler sample preparation steps and rapid detection to acrylamide. The rapid methods for detection of acrylamide are summarized in Table 2.3.

2.5.2.1 Enzyme-linked immunosorbent assay (ELISA) for detection of acrylamide

ELISA detection is based on the specific recognition reaction between antibody and antigen. Due to the high specificity and affinity between antibody and antigen, ELISA offers advantages including good sensitivity and selectivity, not required expensive instrument as in standard method and high-throughput. The application of ELISA in acrylamide determination involved the raising of antibodies, thus synthesizing a suitable antigen for producing high-affinity antibodies is important (Figure 2.4).

In general, a substance with molecular weight lower than 1000 g mol^{-1} does not show immunogenic properties. This is because acrylamide with low molecular weight and lack of strong epitopes cannot elicit raising of antibodies (Hu et al., 2015). However, coupling acrylamide with a carrier protein is an effective way that has been discovered to raise acrylamide antibodies and few approaches have been reported (Preston et al., 2008; Quan et al., 2011; Zhou et al., 2008). A polyclonal antibody that capable of binding acrylamide has been raised after the derivatization of acrylamide with 3-mercaptobenzoic acid (3-MBA) (Preston et al., 2008). The acrylamide derivative (acrylamide-3-MBA) was then coupled to a carrier protein such as bovine tyreoglobulin or human serum albumin, via Michael addition between the unsaturated molecule and protein nucleophilic group (thiol and amine group) (Preston et al., 2008). This detection method produces a specific detection with a LOD of 65.7 μg kg^{-1}.

Another approach was using N-acryloxysuccinimide (NAS) as a hapten instead of acrylamide molecule as reported by Zhou et al. (Zhou et al., 2008). When using direct conjugation of acrylamide to carrier protein that could cause the loss of vinyl bond of acrylamide and this may result in low efficiency of produced antibodies, consequently the drawback can be overcome by synthesizing an antigen for acrylamide by using NAS. NAS is the combination structure of N-hydroxysuccinimide (NHS) and acrylamide

molecule, which contain amino active group that favour NAS to couple with carrier protein. NAS was conjugated to bovine serum albumin (BSA) and application of biotin-avidin system with satisfactory detection affinity towards acrylamide (Zhou et al., 2008).

The application of ELISA for detection of acrylamide possess advantages of specificity, consistence result with the standard method and shorter time detection, however the stability of the obtained antibodies and affinity towards acrylamide itself are still the challenging part of this method.

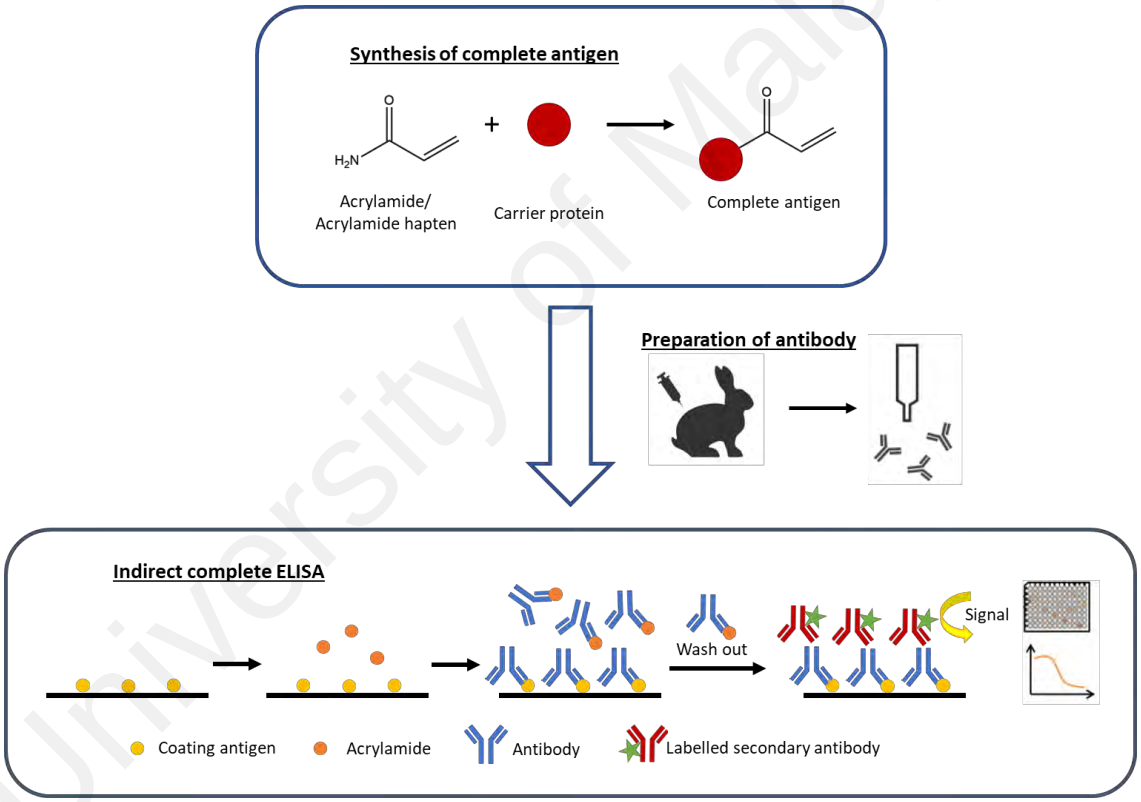

Figure 2.4: Schematic representation of the synthesis of antigen and preparation of antibody for detection of acrylamide via an indirect complete ELISA. (Hu et al., 2015) (adapted with copyright permission from Elsevier)

2.5.2.2 Fluorescent sensing methods for detection of acrylamide

The simple operating steps and ability to perform real time analysis of fluorescent sensing offer significant advantages of this method over standard detection methods (e.g., chromatography method). A novel fluorescent sensing method based on acrylamide polymerization-induced distance increase between quantum dots (QDs) was reported (Hu et al., 2014). In this method, NAS was initially modified with QD. Under the UV radiation, the carbon-carbon double bond of NAS-QDs polymerized with the assistance of photo initiator. The polymerization of QDs caused a decrease in distance between QDs and lead to a decrease of fluorescence intensity (refer Figure 2.5). Nevertheless, with the presence of acrylamide, QDs distance increase and resulting an increase in fluorescence intensity due to the participating of acrylamide in the polymerization. Good correlation between acrylamide concentration and fluorescent respond with $r^2 = 0.94$, a linear range between 3.5×10^5 to 3.5 g L^{-1} and a LOD of 3.5×10^5 g L^{-1} was obtained. However, as compared to other rapid methods especially electrochemical biosensor (referred Table 2.3), this fluorescent sensing method has lower sensitivity and selectivity.

Another simple and rapid fluorescence method was developed based on acrylamide degradation approach (Liu et al., 2014). Through Hofmann reaction, acrylamide degraded to generate vinyl amine. The vinyl amine could react with fluorescamine and resulted pyrrolinone which emitted a strong fluorescence emission that was observed at 480 nm. The emitted fluorescence intensity was then utilized for performing quantitative analysis of acrylamide in the concentration range of 0.05 to 20 μg mL^{-1}. Unfortunately, the main drawback of this approach was due to high temperature reaction conditions required at 90 °C to accelerate Hofmann degradation process which has limited the onsite detection of acrylamide.

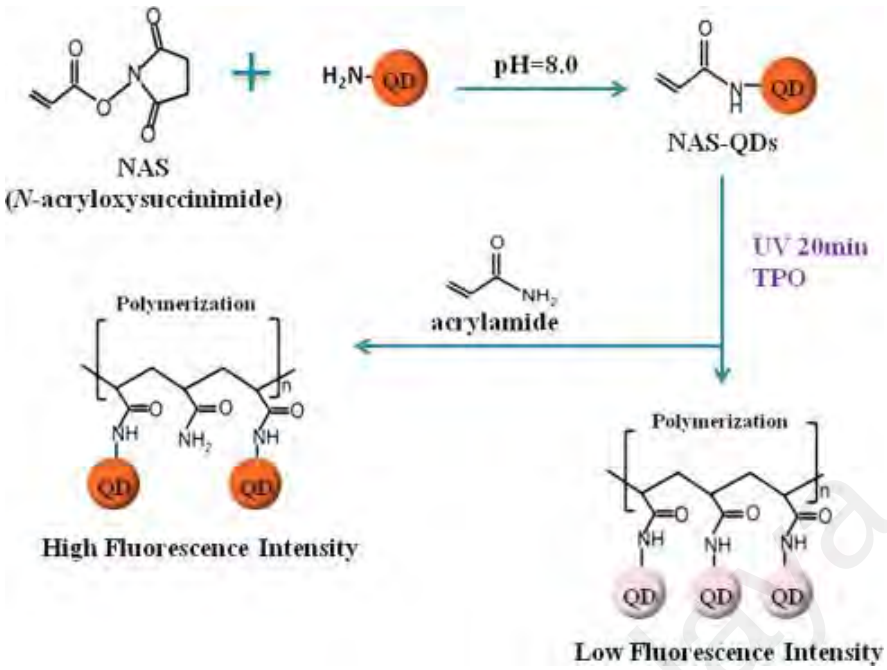

Figure 2.5: Schematic representation of mechanism of fluorescent sensing method based on acrylamide polymerization-induced distance increase between QDs. (Hu et al., 2014) (copyright permission from Elsevier)

2.5.2.3 Microbial electrochemical biosensors for detection of acrylamide

A number of electrochemical biosensors have been reported in pass few years as this method able to perform a simple, specific, sensitive and fast response detection measurement (referred Table 2.3). Majority of the electrochemical biosensing methods are focusing on the modification/preparation of device in order to increase the efficiency of detection for acrylamide. Ignatov et al. (1997) have developed a microbial cell-based biosensor by using *Brevibacterium sp.* cell and Clark oxygen electrode as processer (Ignatov et al., 1997). As mentioned in their published article, specific respiratory activity (SRA) was defined as the difference between the rate of oxygen consumption after the introduction of analyte sample and endogenous cell respiration, since the metabolism of acrylamide and acrylic acid needed participating of oxygen. Hence, the respiratory activity of the microbial cells was selected for detection of acrylamide and acrylic acid in waste water (Ignatov et al., 1997). The reduction of oxygen concentration resulted

changes of current intensity in Clark electrode and can be applied for detection of acrylamide. This method provided sensitive detection (10 mg L^{-1}), short detection time (10−15 mins) and simple sample pre-treatment. Another potentiometric biosensor was fabricated based on the biochemical interaction between bacterial cell, *Pseudomonas aeruginosa* and acrylamide (Silva et al., 2009). This whole cell contained intercellular amidase activity and consequently catalysed the hydrolysis of acrylamide to release acrylic acid and ammonium ion, NH_4^+. The resulted ammonium ion was detected by an ion selective electrode (ISE) as the transducer. Although the reported microbial biosensors have sensitivity detection, however dependence on living organisms can cause a delay in respond. Furthermore, preventing microbial cell/bacterial from environment pollution is another issue of this method.

2.5.2.4 Hb based electrochemical biosensors for detection of acrylamide

Generally, Hb was widely used as the bioreceptor for the detection of acrylamide due to the formation of adduct between acrylamide with Hb (Batra et al., 2013; Garabagiu & Mihailescu, 2011; Li et al., 2020; Stobiecka et al., 2007). The acrylamide-Hb adduct is the product of reaction between α-NH_2 group located at N-terminal valine of Hb and acrylamide molecule. This adduct also is a biomarker used for the determination of exposure of acrylamide to human/animals. The reversible conversion of Hb-Fe^{3+} to Hb-Fe^{2+} contributed to the electroactivity of Hb. During the redox reaction, the formation of acrylamide-Hb adduct could cause irreversible reduction of Hb-Fe^{3+} and alter the electroactivity properties of Hb redox centre (Stobiecka et al., 2007). As a result, changes in current intensity was observed and provided quantitative information on acrylamide content.

For Hb based electrochemical biosensor, the electron transfer to the working electrode and the immobilization efficiency of Hb are the two factors that affecting the performance of biosensor (Hu et al., 2015). Due to the large and three-dimensional structure of Hb, electron transfer process between Hb directly with an electrode is difficult (Stobiecka et al., 2007). The unfavourable orientation of Hb and the distance of redox centre to electrode were reasons for slow electron transfer. Therefore, various electro-mediators were proposed and being modified onto the electrode surface to enhance the electron transfer rate. For examples, poly-3-hydroxybutyrate membrane (Ma et al., 2005), agarose hydrogel films (Wang et al., 2005), carbon paste electrode (Stobiecka et al., 2007), carbon nanotubes (CNTs) (Krajewska et al., 2008) and nanoparticles (Garabagiu & Mihailescu, 2011; Liu et al., 2004; Wang et al., 2011). In addition, the use of nanomaterials such as carbon nanotubes and metal nanoparticles showed a great application to electrode modification (Batra et al., 2013; Garabagiu & Mihailescu, 2011; Kovář et al., 2014). The high surface to volume ratio of nanomaterial not only has increased the amount of immobilized Hb on the electrode, but the excellent electrical conductivity properties of nanomaterial have accelerated the rate of electron transfer and thus lead to sensitive detection.

Krajewska et al. (2008) have designed a voltammetry biosensor by coating glassy carbon electrode with single walled carbon nanotubes (SWCNT) and Hb, the developed sensor presented a low detection limit at 0.071 μg kg^{-1} and the modified electrode showed good resistivity to matrix present in water extracted potato chips (Krajewska et al., 2008). Garabagiu & Mihailescu (2011) proposed gold nanoparticles as the mediator on indium tin oxide (ITO) glass to determine trace content of acrylamide in food products, with a linear range of 0.71 to 710 μg kg^{-1} (Garabagiu & Mihailescu, 2011). An amperometric biosensor based on the combination of metallic nanoparticles with CNTs and conducting polymer has been fabricated by Batra et al. (Batra et al., 2013). A pencil graphite electrode

was modified layer by layer with CNTs, copper nanoparticles (CuNPs), followed by polyaniline and lastly was the immobilization of Hb. The coupled of CNTs and CuNPs worked as a good electron transfer mediator, has improved the analytical performance of developed biosensor with LOD of 1.42×10^{-2} μg kg^{-1} and respond time less than 2 sec (Batra et al., 2013).

Yadav et al. (2018a) have employed nanoparticles of Hb (HbNPs) to replace the native Hb (Yadav et al., 2018a). This protein nanoparticles often in the range of 100 − 200 nm that exhibited faster electron transfer rate than native Hb, high optical, electrical, electronic, thermal properties and also increased the surface area to volume ratio (Yadav et al., 2018b). HbNPs was applied in an amperometric biosensor for the detection of acrylamide, not only economize and simplified the fabrication of biosensor, as well as improved its analytical performance and stability (Yadav et al., 2018a). In addition, Asnaashari et al. (2019) proposed the combination of DNA and Hb as an acrylamide quantification receptor (Asnaashari et al., 2019), since both DNA and Hb could bind to the acrylamide molecule (Hu et al., 2015). Recently, ionic liquid that showed good biocompatibility for electrode preparation and subsequently provided even distribution of Hb in carbon powder due to high viscosity of the ionic liquid (Li et al., 2020). The developed biosensor was used for the detection of acrylamide with a LOD of 3.55×10^{-4} μg kg^{-1} and had advantages such as simple electrode preparation and satisfactory stability.

Electrochemical biosensor based on acrylamide-Hb adduct demonstrated comparatively sensitive determination to acrylamide compound and possess advantages of wide linear range, portable, rapid and high-throughput. However, the acrylamide-Hb adduct formed was found not well correlated with the total intakes of acrylamide. This is because Hb can also bind with acrylamide's epoxide, glycidamide (Bjellaas et al., 2007) and glycidamide that has shown a higher reactivity as compared to acrylamide. Therefore, it was suggested to sum the amount of glycidamide with acrylamide adduct in order to

determine the total acrylamide dietary intake (Wilson et al., 2009). In addition, glycidamide can be formed in food during the heating process (Granvogl et al., 2008) and thus the specificity of Hb to acrylamide is considered not promising.

2.5.2.5 Electrochemical immunosensors for detection of acrylamide

An electrochemical immunosensor for the detection of acrylamide in water and food samples was reported recently (Wu et al., 2019). In this study, a coating antigen (acrylamide-4 mercaptophenylacetic acid-ovalbumin conjugate, acrylamide-4-MPA-OVA) was immobilized on the working electrode. To perform the detection, polyclonal antibody with the analyte (acrylamide-4-MPA) were added at the same time onto the modified electrode. This detection method was based on the competitive assay, where analyte presented in the sample and coating antigen were competing to bind with the antibody (Wu et al., 2019). As a result, a linear respond of decrease in current change with increase concentration of analyte was determined. This developed immunosensor exhibited a working range of 187 ng kg^{-1} to 104 µg kg^{-1} and LOD of 45.9 ng kg^{-1} in drinking water indicating the sensitive analytical detection of immunosensor towards acrylamide. Nevertheless, this detection method has a limitation on performing a direct and rapid detection, this is because the reported immunosensor required pre-mixing of sample with antibody which is not considered as a user intervention free approach.

Table 2.2: Comparison of advantages and disadvantages of standard and rapid detection methods for acrylamide.

Detection method	Principle	Advantages	Disadvantages
Chromatography detection	Acrylamide could be identified from a sample after separation and extraction steps.	✓ High selectivity, specificity and sensitivity. ✓ Useful for quantitative detection.	× Time consuming as requires sample pre-treatment step. × High cost instrument.
ELISA	A specific high affinity of antibody is produced based on a complete antigen via coupling of acrylamide with a suitable carrier protein.	✓ High specificity.	× Production of a high affinity antibody is difficult to achieve.
Fluorescence detection (Hu et al., 2014)	Based on the photophysical properties of QDs and pyrrolinone.	✓ Produce visible signal. ✓ Easy operation steps. ✓ Small instrument scale.	× Lower sensitivity as compared to electrochemical biosensor.
Microbial biosensor	Based on microbial metabolism and biochemical interaction of microbial cell with acrylamide.	✓ Sensitive detection.	× Delay in detection respond. × Require pollution-free microbial cell.

Table 2.2, continued.

Detection method	Principle	Advantages	Disadvantages
Hb based electrochemical biosensor	Utilized reaction of Hb with acrylamide to produce acrylamide-Hb adduct.	✓ High-throughput detection ✓ Sensitive detection.	× Specificity of Hb to acrylamide itself is not promising.
Electrochemical immunosensor (Wu et al., 2019)	Competitive assay of coating antigen with analyte in sample.	✓ Utilise specific interaction between antibody-analyte. ✓ Sensitive detection.	× Require conjugation of target analyte with 4-MPA to increase its immunogenicity. × Could not perform direct detection.

Table 2.3: Reported rapid methods for the detection of acrylamide.

Type of biosensor	Dynamic range/ μg kg^{-1}	LOD/ μg kg^{-1}	Stability/ days	Recovery/ %	Application	Sample preparation	References
3-MBA derivatized acrylamide based ELISA	5.18×10^1 – 3.31×10^3	6.57×10^1	ND	ND	Potato crisps	Solid phase extraction	(Preston et al., 2008)
NAS–BSA conjugate ELISA	1.00×10^1 – 1.00×10^5	0.60×10^1	ND	90.0 – 110.0	Potato fries, biscuits	Solid phase extraction	(Zhou et al., 2008)
Fluorescent sensing method based on polymerization-induced distance between quantum dots	3.50×10^1 – 3.50×10^6	3.50×10^1	ND	ND	Potato chips	Solid phase extraction	(Hu et al., 2014)
Fluorescence method based on acrylamide degradation	5.00×10^1 – 2.00×10^4	1.50×10^1	ND	66.0 – 110.6	French fries, fried puffs, fried chicken roll, bread, biscuits	Hexane extraction	(Liu et al., 2014)
Biosensor based on respiratory activity of microbial cells	1.00×10^4 – 7.50×10^4	ND	<5	ND	Waste water	-	(Ignatov et al., 1997)
Ammonium ion-selective electrode	7.10×10^3 – 7.10×10^4	7.11×10^2	54	95.5	Waste water	-	(Silva et al., 2009)
Voltammetric biosensor based on Hb modified on carbon paste electrode	9.24×10^{-4} – 3.98×10^5	8.53×10^{-3}	30	ND	Potato crisps	Hexane extraction, Carrez purification	(Stobiecka et al., 2007)
Voltammetric biosensor based on glassy carbon electrode modified SWCNT/Hb	7.11×10^{-4} – 7.11×10^4	7.11×10^{-2}	14	ND	Potato crisps	Hexane extraction, Carrez purification	(Krajewska et al., 2008)

Table 2.3, continued.

Type of biosensor	**Dynamic range/ µg kg^{-1}**	**LOD/ µg kg^{-1}**	**Stability/ days**	**Recovery/ %**	**Application**	**Sample preparation**	**References**
Amperometric biosensor based on Hb modified on pencil graphite electrode	3.55×10^{-1} – 5.33×10^{6}	1.42×10^{-2}	100	95.4 – 97.6	Potato crisps	Hexane extraction, Carrez purification	(Batra et al., 2013)
Hb modified on glassy carbon electrode	2.13×10^{-3} – 1.07×10^{1}	7.11×10^{-4}	28	98.8 – 101.4	Potato crisps	Hexane extraction, Carrez purification	(Varmira et al., 2018)
HbNPs based amperometric biosensor	7.11×10^{-3} – 7.11×10^{6}	7.11×10^{-3}	120	98.2 – 99.0	Biscuits, cakes, chips, fried cereal, nuts and kurkure	Carrez purification	(Yadav et al., 2018a)
Hb-oligonucleotides modified electrode	1.42×10^{2} – 3.55×10^{6}	1.12×10^{1}	60	91.0 – 120.0	Potato fries	Hexane extraction, Carrez purification	(Asnaashari et al., 2019)
Electrochemical immunosensor by competitive assay	1.87×10^{-4} – 1.04×10^{-1}	4.59×10^{-5}	42	86.0 – 115.0	Drinking water, coffee, potato chips	Solid phase extraction	(Wu et al., 2019)
Electrochemical immunosensor via displacement assay	0.10×10^{2} – 3.50×10^{4}	0.38×10^{1}	28	90.8 – 99.7	Coffee, cocoa powder, prune juice	-	Current study (Lau et al., 2019)

ND = Not detected, LOD = Limit of detection, Hb = Hemoglobin, SWCNT = single walled carbon nanotubes.

2.6 Electrochemical control on antibody-antigen binding interaction

Electrochemical control or described as electrochemical stimulation can be applied in immunosensor and triggered the interaction between bio-molecules with antigen by electrical field (Asanov et al., 1998; Brod et al., 2008; Liron et al., 2002). There are few reasons were reported that caused the dissociation of antibodies. Brod et al. (2008) proposed the application of a bias at negative voltage causes enhancement of local pH to a higher pH value near the electrode, consequently caused deprotonation of the amino-acid functional group found in the immobilized antigen (Brod et al., 2008). Antibody-antigen binding depends on several interactions and one of them was electrostatic interaction. After undergoing the deprotonation step, the antigen's amino acid loses their native electrostatic binding ability towards antibody, leading to the rapid detachment of antibody.

Furthermore, the electrochemical control method can be used for regenerating the electrode surface where a dissociation of a surface bound antibody from surface bound hapten could occur more completely. Asanov et al. (1998) reported that by applying electrode polarization resulted in changes of electrostatic properties and hydrophobicity of electrode surface. However, these two factors do not give much impact on protein absorption or desorption. Other factors that could be taken into account including the changes of surface properties with parameter in the double electric layer (DEL) and local changes of pH in DEL (Asanov et al., 1998). Another possible reason for the electrical stimulation on the dissociation of bio-specific complexes is that protein has inadequate time to adapt itself to the conformation or orientation with respect to the new surrounding/charge electrode surface when pulsing is applied, hence cause a desorption.

All these reported studies indicated that the electrochemical modulation could control the antibody-antigen interaction, typically the negative potential could inhibit the antibody and antigen binding or even cause a dissociation of antibody from antibody-

antigen complex. This is because antibody is negatively charged or acted as an anion in neutral conditions (Gooding et al., 2004), hence impeded the antibody-antigen binding during application of negative potential. This approach also suggested as a possible way to minimize the non-specific absorption as well as to suppress cross reactivity binding (Asanov et al., 1998; Liron et al., 2002). Most importantly, the non-covalent antibody-antigen binding can be reversible without a significant damage/effect after the negative pulsion (Brod et al., 2008). A good evidence for the regeneration of immunosensor with aid of electrochemical pulsion has been reported by Khoo et al. (2016). The repeatable biotin immunosensor surface remained its detection ability towards the analyte even after five regenerations and no physically damage was observed (Khoo et al., 2016).

2.7 Response surface methodology

The optimization of the analytical methods is commonly practiced in order to obtain the maximum or the best performance. The hand-on experimental is normally carried out by monitoring the influence of one variable at a time while the other variables are maintained at a constant parameter. To optimize all of the effect of variables on experimental performance may lead to an increase in number of experiments and then possessed disadvantages such as increase in the use of reagent and time consuming. As a consequence, multivariate statistic technique which is a chemometric tool with combinations of mathematical and statistical techniques has been applied (Bezerra et al., 2008). It is very useful typically for analysis involving numerous variables influencing the performance with the objective of optimizing the experiment performance (Sharma et al., 2009). In response surface study, the independent experimental variables that can be changed independently is defined as factors; while the dependent variable is the measured results from experimental which is the responses. This method allows the development of a mathematical model to be fitted in a predicted polynomial equation that describes the

performance of experimental data sets, evaluating the interaction effects between the factors as well as optimizing the parameters of factors to attain the best performance (Bezerra et al., 2008).

Box-Behnken design is one of the experimental designs for response surface methodology. It has a higher efficiency than other experimental designs such as central composite design or Doehlert matrix, and exhibits an equal efficiency with Doehlert Matrix when three factors are studied (Ferreira et al., 2007). Due to its lower number of experiments with only 17 trails with shorter operating time, Box-Behnken design has been widely applied as alternative way for optimization the analytical analysis, for instant optimizing the phenolic extraction condition in HPLC (Gomes et al., 2017), optimizing the ultrasound-assisted extraction condition in GC-MS (Araujo et al., 2017) and optimizing the optimal conditions for cadmium detection using square wave voltammetry (Zhao et al., 2016). Another advantage of this experimental design is Box-Behnken design has excluded the combinations of the factors at the highest or lowest level (Ferreira et al., 2007). As a consequence, Box-Behnken experimental design is particularly useful in avoiding the trials under extreme experimental combinations to avoid the undesirable result.

2.8 Working principle of equipment

2.8.1 Potentiostat

Potentiostat is an electronic instrument that measures and controls the potential difference between the working electrode and the reference electrode (voltage) (EC08, 2011). The potentiostat works commonly in an electrochemical cell with three electrodes, the working electrode, the reference electrode and the counter electrode needed (Beach et al., 2005). The working electrode is where the potential is regulated and current is

measured, and is usually an "inert" material such as glassy carbon, gold or platinum. The reference electrode is the electrode with constant potential, whereas the counter electrode is a conductor electrode for completing the cell circuit. When potentiostat applies potential on the electrode surface, electrode surface modification triggers the delivery of electrons and causes changes in the transfer rate of electrons, this can be measures by the potentiostat (Butterworth et al., 2019; Mercer et al., 2019).

2.8.2 Field Scanning Electron Microscope (FE-SEM)

FESEM is a well-known analytical method, generating signals containing topographical and sample surface composition information. FESEM is a microscope working with high-energy electron beams. The electrons produced from a source of field emissions are accelerated in a high gradient of the electric field under high vacuum column (Erlandsen et al., 2000). The electron beam travelled through electromagnetic lenses, concentrated on the surface or specimen of the sample. The electrons emitted detected by the electron detector and the strength of the electron signal emitted are shown in digital image form, which can be seen on a monitor (Wijeyesekera et al., 2016). Besides, FESEM can couple with an Energy Dispersive X-Ray Analyzer (EDX) to provide information on elementary identification and quantitative compositional information (Kambham et al., 2019; Mani et al., 2012). This analysis depends on the intensity of backscattered electrons generated by electron bombardment to characterize the elementary composition of the volume analysed.

2.8.3 Fourier Transform Infrared (FT-IR)

FT-IR is a useful analysis for determining the existence in samples of certain functional groups (Mohamed et al., 2017). As radiation passes through the sample, FTIR

tests the IR portion of the electromagnetic radiation spectrum. The IR spectrum represents the molecule's absorption and transmission resulting from the absorption of light at different wavelengths, thus producing the analysed sample's molecular fingerprint (Nguyen et al., 2019; Ramírez-Hernández et al., 2019).

2.8.4 Gas chromatograph mass spectrometry (GC-MS)

GC-MS is an analytical technique consisting of a gas chromatograph (GC) coupled with a mass spectrometer (MS) for separating complex mixtures, defining and quantifying the analytes in samples (Hussain & Maqbool, 2014; Stan, 2005). This makes GC-MS suitable for the study of compounds with low molecular weight in environmental and food samples (Bianchi et al., 2007; Bueno et al., 2019; Domínguez et al., 2016). The analysed compound using this technique should be highly volatile and stable at high temperatures (Hussain & Maqbool, 2014). GC is where the sample separation occurs, each compound elutes at different times out of the gas column and this is referred to as retention time. After the compound leaves the GC column, MS ionizes the compound and generates signal strength according to the mass-to-charge ratio.

CHAPTER 3: METHODOLOGY

3.1 Materials and reagents

1,3- dicyclohexylcarbodiimide, 1,4-phenylenediamine , 2-[2-(2-methoxyethoxy)ethoxy]acetic acid (antifouling agent), 4-nitroaniline, 20 nm gold nanoparticles (AuNPs), acrylamide, maleamic acid, methacrylic acid, N,N'-dimethylenebis(acrylamide), potassium chloride (KCl), potassium phosphate dibasic (K_2HPO_4), potassium phosphate monobasic (KH_2PO_4), sodium chloride (NaCl), sodium nitrate ($NaNO_2$) and sodium phosphate dibasic (Na_2HPO_4) were purchased from Sigma Aldrich, USA. Potassium ferricyanide ($K_3Fe(CN)_6$) was purchased from Acros, USA. Acrylic acid, acetonitrile, propionic acid and N,N-dimethylformamide were purchased from Merck, Germany. Ethyl alcohol (EtOH) and hydrochloric acid (HCl) were purchased from R&M Chemicals, UK. Micro-cloth pad and micropolish alumina powder (1.0, 0.3 and 0.05 μm) were purchased from Buehler, USA. Polyclonal anti-acrylamide IgY antibody (host: chicken) was purchased from Mybiosource, USA. All reagents were used as received, and all solutions were prepared with Milli-Q water with resistivity 18.2 MΩ•cm at 25 °C (Millipore, Sydney, Australia). Phosphate buffer solution was prepared by using 50 mM of KCl, KH_2PO_4 and K_2HPO_4. Phosphate buffer saline (PBS) was prepared by using 2 mM of KH_2PO_4, 10 mM of Na_2HPO_4, 2.7 mM of KCl and 137 mM of NaCl. Both of the buffer solutions were adjusted to pH 7.0 and pH 7.4, respectively with NaOH nd HCl solution. For the purpose of method comparison to a standard method, GC-MS analysis was performed. Acrylamide extraction from liquid food samples (cocoa, coffee and prune juice) was performed using Bond Elut QuEChERS purchased from Agilent Inc., USA.

3.2 Electrochemical measurements

All of the electrochemical measurements including cyclic voltammetry (CV) and EIS impedance measurement were carried out by using an AutolabIII potentiostat PGSTAT204 from Metrohm, Netherlands. A conventional three-electrode cell system was utilized for the electrochemical experiments, with a glassy carbon plate as the working electrode. A platinum wire and Ag/AgCl (3 M KCl) as the counter electrode and a reference electrode, respectively. A Plate Material Evaluating Cell is made up from a Teflon cell body and a Teflon cell base. The glassy carbon plate was "sandwiched" between Teflon blocks and attached by using two 20 mm screws. A rubber O-ring was placed between the glassy carbon plate and the Teflon cell body to prevent leakage of electrolyte. The counter and reference electrodes were placed in the Teflon cap and later being inserted to the Teflon evaluating cell. All CV for surface characterization was carried out at 0.7 V to -0.2 V scanning potential at a scan rate of 100 mV s^{-1}, while the EIS measurement was performed with direct potential of 0.2 V, frequency range between 0.1 − 10,000 Hz and amplitude of 0.01 V. Both CV and EIS analysis were carried out in phosphate buffer solution containing 1 mM of $[Fe(CN)_6]^{3-/4-}$ redox active species. All electrochemical measurements were carried out at 25 °C, at room temperature.

3.3 Apparatus and instrumentations

Hitachi SU8220 Field Scanning Electron Microscope (FE-SEM) (Tokyo, Japan) coupled with energy dispersive X-ray analysis (EDX) was used for the surface characterization of bare glassy carbon plate and AuNPs modified electrode surface. ImageJ (NIH, USA) image processing software was used for the determination of AuNPs size distribution. Surface characterizations using Fourier Transform Infrared (FT-IR) were analysed within the range of 450–4000 cm^{-1} performed using Spectrum™ 400

(Perkin Elmer, USA). Box-Behnken statistical analysis was conducted using Design Expert software (Trial Version, Stat-Ease Inc., USA). Acrylamide determination with the standard method was performed using Shidmazu (Japan) gas chromatography mass spectroscopy system (GC2010) equipped with mass detector (QP2010 Ultra), electron impact ionization source, and auto sampler (AOC 20i). The solgel-wax column with the dimension of 30 m length × 0.25 mm internal diameter from SGE Analytical Science, USA was used for acrylamide separation from samples matrix prior to GC-MS analysis.

3.4 Stepwise fabrication of the electrochemical immunosensor for acrylamide detection

Prior to the fabrication steps, the glassy carbon plate was polished successively with 1.0, 0.3, and 0.05 μm alumina slurries, respectively on a micro-cloth pad. After each polishing step, the glassy carbon plate was then rinsed thoroughly with Milli-Q water. The immunosensor fabrication steps is as shown in Figure 3.1. Firstly, the mixture solution of 4-niroaniline and 1,4-phenylenediamine with a ratio of 1:1 was solubilized in 0.5 M HCl containing two times molar amount of $NaNO_2$. After that, this diazonium salt mixture solution was deaerated with purified nitrogen gas and allowed to react for 15 min. The modification step of diazonium salt via electrochemical reduction was recorded by scanning the clean glassy carbon plate for 2 cycles between the potential of -0.6 V with 0.2 V to produce the mixed monolayer of the aryldiazonium salt and formed Surface 1 (Figure 3.1). After washing with Milli-Q water, the glassy carbon plate was treated with $NaNO_2$ that initially dissolved in 0.5 M of HCl before the incubation of AuNPs dispersion for 4 hrs at 25 °C. The AuNPs were covalently bound to the amino linker on glassy carbon plate by forming Au-NH linkage to form Surface 2 (Figure 3.1). Subsequently, 4-aminophenyl was formed after undergoing electrochemical reduction of 4-nitrophenyl in a protic solution prepared from 1:9 v/v EtOH-H_2O containing 0.1 M of KCl. The

electrochemical reduction was conducted using CV method with potential ranged between 0.0 V to 1.6 V for three cycles. To obtain Surface 3, 10 mM of 2-[2-(2-methoxyethoxy)ethoxy]acetic acid (antifouling agent) was activated in ethanol solution containing 40 mM N,N-dicyclohexylcarbodiimide for 30 min. Antifouling agent was modified on the electrode to prevent non-specific binding of protein on the electrode surface. A volume with 60 µL of the activated anti-fouling agent was later added on the glassy carbon plate and incubated for 6 hrs at room temperature (25 °C). The glassy carbon plate was further modified with 1,4-phenylenediamine by scanning potential between -0.6 V and 0.2 V for 2 cycles in 0.5 M HCl solution containing 10 mM of $NaNO_2$ and to generate Surface 4 (Figure 3.1). The modification of aryldiazonium salt had provided a binding side for hapten on AuNPs. The overnight incubation of modified glassy carbon electrode in 5 mM of maleamic acid with 20 mM of N,N-dicyclohexylcarbodiimide in ethanol solution resulted a binding site (surface bound hapten) for acrylamide antibody (Surface 5) (Figure 3.1). The final step of the immunosensor interface for acrylamide detection (Surface 6) produced by incubating the fabricated electrode in 0.5 µg mL^{-1} of acrylamide antibody prepared in PBS at pH 7.4. The antibody solution was incubated for 30 min at the temperature of 4 °C. The fabricated immunosensor surface was rinsed thoroughly with PBS at pH 7.4 before and after the incubation of antibody.

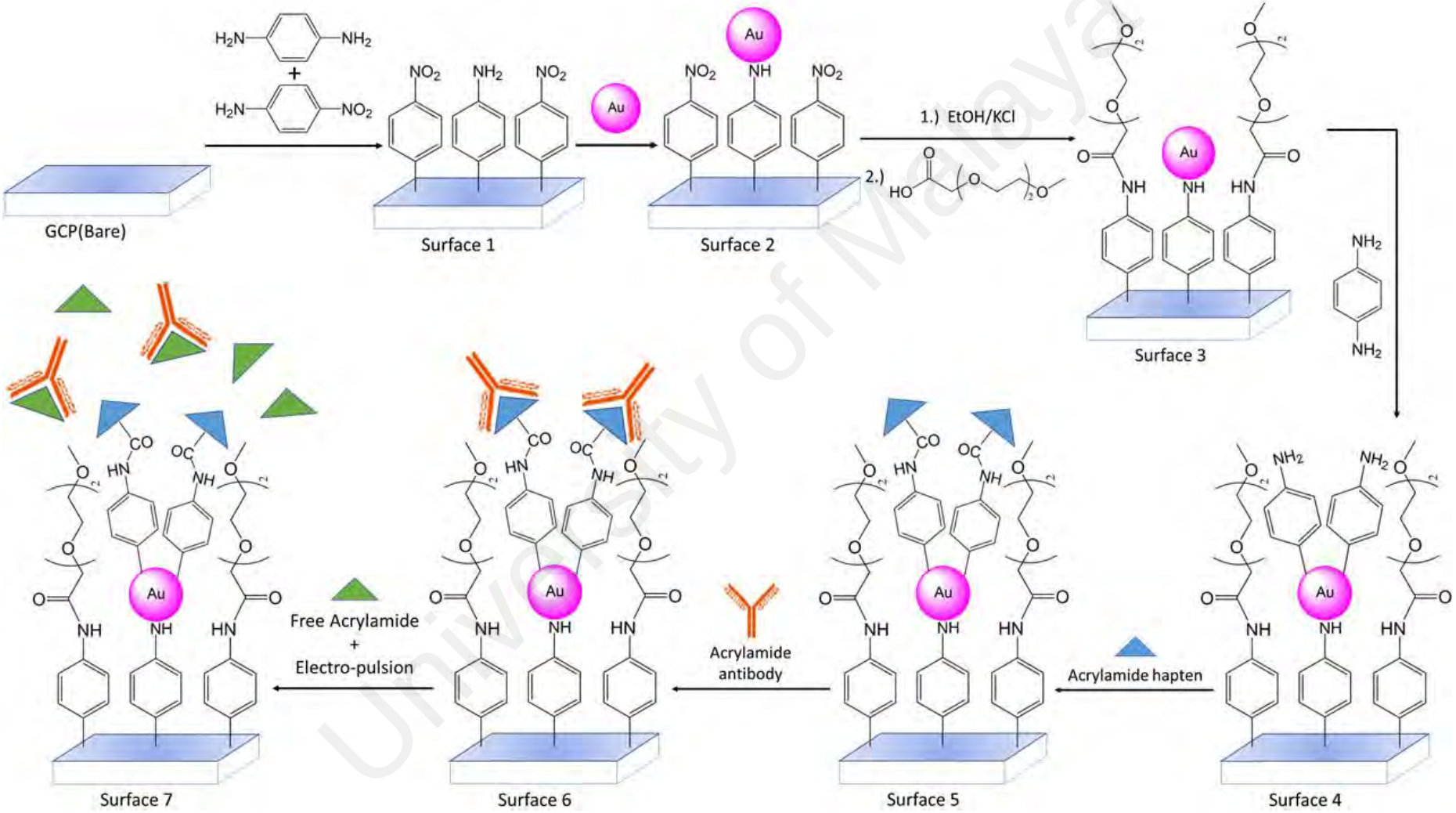

Figure 3.1: The stepwise interfacial fabrication steps of the developed electrochemical immunosensor interface for detection of acrylamide.

3.5 The dissociation of surface bound antibody via a displacement assay

The developed electrochemical immunosensor interface was fabricated as described in Section 3.4. The immunosensor surface was then introduced with 30 μg mL^{-1} of acrylamide for surface bound antibody to dissociate from hapten. The acrylamide solution was incubated on the modified glassy carbon plate electrodes for 5, 10, 15, 20, 30 and 60 min. The resistivity of electrode before and after the introduction of acrylamide was determined by using EIS method. Each reading was repeated for three replicates with newly-prepared electrode.

3.6 Electro-pulsing effect on enhancement of the dissociation of antibody from surface bound hapten

A series of electrode pulsing (electro-pulsion) were carried out at various pulsing potentials and pulsing charges for different pulsing durations to optimize the optimal conditions for a displacement assay. The electrode pulsion was conducted by using chronoamperometry method. The EIS measurement on the electrode was performed before and after the electrode pulsion with presence of a constant concentration, 30 μg mL^{-1} of acrylamide. The changes in resistivity (R_{ct}) before and after the electro-pulsion was obtained in order to determine the optimal electro-pulsing condition for the dissociation of the surface bound antibody from the surface bound hapten. In addition, two sets of control experiments have been conducted: (i) the electrode was pulsed with -800 mV for 10 min in PBS at pH 7.4 without the presence of free acrylamide, and (ii) secondly, the electrode was incubated in PBS at pH 7.4 without the presence of free acrylamide. The resistivity changes of the electrode were evaluated by using EIS method.

3.7 Box-Behnken experimental design

A three-level three-factorial Box-Behnken experimental design was employed to investigate the effect of the displacement assay factors (e.g., pulsing duration, pulsing potential and concentration of acrylamide) on the resistivity changes observed in a displacement assay. Pulsing duration (from 5 to15 min), pulsing potential (from -700 to -900 mV) and acrylamide concentration (from 0 to 30 μg mL^{-1}) are the variable input parameters, while the difference in resistivity of the electrode upon dissociation of antibody with the aid of electro-pulsing effect is the response. Table 3.1 shows the experimental parameters and the experimental Box-Behnken design levels applied in the statistical software (Design Expert). The factor levels were coded –1 as low, 0 as central point and 1 as high. As based on the actual experimental results that using all the studied positive potential did not show any significant dissociation of antibody from the surface bound hapten, hence no positive potential was included in this present statistical study since the main objective of performing a displacement assay is the dissociation of antibody from the surface bound hapten.

First of all, three important tests (lack of fit test, model summary statistics and sequential model sum of squares tests) were conducted to evaluate the most suitable model to be fitted for the obtained experimental data. Next, a second-order quadratic equation can later be described from the fitted model to predict the response (difference in resistivity). Subsequently, the three-dimensional response surface graph was plotted to determine the relationship between the three studied factors with respect to the difference in resistivity. Other than that, the most significant factor that affecting the displacement assay was determined. A desirability function was used for the determination of the optimal conditions for a displacement assay and evaluated based on the maximum response (maximizing the difference in resistivity).

Table 3.1: Experimental design levels of chosen factors.

Factors	Level		
	Low (-1)	Middle (0)	High (+1)
A: Pulsing duration/ min	5	10	15
B: Pulsing potential/ mV	-900	-800	-700
C: Concentration of acrylamide/ µg mL^{-1}	0	15	30

3.8 Reproducibility and repeatability assessment

Reproducibility refers to the capability of the developed immunosensor to produce a uniform result when repeating the test under similar experimental conditions and at a constant concentration. High reproducibility is related to the reliability and consistency of the developed electrochemical immunosensor. The reproducibility test was conducted with five different electrodes and each electrode was tested for three replicates. After the modification steps (as in Figure 3.1), the electrode surface was exposed in 15 µg mL^{-1} of free acrylamide prepared in PBS pulsed with electro-pulsion at -800 mV for 10 min. Then, EIS measurement was taken for each electrode before and after the displacement assay where dissociation of surface bound antibody from the surface bound hapten occurred.

Precision assessment was described as the closeness of the obtained result with no significant variation. The experiment was conducted by testing the developed immunosensor with a series of different concentration (low, medium and high concentration from dynamic range) of acrylamide under similar experimental conditions. In intra-day precision study, the fabricated immunosensor was tested in 5 µg mL^{-1}, 15 µg mL^{-1} and 25 µg mL^{-1} of free acrylamide prepared in PBS with the electro pulsion at -800 mV for 10 min. The decrease in resistivity resulted from the displacement assay for each electrode was measured on the same day and measured by using EIS method. Each concentration was tested for five replicates. On the other hand, the inter-day precision

study was carried out for five continuously and subsequent days and for each day, three different concentration of acrylamide solutions were tested. Each concentration was tested for triplicates. The fabricated immunosensor was pulsed with -800 mV for 10 min in 5 μg mL^{-1}, 15 μg mL^{-1} and 25 μg mL^{-1} of free acrylamide prepared in PBS. The experiment was repeated on day 2, 3, 4, and 5 on newly prepared immunosensor surface.

3.9 Selectivity and stability tests

The selectivity test was conducted to ensure the specificity of immunosensor towards acrylamide and without showing any significant response to others interference molecules. The fabricated immunosensor interface was evaluated in four different types of small organic molecule solutions, including acrylic acid, methacrylic acid, propionic acid and N,N'-dimethylenebis(acrylamide). These molecules were selected because they have a high similarity in chemical structure as acrylamide. Firstly, the decrease in resistivity of the fabricated electrode after pulsing at -800 mV for 10 min in 15 μg mL^{-1} of acrylamide prepared in PBS was recorded. Subsequently, the four others small organic molecule solutions were assessed at the concentration of 15 μg mL^{-1} in PBS with the newly prepared electrode surface. The resistivity changes were measured with EIS before and after the exposure of immunosensor to acrylamide and other small organic molecules.

To fulfil one of the commercialization criteria of developed immunosensor, long-term stability test has to be performed on the immunosensor in order to ensure the consistent detection ability after storage. Stability assessment was tested using different electrodes and the fabricated electrodes were stored in PBS at 4 °C. The EIS measurement was taken on days 1, 2, 3, 4, 5, 7, 14, 21 and 28, respectively for each electrode. For determining the resistivity changes, each of the electrode was pulsed with -800 mV for 10 min in a 10 μg mL^{-1} of free acrylamide prepared in PBS. The EIS measurement was taken before and

after the displacement assay with aid of electro-pulsion. In addition, the stability evaluation was conducted with storage of the developed immunosensor at room temperature, 25 °C. The reading of the EIS was taken during days 1, 2, 3, 4, 5, 7 and 14.

3.10 Method comparison where analysis of acrylamide in food samples by standard method, GC-MS

In GC-MS analysis, the diluent for sample and calibration standard was prepared from 50% acetonitrile solution. The standard stock solution of 1000 μg mL^{-1} acrylamide was prepared in 50% acetonitrile solution. For determination of acrylamide in food samples, an external calibration method was utilized, where five standard calibration with concentration of 0.05, 0.1, 1.0, 5.0 and 10.0 μg mL^{-1} were prepared. The concentration of 1.0, 5.0 and 10.0 μg mL^{-1} were prepared from the stock acrylamide standard solution, while for the concentration of 0.05, and 0.1 μg mL^{-1} were prepared from 1.0 μg mL^{-1} of standard stock.

1.0 g of food samples were weighed and dispersed in 5 mL of diluent solution (50% acetonitrile). The sample solution was vortexed for 1 min, and followed by 10 min sonication. After that, the solution was centrifuged for 5 min at 2600 g rotational centrifugation force (RCF) to discard the undissolved matter. Then, the upper solution layer (1 mL) was transferred into Agilent bond Elut QuEChERS. The solution was vortexed until well dispersed and later been centrifuged at 3000 g. A well-defined of two distinct layers of the solution has been observed, 0.22 μm RC syringe filter was used to filter the upper layer of the solution and the solution was transferred into a GC-MS vial for acrylamide analysis.

In GC-MS analysis (for acrylamide), helium gas was used as the mobile phase with 1.4 mL min^{-1} of column gas flow. Besides, the GC sample injector temperature was set

at 200 °C, with split mode ratio of 5.0. In the column oven, a gradient separation mode was used with the initial temperature start at 80 °C. The temperature was gradually ramp to 250 °C with the rate of 10 °C min^{-1}. The ion mass scan range was set at 35 to 500 m/z with the ion source temperature at 200 °C. The acrylamide peak was identified at retention time of 9.37 min, with target ion mass at 71 (parent ion) and qualify ion mass at 44.

3.11 Analytical performance of developed electrochemical immunosensor in real food samples

Three types of food samples (coffee, coco and prune juice) were selected for the real food analysis and were purchased from a local supermarket. The dissolving or diluting of food samples in PBS was the only sample preparation step for electrochemical immunosensor detection. 2 g of coffee powder was dissolved in 10 mL of PBS and repeated the similar procedures for coco powder. While 2 mL of prune juice was diluted to a total volume of 10 mL with PBS at pH 7.4. Each food sample was aliquoted to five vials and the food samples were spiked with 10 μg mL^{-1} of acrylamide to the final volume of 3 mL. Standard addition method was used by spiking different volume of acrylamide to each vial of the sample solution, which were 0, 10, 20, 30 and 40 μL, respectively. The standard addition was performed for triplicates for each concentration. The changes in resistivity was determined by using EIS method, tested before and after the exposure of electrode surface to food samples. A linear standard addition graph with difference in resistivity against the concentration of acrylamide was plotted for the determination of the unknown concentration of acrylamide presence in food samples. On the other hand, the recovery test was carried out by adding the food samples with three different concentration of acrylamide solutions (40, 80, 120 ng mL^{-1} for coffee and coco samples, 400, 800, 1200 ng mL^{-1} for prune juice).

CHAPTER 4: RESULTS AND DISCUSSION

4.1 Surface characterization of the immunosensor modified interface

4.1.1 Electrochemical characterization of fabricated electrode surface using CV

CV is the most commonly used electrochemical characterization method for monitoring the feature of the fabricated electrode surface. This technique was selected to investigate the electrochemical properties after each modification step. Figure 4.1 shows the CV curves of the step-wise surface characterization of modified working electrode. In order to allow the CV curves shown in Figure 4.1 to be clearly distinguished, the corresponding zoom of Figure 4.1 is shown in Figure 4.2 (a) and (b).

A couple of distinct and well-defined $[Fe(CN)_6]^{3-/4-}$ redox peaks can be clearly seen in Figure 4.1 (i). The bare glassy carbon plate has the maximum redox peak (blue curve) was attributed to the high electron transfer capability of the clean bare electrode. After electrode surface modification with the mixed layer of diazonium salt consisting 1,4-phenylenediamine and 4-nitroaniline, this has significantly reduced the peak current and hence indicating the diazonium salt mixed layer has prevented the access of $[Fe(CN)_6]^{3-/4-}$ redox species to glassy carbon plate electrode surface. This also means that the aryl diazonium salt modification layer could reduce the electron transfer rate across the working electrode surface. After the modification of AuNPs on glassy carbon plate through the covalent binding with amino-phenyl group (surface 2), the peak current increased dramatically as shown in Figure 4.1(iii) indicating the AuNPs may accelerate the transportation of electron (Liu et al., 2011). The modification of AuNPs on glassy carbon plate electrode surface not only has increased the total surface area of electrode for the immobilization of biorecognition molecules, but also has increased the electronic coupling between redox active species and transducer surface attributed to its good electron transfer ability (Pingarrón et al., 2008; Shein et al., 2009). When (2-[2-(2-methoxyethoxy)ethoxy]acetic acid) anti-fouling agent has been modified on the glassy

carbon plate surface and formed surface 3, the peak current was found decreased obviously (refer to Figure 4.1 iv). The CV curve showed the modification of organic layer on the electrode surface has hindered the electron transfer of redox active species, therefore resulting a reduction in the faradaic peak. As shown in Figure 4.2 from surface 4 to 6, the peak current was decreasing after the multiple surface modifications which should be due to the blocking effect of modification layers and consequently decreased the electron transfer rate. After the free acrylamide was introduced to the immunosensor surface and with the aid of electro-pulsion effect, an increment in peak current has been observed indicating the dissociation of the surface bound antibody from hapten (Figure 4.2 b viii). Since the reduction and oxidation peak from surface 4 to surface 7 were not significantly observed in curved CV, the EIS approach was chosen as an alternative way of investigating and checking each modification layer on the surface of the electrodes.

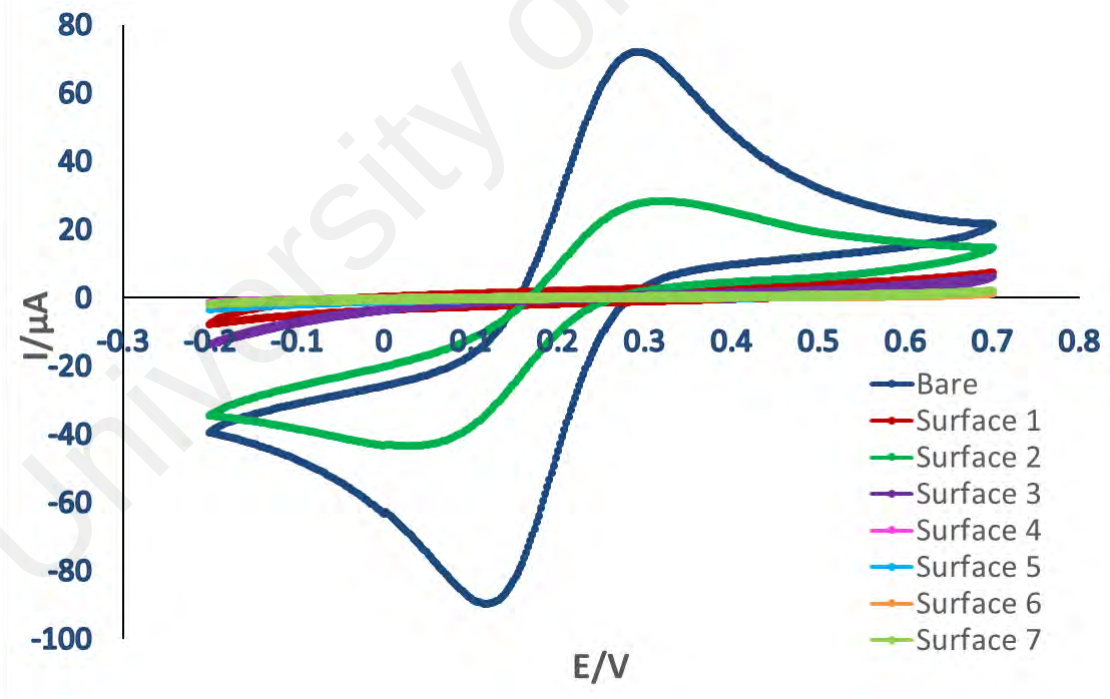

Figure 4.1: Surface characterization of glassy carbon plate using CV. The cyclic voltammograms of: (i) bare electrode (blue), (ii) surface 1 (red), (iii) surface 2 (green), (iv) surface 3 (purple), (v) surface 4 (pink), (vi) surface 5 (light blue), (vii) surface 6 (orange), and (viii) surface 7 (light green).

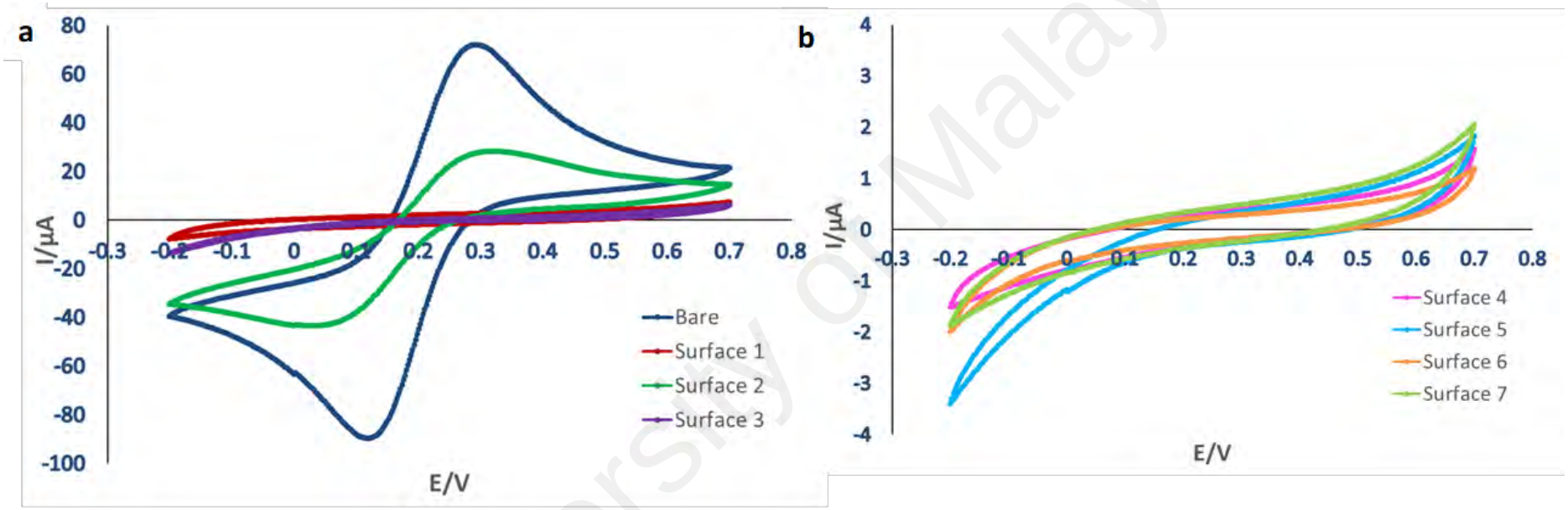

Figure 4.2: (a) Corresponding zoom of Figure 4.1 − Cyclic voltammograms of: (i) bare electrode (blue), (ii) surface 1 (red), (iii) surface 2 (green) and (iv) surface 3 (purple), (b) Corresponding zoom of Figure 4.1 − Cyclic voltammograms of: (v) surface 4 (pink), (vi) surface 5 (light blue), (vii) surface 6 (orange), and (viii) surface 7 (light green).

4.1.2 Electrochemical characterization of fabricated electrode surface using EIS

EIS analysis is a useful tool to investigate the step-wise interfacial properties of the electrode surface. The obtained Nyquist plots of each fabricated surface are shown in Figure 4.3. By fitting the Nyquist plot to an equivalent electric circuit (inset in Figure 4.3), the value of each parameter is given in Table 4.1. The electric circuit consisted the parameters of resistance of the electrolyte/solution (R_s), in series with the double layer capacitance (C_{dl}) and the resistance of charge-transfer (R_{ct}). R_s was representing the solution resistance between the reference electrode and the working electrode. The resistance of an ionic solution is mainly depending on the ionic concentration, the ions type, the temperature and the geometry of the area which current is carried (namely the distance of the cross-sectional area of solution linked to electrode surface and the electrode) are factors that affecting the reading of R_s (Khoo et al., 2016). Unfortunately, a uniform current distribution through a definite electrolyte area could not be achieved for most electrochemical cells. Therefore, the R_s is usually determined by the geometry of media (electrolyte) that carries the current and the current flow path (Lvovich, 2012). In short, the differ in R_s values taken in Table 4.1 is observed not be altered by the stepwise electrode surface modifications

C_{dl} and R_{ct} are the parameters related to the double layer and insulating properties at the electrode/electrolyte interface. Therefore, the varying in values of these two elements could be affected by the modification of electrode surface. Due to the deformation and broadening of the semicircle Nyquist plot, a normal Randles equivalent circuit could not be fitted in. The deformation of impedance semicircle might be attributed to the roughness of the electrode-electrolyte interfaces or the inhomogeneity in the local distribution of defects in the vicinity of grain boundaries (Abouzari et al., 2009). However, after the experiment study, Abouzari et al. (2009) suggested that the deformation of impedance semicircle was mostly influenced by the presence of ionic charge carriers instead of the

interface roughness. Therefore, this problem can be solved using a parallel connection of an ohmic resistor (R_{ct}) and a constant phase element (CPE). For CPE, Q is the pre-factor of the CPE, and n is its exponent. The n value of CPE may vary between 0 to 1. When n = 1, the CPE was described as an ideal capacitor whereby Q = C_{dl}. For n < 1, the C_{dl} has to be calculated using the equation follows:

$$C_{dl} = R_{ct}^{\frac{1-n}{n}} . Q^{\frac{1}{n}} \quad (4.1)$$

The calculated value of C_{dl} for each fabricated layer on the working electrode is shown in Table 4.1 (from bare glassy carbon plate to surface 7). From Table 4.1, as C_{dl} value did not show significant change as compared to R_{ct}, thus the value of R_{ct} was selected as the parameter to determine each fabricated step made on the electrode surface. Additionally, the value of n is related to the defection of the modification layer being modified on the electrode surface (Khoo et al., 2016). As observed, the values of n in Table 4.1 were close to 1, indicating the low deficiency of glassy carbon plate surface after the stepwise fabrication.

As referred in Table 4.1, after the electrochemical reduction modification of diazonium salt, the aryl diazonium salt layer has resisted the redox active species from accessing the electrode surface and consequently increase the value of R_{ct}. A significant decreased in R_{ct} has been noted after the modification of AuNPs on the electrode. This indicated the AuNPs showed an electron conducting properties that could act as an electron mediator which accelerate the electron transfer rate between $[Fe(CN)_6]^{3-/4-}$ and electrode surface. Hence, causing a decrease in R_{ct} value and reduced in resistivity of the electrode surface. An expected increase in R_{ct} values from surface 3 to surface 6 have been observed as shown in Table 4.1. This was due to the increased in modification layers that have blocked the assessment of redox active species from reaching the electrode surface and give raised to the charge-transfer resistance, consequently increased the value of R_{ct}. For surface 7,

after free acrylamide was added, R_{ct} showed a decreased in resistivity, which was suggested that the displacement assay has been successfully occurred upon the dissociation of surface bound antibody from hapten. The EIS analysis has showed a good correlation with the CV obtained from Section 4.1.1, in which the current peak decreased as the impedance/resistivity increased.

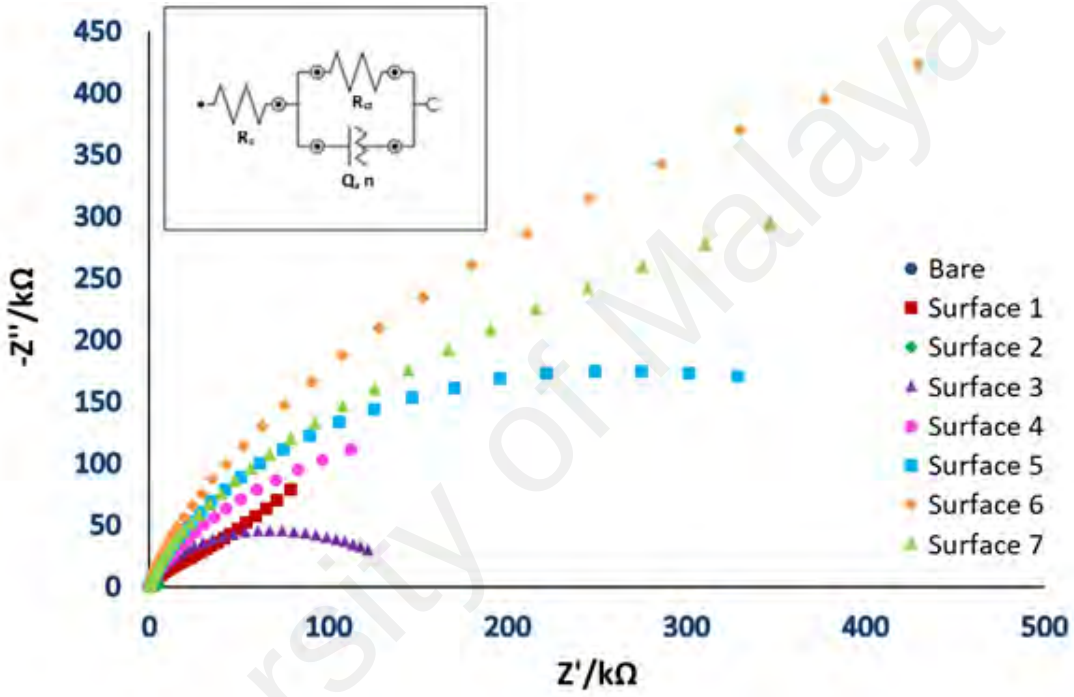

Figure 4.3: Surface characterization of glassy carbon plate using EIS analysis, and the Nyquist plots recorded for impedance measurement of: (i) bare electrode (blue), (ii) surface 1 (red), (iii) surface 2 (green), (iv) surface 3 (purple), (v) surface 4 (pink), (vi) surface 5 (light blue), (vii) surface 6 (orange), and (viii) surface 7 (light green). Inset: Equivalent circuit fitted to Nyquist plot.

Table 4.1: The equivalent circuit parameters values of fitting curves for each interface of fabricated electrochemical impedance immunosensor by NOVA software.

Electrode	R_s/Ω	R_{ct}/Ω	Q/Mh_o	n	C_{dl}/F
Bare GCP	16.496	9.252×10^{2}	2.576×10^{-6}	0.779	8.903×10^{-5}
Surface 1 (Ph-NH_2:Ph-NO_2/GCP)	13.219	1.056×10^{5}	4.778×10^{-6}	0.774	3.914×10^{-6}
Surface 2 (AuNPs/Ph-NH_2:Ph-NO_2/GCP)	36.095	2.785×10^{3}	5.747×10^{-6}	0.740	1.343×10^{-6}
Surface 3 (Antifouling/AuNPs/Ph-NH_2:Ph-NO_2/GCP)	15.911	1.235×10^{5}	1.975×10^{-6}	0.826	1.468×10^{-6}
Surface 4 (Ph-NH_2/Antifouling/AuNPs/Ph-NH_2:Ph-NO_2/GCP)	43.067	2.280×10^{5}	5.818×10^{-6}	0.843	6.133×10^{-6}
Surface 5 (Hapten/Ph-NH_2/Antifouling/AuNPs/Ph-NH_2:Ph-NO_2/GCP)	28.296	4.207×10^{5}	1.550×10^{-6}	0.845	1.433×10^{-6}
Surface 6 (Antibody/Hapten/Ph-NH_2/Antifouling/AuNPs/Ph-NH_2:Ph-NO_2/GCP)	24.467	7.604×10^{5}	1.251×10^{-6}	0.886	1.244×10^{-6}
Surface 7 (Hapten/Ph-NH_2/Antifouling/AuNPs/Ph-NH_2:Ph-NO_2/GCP)	18.947	5.129×10^{5}	1.417×10^{-6}	0.855	1.343×10^{-6}

GCP = Glassy carbon plate, Ph-NH_2 = 1,4-phenylenediamine, Ph-NO_2 = 4-nitroaniline

4.1.3 Surface characterization of AuNPs modification on electrode surface using FE-SEM

FESEM method was used to analyse the attachment of AuNPs onto the electrode surface (surface 2). Figure 4.4 (a) shows the FE-SEM image of the bare glassy carbon plate surface and illustrated a smooth black electrode surface without any residues deposited. After the attachment of AuNPs as shown in Figure 4.4 (b), bright white dots were clearly seen and the white dots were further analysed by using the EDX analysis. As referred in EDX spectrum shown in Figure 4.5 (a), Au element was observed and confirmed that the electrode surface has been successfully decorated with AuNPs. In addition, peaks assigned for carbon (C), nitrogen (N) and oxygen (O) elements were attributed to the aryl diazonium salt group that been modified on the electrode surface in previous surface modification step (surface 1). As shown in FE-SEM image (Figure 4.4 b), AuNPs were uniformly distributed on the surface of glassy carbon plate which could provide binding sites for 2-[2-(2-methoxyethoxy)ethoxy]acetic acid (the antifouling agent). The density of AuNPs was calculated as 4.29×10^8 cm^{-2} with n = 3 and the calculations were attached in Appendix.

Moreover, the average size of deposited AuNPs was measured from the FE-SEM zoom-in image displayed in Figure 4.5 (b). The AuNPs were approximately 20 nm in diameter and were all in spherical shape. The FE-SEM image was further processed with ImageJ digital image processing software to measure the average diameter of AuNPs distributed on the glassy carbon electrode. The average particles size of AuNPs was calculated as 18 nm using ImageJ based on 297 AuNPs in total. The size distribution of AuNPs on the electrode surface was mostly at 20 nm as shown in Figure 4.5 (c). The result obtained from ImageJ agreed relatively well with FE-SEM technique, indicating the modification step of AuNPs did not make significant changes or influences on the original size of AuNPs.

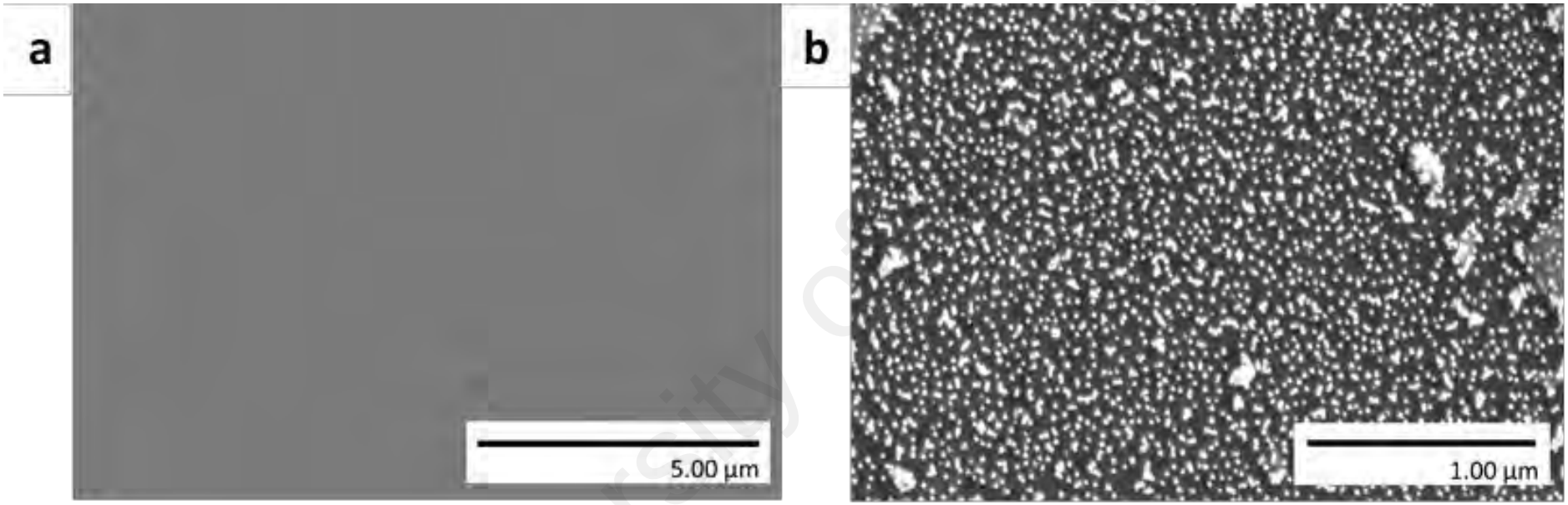

Figure 4.4: Surface characterization of glassy carbon plate using FE-SEM. The FE-SEM images of (a) bare glassy carbon plate with a magnification of 10 k, (b) surface 2 with 40 k of magnification.

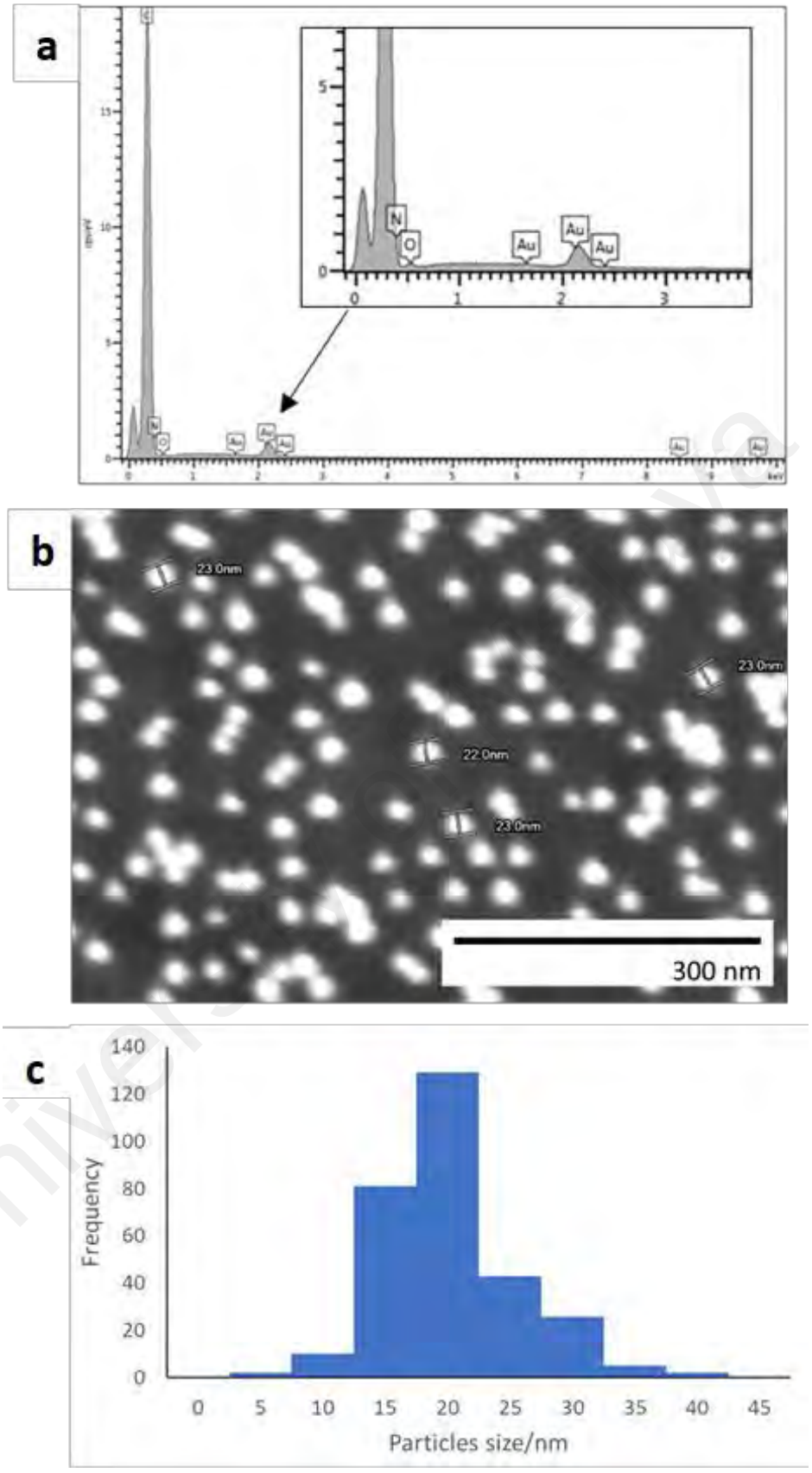

Figure 4.5: (a) EDX spectrum of surface 2, (b) Diameter of AuNPs measured by FE-SEM, (c) Size distribution of AuNPs calculated using ImageJ software and plotted with histogram.

4.1.4 Surface characterization of fabricated electrode surface using FT-IR

The FT-IR analytical technique was applied to analyse the functional group on the electrode surface after each fabrication steps. Figure 4.6 shows the IR spectrum obtained from a bare glassy carbon plate to surface 7. The IR spectrum of fabrication made on surface 1 showed the presence of nitro group at the region approximately 1404 cm^{-1}, aromatic group at 1616 cm^{-1}, and amino group at 3401 cm^{-1}. This suggested the mixed layer of aryl-diazonium salt containing 4-nitroaniline and 1,4-phenylenediamine have been successfully modified onto the glassy carbon plate surface via the electrochemical reduction process. The AuNPs attachment in the modification of surface 2 caused the NH_2 stretching disappeared, indicating AuNPs were bind to amino-phenyl group rather than nitro-phenyl group. Nevertheless, the nitro and aromatic group bands were still can be observed in IR spectrum similar as in surface 1. The presence of a significant peak of N-H stretching at the region of 3327 cm^{-1} and C=O stretching at 1625 cm^{-1} on surface 3 could represent the modification of the 2-[2-(2-methoxyethoxy)ethoxy]acetic acid antifouling agent on the electrode. This explained an amide covalent bond has been formed between a reaction of the amino-phenyl group (resultant from the reduction of nitro-phenyl) and the COOH group of 2-[2-(2-methoxyethoxy)ethoxy]acetic acid. Furthermore, the appearance of stretching band observed at the region between 1000 – 1300 cm^{-1} was attributed to the stretching vibration of C-O in ether group presented in the antifouling agent. For IR spectrum of surface 4, the occurrence of peak approximately at approximately 3747 cm^{-1} was assigned to the amine group after the modification of 1,4-phenylenediamine on AuNPs. In addition, the stretching vibration of aromatic group, N-H, C=O and C-O group from previous fabrication steps still occurred in the IR spectrum of surface 4. Surface 5 involved the surface bound hapten modification on the electrode surface and resulted the increasing peak of NH_2 stretching band at 3678 cm^{-1}, indicating the successful immobilization of hapten on glassy carbon plate. Other than that,

no significant change of IR spectrum could be observed for others functional group stretching. The IR spectrum for surface 6 and 7 showed a similar stretching as in surface 5, where appearance of NH_2 stretching at 3683 cm^{-1}, N-H stretching at 3324 cm^{-1}, C=O stretching at 1582 cm^{-1}, ether group stretching vibration at between 1300 – 1000 cm^{-1}, aromatic group C-H stretching band at 2969 – 2821 cm^{-1} and aromatic C-C stretching region at approximate 1567 – 1437 cm^{-1}. This was due to the immobilization of antibody on the electrode surface and antibody is a complicated structure which consists of multiple functional groups, causing the IR spectra difficult to be assigned for a certain specific band. However, even after a strong negative electro-pulsion at -800 mV for 10 min, the step-wise surface modification layers were remained attached on the electrode surface and indirectly indicated the strong and stable interfacial design of immunosensor.

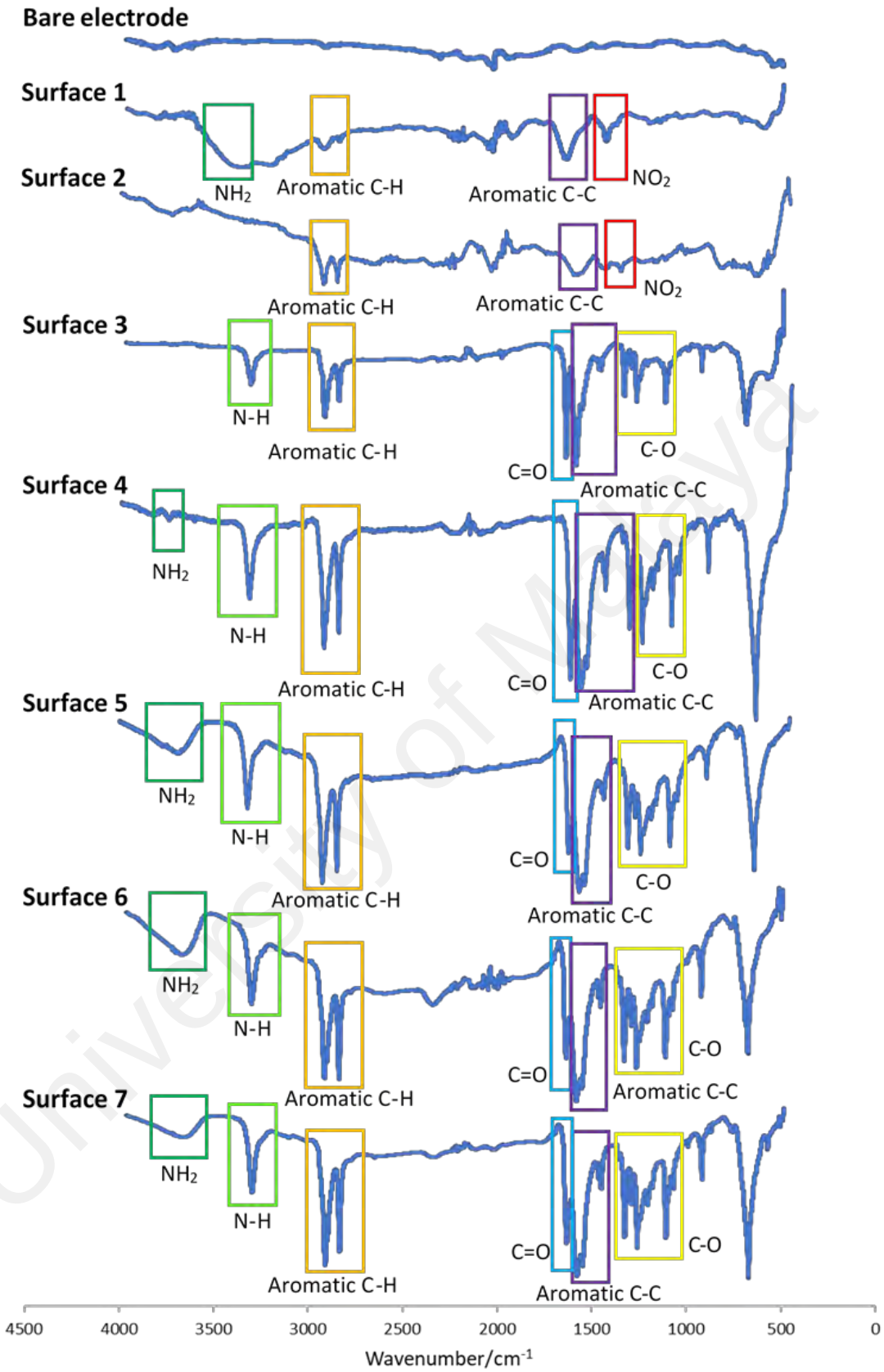

Figure 4.6: Surface characterization of fabrication step on glassy carbon plate using FT-IR. The FT-IR spectra from bare glassy carbon plate to surface 7 [NH_2 (green), amide N-H (light green), aromatic C-H (orange), C=O (light blue), aromatic C-C (purple), ether C-O (yellow) and NO_2 (red)].

4.2 Optimization of a displacement assay conditions for dissociation of surface bound antibody

4.2.1 Dissociation of surface bound antibody from surface bound hapten via a displacement assay

This assessment was conducted to demonstrate the dissociation of antibody via a displacement assay which was mainly due to the presence of free acrylamide. The fabricated glassy carbon electrode was exposed with free arylamide solutions and after incubation for a period of time, the difference in resistivity is displayed in Figure 4.7. The resultant decrease in resistivity was increased from 5 min to 15 min of incubation. This indicated the acrylamide antibody exhibited a higher binding affinity towards free acrylamide as compared to hapten, and consequently caused a dissociation of antibody from the surface bound hapten. After 20 min of incubation, the decrease in resistivity did not show a significant enhancement in the dissociation of antibody and subsequently showed an increasing in resistivity after incubation for 60 min. This could be caused by the strength of binding affinity between the antibody and hapten after long time of incubation. The binding force between the antibody and hapten increases as the incubation period rises, which allows the antibody to hardly dissociate from the hapten attached to the surface. On the other hand, the binding force between an antibody and hapten was not too high within 15 to 20 min of incubation time and therefore permitted the dissociation of the surface bound antibody. Hence, for the displacement assay to be taken place, the immunosensor interface should be incubated in free acrylamide for 15 min.

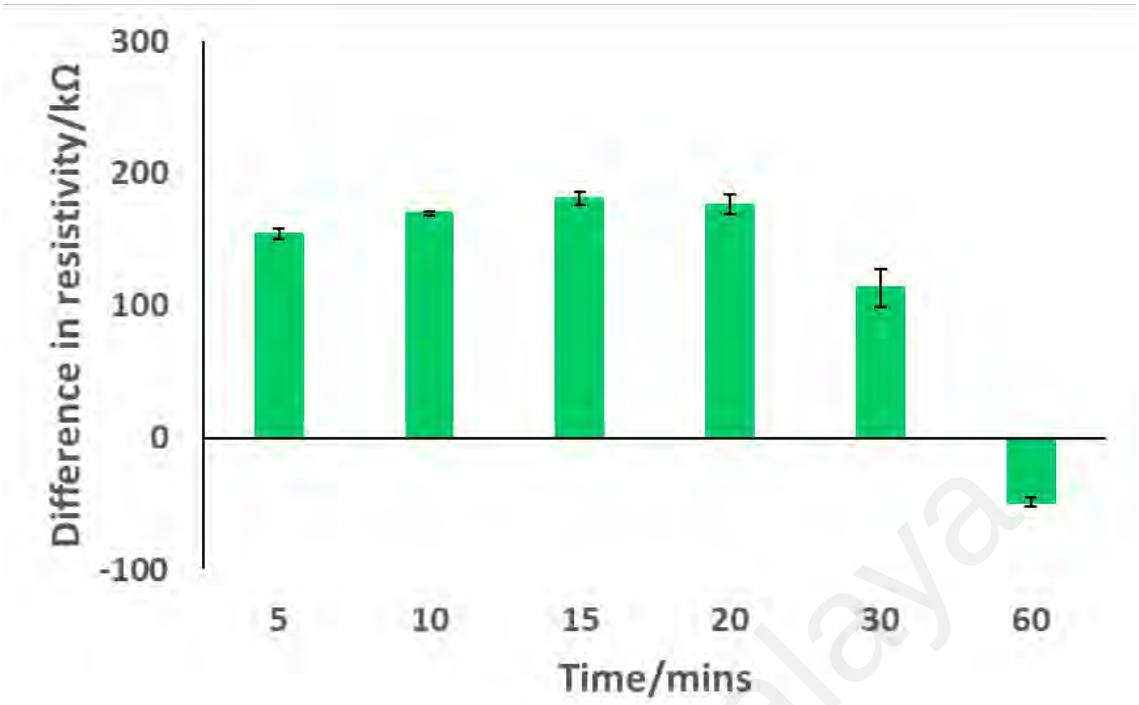

Figure 4.7: The dissociation of antibody from surface bound hapten after 5, 10, 15, 20, 30, and 60 min of incubation in 30 μg mL^{-1} of free acrylamide solution.

4.2.2 An enhancement of dissociation of antibody from the surface bound hapten with the aid of electro-pulsion for the occurrence of a displacement assay

The optimization study on the dissociation of surface bound antibody via a displacement assay was carried out by varying the pulsing potentials and pulsing durations, the tested pulsing conditions are illustrated in Figure 4.8. Electro-pulsion at -800 mV with pulsing duration of 10 min was determined as the optimal conditions. This is because the immunosensor achieved the highest decrease in resistivity after electro-pulsion of -800 mV for 10 min. The value of changes in resistivity (R_{ct}) is defined as the decrease in resistivity before R_{ct} (x) and after R_{ct} (y) the surface bound antibody being dissociated from the electrode surface ($R_{ct} = R_{ct}$ (x) – R_{ct} (y)). However, at a lower pulsing potential (at -700 mV) did not show any enhancement of dissociation of antibody. By pulsing the electrode at -900 mV also did not illustrate any significant difference in resistivity. Furthermore, an extended pulsing duration (pulsed for 15 min) or shorten of

the pulsing duration from 10 min (pulsed the electrode for 5 min) even have a lower decrement in resistivity. As compared to Section 4.2.1 (Figure 4.7), the difference in resistivity in Figure 4.8 shows a greater decrease in resistivity, showing that the electro-pulsing effect has improved the dissociation rate of surface bound antibody by extensively decreased the time taken for a displacement assay (from 15 min to 10 min) as well as amplified the amount of antibody been dissociated (increased the difference of resistivity). Based on the optimization study (Figure 4.8), the cathodic pulsion has caused dissociation of antibody. Conversely, the use of anodic pulsion caused adsorption and the resistivity increased. The dissociation of antibody could cause by the electrostatic force during pulsion (Khoo et al., 2016) or due to the presence of carboxylate group ($-COO^-$) in antibody protein structure. Thus, the negatively charged protein preferred to interact with anodic charged electrode surface (Omanovic & Roscoe, 1999) and vice versa in cathodic pulsed electrode. Another possible reason that caused the dissociation of antibody was due to the isoelectric point (pI) of antibody. When the pH of environment lower than pI, the antibody protein carried a net positive charge and reversely antibody carried a negative charge if the pH of the surrounding environment was higher than pI. The previous studies reported by Khoo et al. (2016) and Khor et al. (2011) used IgG antibody and the IgG antibody showed a dissociation during the negative electro-pulsion (Khoo et al., 2016; Khor et al., 2011). Interestingly, the IgY antibody applied in the current study has a slightly lower pI value range as compared to IgG antibody (Dávalos-Pantoja et al., 2000), where IgY's pI value range was 5.7–7.6 while IgG was within 6.1–8.5. Therefore, at the similar neutral condition (pH 7.4), IgY antibody could demonstrated an expected dissociation when electrode was pulsed with a negative charge. Since the acrylamide IgY antibody repelled negatively charged electrode surface and preferred binds to the positive charge, thus this indicates that the net charge of anti-acrylamide antibody was suggested to be negative in PBS at pH 7.4.

The control experiment with the absence of free acrylamide is displayed in Figure 4.9. The resistivity changes were hard to be observed in Figure 4.9 (a) and (b) without the presence of free acrylamide in PBS solution. These observations submitted an evidence that the dissociation of surface bound antibody from surface bound hapten on electrode was critically dependence on the presence of free acrylamide. In addition, the aid of negative electro-pulsion on electrode has shown an enhancement on the dissociation rate of surface bound antibody and also maximized the amount of dissociated antibody from surface bound hapten.

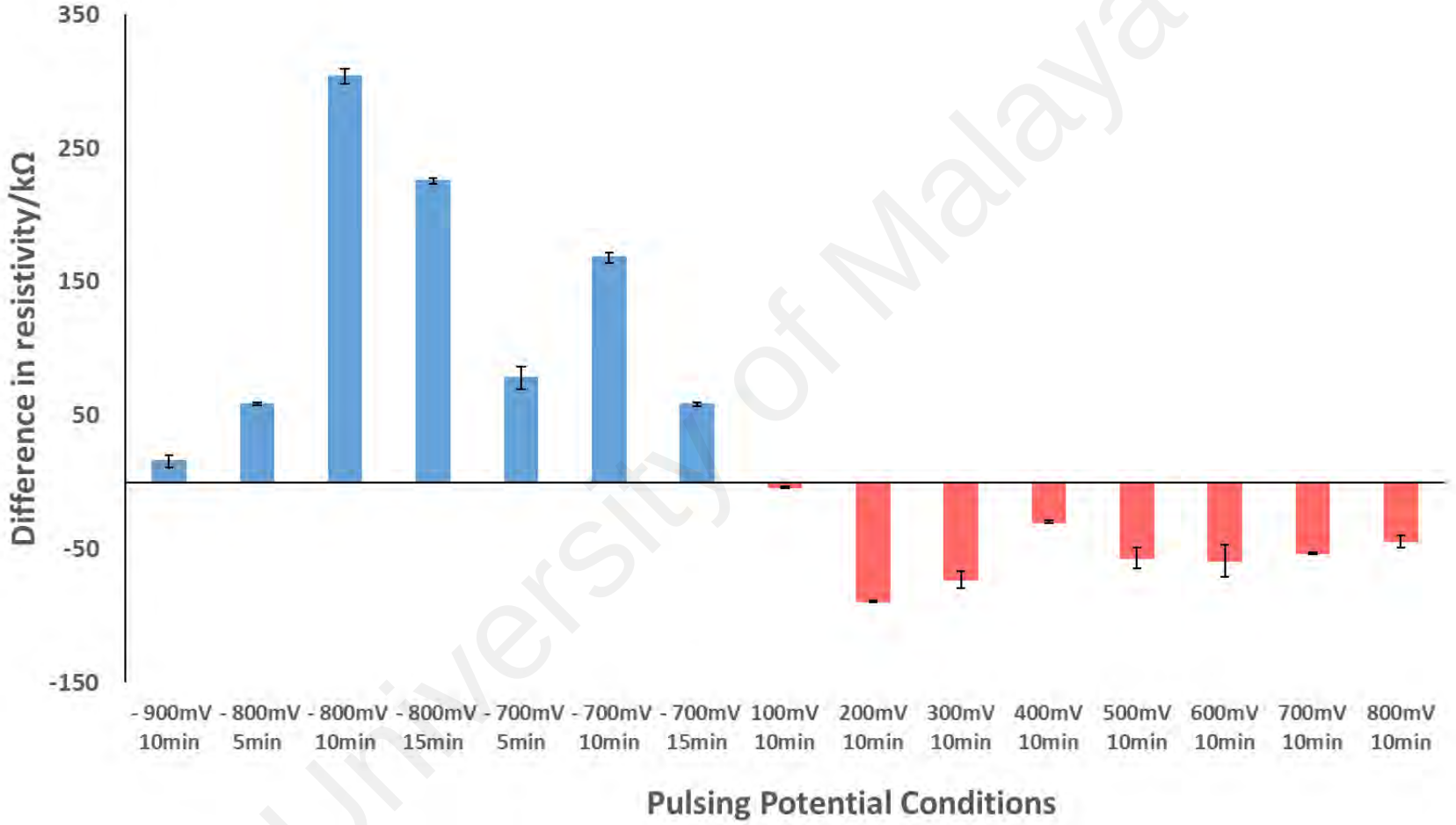

Figure 4.8: The optimization of electro-pulsing conditions for maximum dissociation of antibody from surface bond hapten demonstrated on fabricated electrode surface at different pulsing potentials and varying pulsing durations.

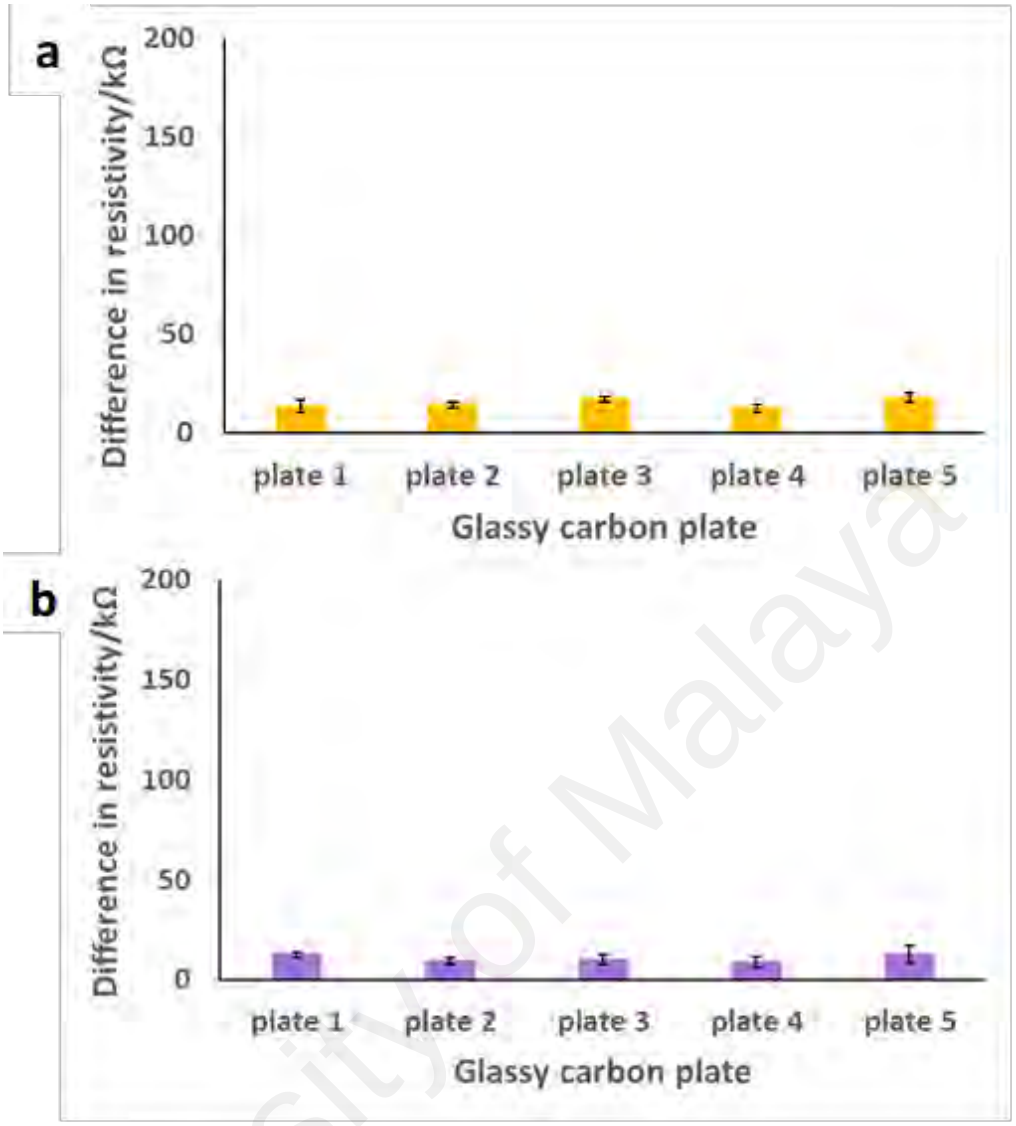

Figure 4.9: The optimization study on dissociation of surface bound antibody from hapten without the presence of free acrylamide. (a) Decrease in resistivity after electro-pulsion of -800 mV for 10 min in PBS at pH 7.4, (b) Decrease in resistivity after incubation in PBS at pH 7.4 without electro-pulsion.

4.2.3 Box-Behnken experimental design

The effect of pulsing potential, pulsing duration and concentration of acrylamide were investigated simultaneously by applying the Box-Behnken design under response surface methodology using Design Expert software and the optimal conditions were determined to achieve the maximum response (difference in resistivity). The optimal conditions predicted from this statistical study was then compared to the conditions obtained from the experimental study (Section 4.2.2).

4.2.3.1 Box Behnken analysis

The experiments were performed with different combinations of factors and the measured response using statistically design experiments suggested by the Box-Behnken design. The experiment combinations consisted of 17 trails as shown in Table 4.2. The linear, the interaction of two factors (2FI), quadratic and cubic models were fitted to the experimental data to obtain the regression equations. Three tests were carried out including the lack of fit test as shown in Table 4.3, model summary statistics as given in Table 4.4 and the sequential model sum of squares as displayed in Table 4.5, in order to determine the acceptability of fitness of these models with respect to the difference in resistivity. The model summary statistics (Table 4.4) indicated that the cubic model was found to be aliased and therefore has been excluded. On the other hand, the p-value for the quadratic model was only 0.0007 (Table 4.5), where p-value < 0.05 indicated the significance of the model. In table 4.3, the lack of fit test was found insignificant for the selected model. The p-value of 0.0455 for quadratic model was the highest value among all the tested models and explained this model was suggested to describe the experimental data. Therefore, the quadratic model was selected as the most suitable model to be fitted and applied for further analysis.

Table 4.2: Box-Behnken experimental design for three factors used in the displacement condition and response.

Run	Factor 1	Factor 2	Factor 3	Response 1
	A: Pulsing Duration/min	B: Pulsing Potential/mV	C: Concentration of Acrylamide/ μg mL^{-1}	Difference in resistivity/kΩ
1	10	-700	30	161.65
2	5	-800	30	58.67
3	10	-900	30	113.5
4	10	-800	15	163.06
5	5	-800	0	15.2276
6	10	-800	15	187.35
7	10	-900	0	12.1243
8	10	-700	0	12.008
9	15	-900	15	95.176
10	5	-900	15	69.55
11	15	-700	15	64.044
12	10	-800	15	166.96
13	5	-700	15	45.804
14	10	-800	15	187.117
15	15	-800	0	15.4522
16	10	-800	15	164.14
17	15	-800	30	225.812

Table 4.3: Lack of fit tests.

Source	Sum of Squares	df	Mean Square	F-value	p-value	Remark
Linear	46042.79	9	5115.87	33.20	0.0021	-
2FI	38481.39	6	6413.57	41.62	0.0015	-
Quadratic	**3231.37**	**3**	**1077.12**	**6.99**	**0.0455**	**Suggested**
Cubic	0.0000	0	-	-	-	Aliased
Pure Error	616.37	4	154.09	-	-	-

Table 4.4: Model summary statistics.

Source	Std. Dev.	R^2	Adjusted R^2	Predicted R^2	PRESS	Remark
Linear	59.91	0.4452	0.3171	0.1293	73222.23	-
2FI	62.53	0.5351	0.2561	-0.1801	99246.35	-
Quadratic	**23.45**	**0.9542**	**0.8954**	**0.3738**	**52665.01**	**Suggested**
Cubic	12.41	0.9927	0.9707	-	-	Aliased

Table 4.5: Sequential model sum of squares.

Source	Sum of Squares	df	Mean Square	F-value	p-value	Remark
Mean	1.817E+05	1	1.817E+05	-	-	-
Linear	37438.65	3	12479.55	3.48	0.0475	-
2FI	7561.40	3	2520.47	0.6447	0.6038	-
Quadratic	**35250.02**	**3**	**11750.01**	**21.38**	**0.0007**	**Suggested**
Cubic	3231.37	3	1077.12	6.99	0.0455	Aliased
Residual	616.37	4	154.09	-	-	-
Total	2.658E+05	17	15636.61	-	-	-

4.2.3.2 Fitting the second-order polynomial equation and statistical analysis

The quadratic response model can be described as polynomial equation as follow:

$$Y = \beta_0 + \beta_1 x_1 + \beta_2 x_2 + \beta_3 x_3 + \beta_{12} x_1 x_2 + \beta_{13} x_1 x_3 + \beta_{23} x_2 x_3 + \beta_{11} x_1^2 + \beta_{22} x_2^2 + \beta_{33} x_3^2 \quad (4.2)$$

where Y is the predicted response; β_0 is the constant; β_1, β_2 and β_3 are the coefficient of the linear parameters; β_{12}, β_{13} and β_{23} are the coefficient of the interaction parameters; β_{11}, β_{22} and β_{33} are the coefficient of the quadratic parameters; and x_1, x_2 and x_3 are the variables.

The following second-order polynomial equation was obtained from the basis of Box–Behnken experimental design model and was applied in the actual term generated for the resistivity changes in the displacement assay:

Difference in resistivity = – 3668.81923 + 34.42536 × Pulsing Duration – 8.81643 × Pulsing Potential + 10.99562 × Concentration of Acrylamide – 0.003693 × Pulsing Duration × Pulsing Potential + 0.556391 × Pulsing Duration × Concentration of Acrylamide + 0.008044 × Pulsing Potential × Concentration of Acrylamide – 2.02224 × Pulsing Duration^2 – 0.005453 × Pulsing Potential^2 – 0.197240 × Concentration of Acrylamide^2

This equation was applied for the prediction of resistivity difference by providing the values of each factor (pulsing duration, pulsing potential and concentration of acrylamide) which is an applicable way to reduce chemicals used and time saving.

The analysis of variance (ANOVA) result for a displacement assay is listed in Table 4.6. The large F-value of the model implies that the variation in the response can be explained by the model and as observed the F-value was 16.22 indicated the model term was significant to the response. Furthermore, the p-value of the model (0.0007) was lower than 0.05 implied the statistical significance of the model. The determined coefficient (R^2

= 0.9542), indicating 95.42% of the variability in the response can be predicted by the model. In addition, the value of predicted R^2 is the measure of the variation in data explained by the model (Kumar et al., 2008). When the difference between predicted R^2 with adjusted R^2 is larger than 0.2, this may due to the possible problem with either the model and/or the data. The adequate precision was measured from the signal to noise ratio, with greater than 4 is desirable and found to be 11.747. This has confirmed that this model was significant for optimizing the displacement assay conditions. Besides, the response was most significantly affected by the factor of concentration of acrylamide with p-value of 0.0001 (< 0.05) and F-value of 57.95, indicating the presence of acrylamide was the dominant factor for a displacement assay to occur. In addition, Figure 4.10 shows the relationship between the predicted and the actual response of difference in resistivity for a displacement assay. The residuals tend to be closed to the diagonal line represented the developed model was sufficient to be applied in present study.

Table 4.6: ANOVA for quadratic model.

Source	Sum of Squares	df	Mean Square	F-value	p-value	Remark
Model	80250.07	9	8916.67	16.22	0.0007	significant
A- Pulsing Duration	5577.40	1	5577.40	10.15	0.0154	-
B- Pulsing Potential	5.86	1	5.86	0.0107	0.9207	-
C-Concentration of Acrylamide	31855.39	1	31855.39	57.95	0.0001	-
AB	13.64	1	13.64	0.0248	0.8793	-
AC	6965.35	1	6965.35	12.67	0.0092	-
BC	582.41	1	582.41	1.06	0.3376	-
A^2	10761.73	1	10761.73	19.58	0.0031	-
B^2	12518.20	1	12518.20	22.77	0.0020	-
C^2	8292.59	1	8292.59	15.09	0.0060	-
Residual	3847.74	7	549.68	-	-	-
Lack of Fit	3231.37	3	1077.12	6.99	0.0455	significant
Pure Error	616.37	4	154.09	-	-	-
Cor Total	84097.81	16	-	-	-	-

$R^2 = 0.9542$, Adjusted $R^2 = 0.8954$, Predicted $R^2 = 0.3738$, Adeq Precision = 11.7470

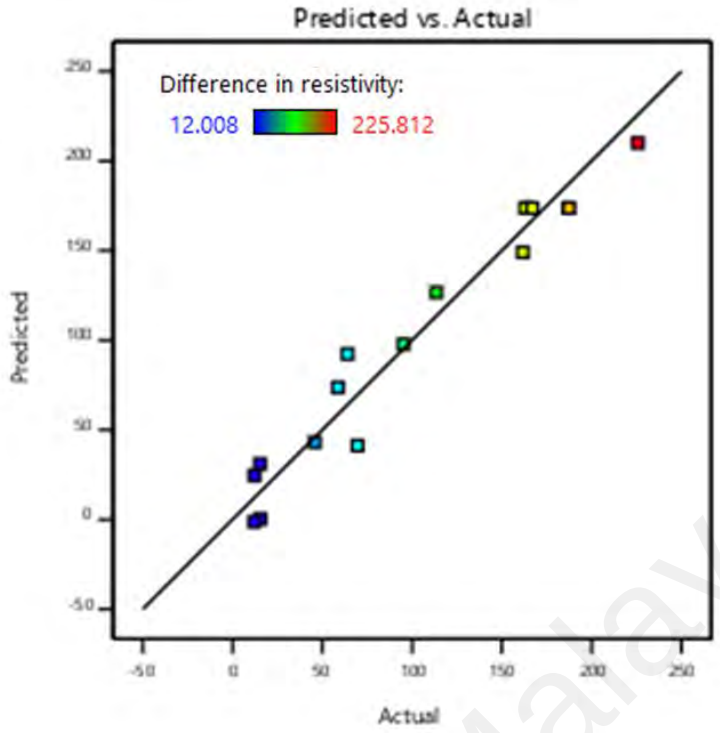

Figure 4.10: Scatter diagram of predicted response versus actual response (analytical response refers to the difference in resistivity) for the displacement assay.

4.2.3.3 Effect of factors on the difference in resistivity

Figure 4.11 shows the respond surface plot for the relationship between pulsing potential, pulsing duration and concentration of acrylamide on the difference in resistivity. All individual factors were found to have their own effect on the response. The effect of pulsing duration and pulsing potential on the difference in resistivity by varying from 5 to 15 min and -700 to -900 mV as shown in Figure 4.11 (a). At fixed pulsing potential, the difference in resistivity increased as the pulsing duration increased from 5 min to 10 min and then the difference in resistivity decreased when the pulsing duration exceed 10 min and above. This indicated that pulsing the electrode for 15 min does not improve the dissociation of antibody. While the pulsing potential exhibited the largest difference in resistivity at approximately -800 mV (Figure 4.11 a and b), indicated pulsing at -800 mV could dissociate the highest amount of surface bound antibody. For the concentration of acrylamide, the difference in resistivity increase with an increase in concentration (Figure

4.11 b and c). This was due to the increased in the concentration of acrylamide can cause more antibody to dissociate from hapten and thus decreased the resistivity, consequently contributed to the quantitative detection ability of the developed immunosensor.

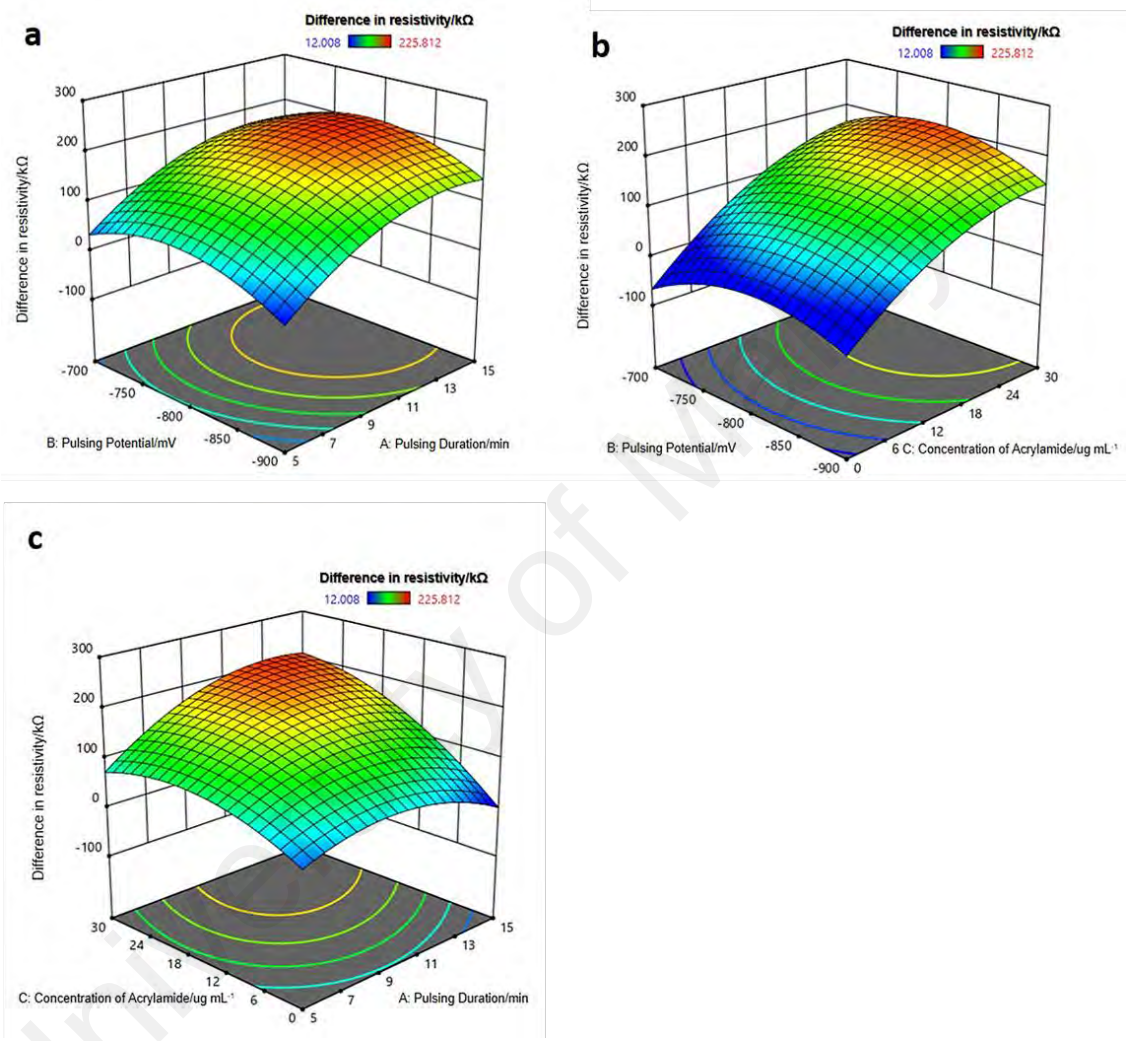

Figure 4.11: The three-dimensional response surface plot demonstrated the effect of factors on response. (a) The effect of pulsing duration and pulsing potential on the difference in resistivity, (b) The effect of pulsing potential and concentration of acrylamide on the difference in resistivity, (c) The effect of pulsing duration and concentration of acrylamide on the difference in resistivity.

4.2.3.4 Desirability function for optimization

The desirability function was the most frequently used method for optimization of the analytical procedure (Ferreira et al., 2007). The scale of desirability function range between 0 to 1. The desirability = 1 represented a fully desired response, while desirability = 0 is for a completely undesirable response. The desirability for a response can be obtained by specifying the goal of the response, with either minimized the response, maximized the response or target the response (Ragonese et al., 2002). In the current study, the maximized respond should be taken to represent the largest difference in resistivity for optimization of displacement assay conditions. When the response was maximized, pulsing at -790.917 mV, for 13.36 min and with the presence of 30 μg mL^{-1} of free acrylamide were determined as the optimal conditions. In Figure 4.12, the overall desirability of 0.953 was obtained. Since the value of desirability was closed to 1, the reflected result generated was favourable. The optimized conditions for a displacement assay based on the Box-Behnken design showed a good correlation with the displacement assay conditions optimized from experimental study. Hence, the electrochemical pulsing with -800 mV for 10 min was applied to all of the experiments for the detection of acrylamide in PBS.

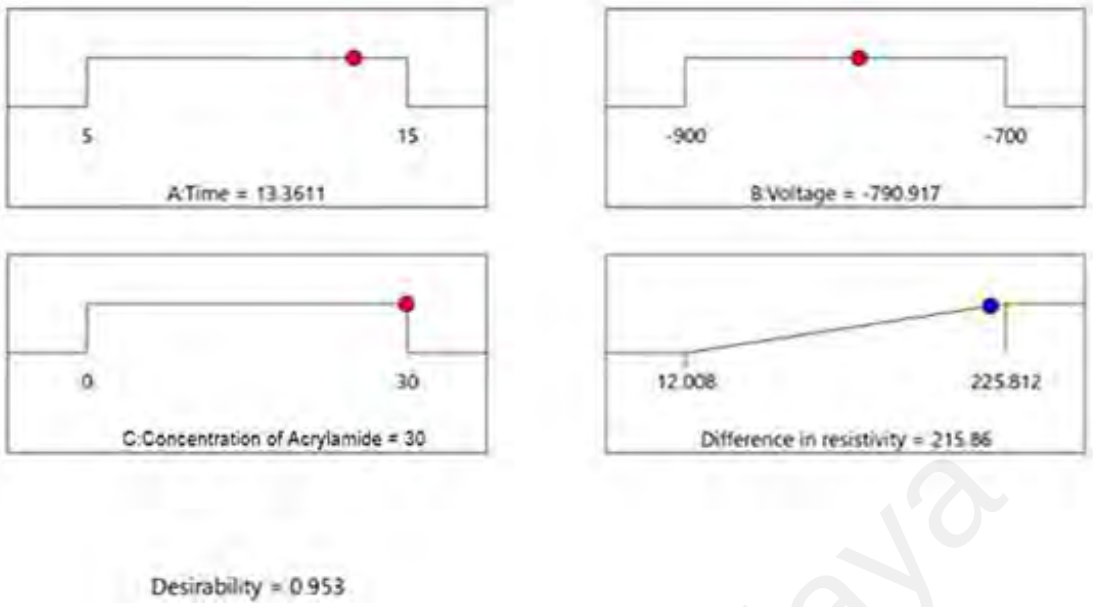

Figure 4.12: Desirability ramp for optimization.

4.3 Quantitative detection of acrylamide using the developed immunosensor

Under the optimized displacement assay conditions, the developed immunosensor was further applied for quantitative detection of acrylamide in PBS. The calibration plot of developed immunosensor showed a good linear relationship between the decrease in resistivity and an increase in the concentration of acrylamide as illustrated in Figure 4.13. The immunosensor surface has been tested in a range of concentration within 5 ng mL^{-1} to 45 µg mL^{-1} of free acrylamide and was plotted as shown in Figure 4.13 (a). As referred in Figure 4.13 (c), a linear relationship between the concentration of acrylamide and difference in resistivity was established in the range of 0.01 to 35.00 µg mL^{-1}. Hence, the immunosensor displayed a linear dynamic range within 0.01 to 35.00 µg mL^{-1}. The LOD and limit of quantification (LOQ) were measured as 3.84 ng mL^{-1} and 2.01 µg mL^{-1}, defined by using the equations 4.3 and 4.4, respectively (Little, 2015).

$$LOB = \text{Mean blank} + 1.645\ SD \quad (4.3)$$

$$LOD = \text{Mean blank} + 3.3\ SD \quad (4.4)$$

$$LOQ = \text{Mean blank} + 10\ SD \quad (4.5)$$

where LOB is the limit of blank and SD is the standard deviation of blank.

The reported dynamic range and LOD in various analytical techniques have been listed in Table 2.2. Compared to the previously reported biosensor, the developed immunosensor showed a narrower dynamic range. However, the developed immunosensor performed a lower LOD when comparing with electrochemical biosensor developed by Asnaashari et al. (2019) with LOD of 11.2 ng mL^{-1} (Asnaashari et al., 2019) and fluorescent sensing method displayed LOD of 35 ng mL^{-1} (Hu et al., 2014). The reason of sensitive detection of fabricated immunosensor was attributed to the AuNPs modification step. AuNPs possess the properties of high surface area to volume ratio, thus has increased the amount of immobilized hapten. Consequently, enhanced the amount of surface bound antibody and thus improved the sensitivity of immunosensor.

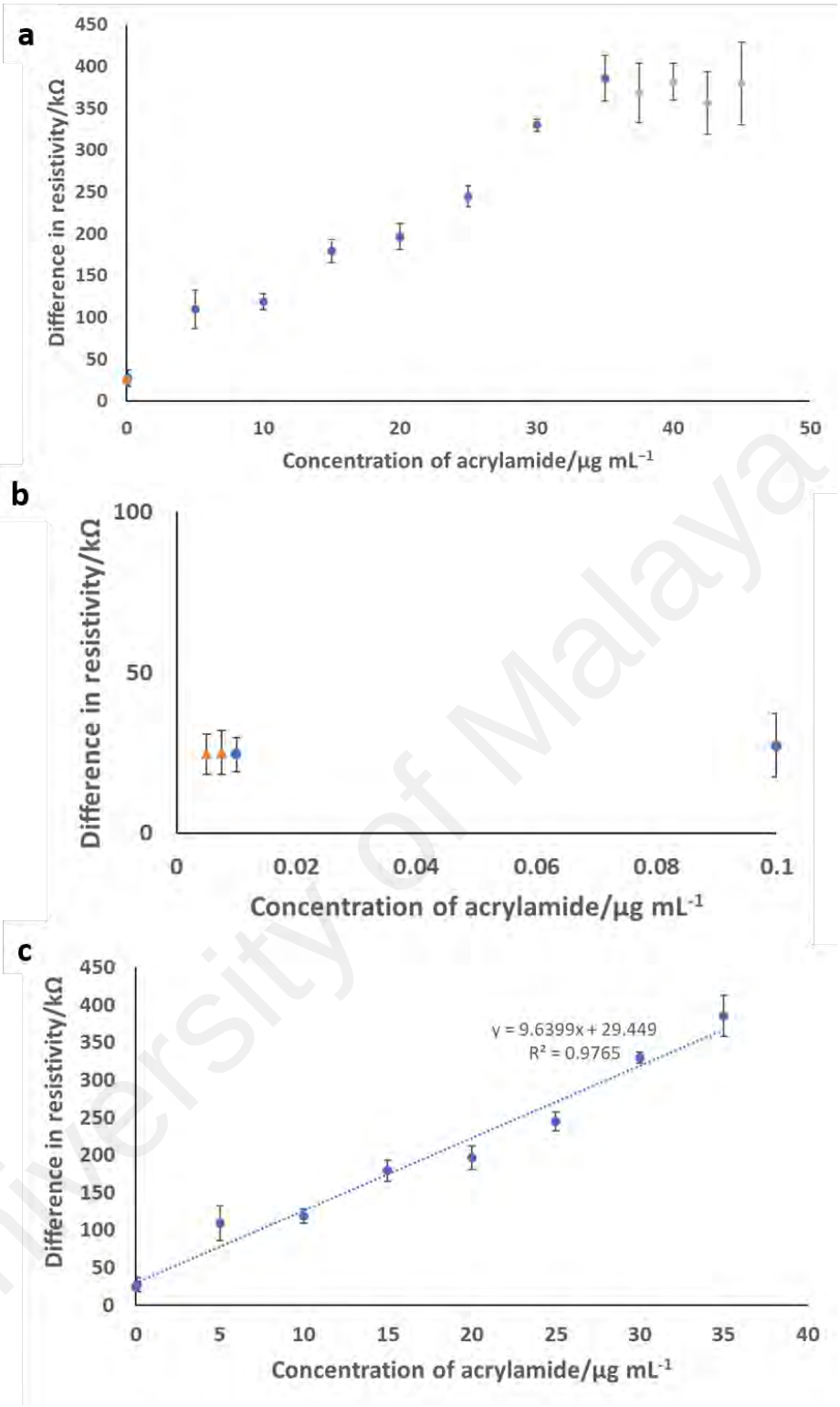

Figure 4.13: (a) The calibration plot corresponding to the difference in resistivity of immunosensor after the addition of free acrylamide, the concentration of acrylamide ranged from 5 ng mL^{-1} to 45 µg mL^{-1} prepared in PBS at pH 7.4 with the aid of electro-pulsion at -800 mV for 10 min. (b) The calibration plot from 5 ng mL^{-1} to 0.1 µg mL^{-1} of acrylamide. (c) The linear dynamic range from 0.01 µg mL^{-1} to 35.00 µg mL^{-1} of acrylamide (obtained from (a)).

4.4 Reproducibility assessment on the developed immunosensor

To investigate the reproducibility of developed immunosensor, the assessment was applied in five different electrode surfaces. It was conducted within a day with the same manner and tested in the same concentration of free acrylamide. After three successive measurements on each electrode, the relative standard deviation (RSD) responded to 15 µg mL^{-1} of acrylamide was obtained to be 3.13% as shown in Figure 4.14. This demonstrated the high reproducibility (RSD < 10%) of immunosensor was obtained. The high reproducibility of immunosensor was mainly contributed from the sensor fabrication procedures and immunosensor interface design (Darwish et al., 2016). Hence, the present immunosensor has a stable and rigid surface modification design in order to produce a high reproducibility acrylamide detection.

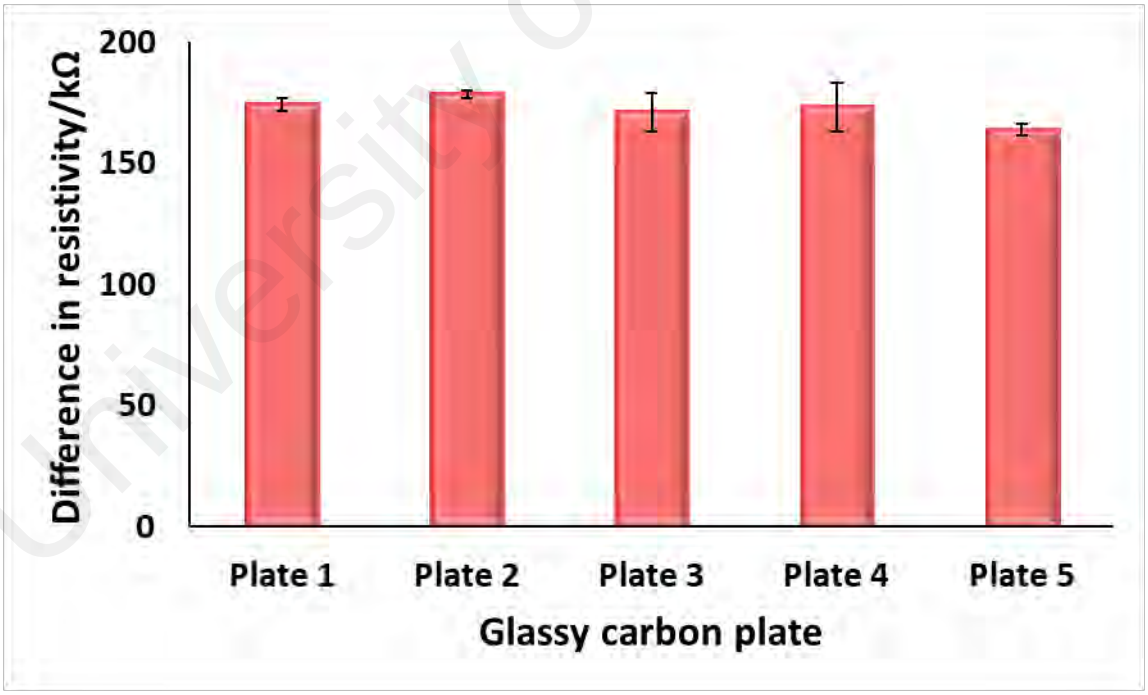

Figure 4.14: Reproducibility study of the developed immunosensor on 5 different electrodes.

4.5 Repeatability test on the developed acrylamide immunosensor

The repeatability study was evaluated in three different concentrations of acrylamide on the same day and continuously for five days. The acrylamide solution with concentration of 5 μg mL^{-1}, 15 μg mL^{-1} and 25 μg mL^{-1} were prepared in PBS at pH 7.4. The obtained results are shown in Figure 4.15 (a) and (b) where each concentration was repeated for five times analysis for intra-day and three replicates for inter-day. The RSD for intra-day repeatability was calculated to be 8.22%, 7.06% and 5.77% in 5 μg mL^{-1}, 15 μg mL^{-1} and 25 μg mL^{-1} of free acrylamide, respectively (Figure 4.15 a). The intra-day repeatability was assessed on the same day but at different time and three concentration of acrylamide was tested at the same time. Subsequently for inter-day repeatability study, three concentration of acrylamide were tested at one time on the same day with different electrodes and the experiment was conducted for continuous five days. The RSD was calculated and determined to be 7.33%, 5.49% and 7.97% based on 5 μg mL^{-1}, 15 μg mL^{-1} and 25 μg mL^{-1} of acrylamide (Figure 4.15 b). The RSD obtained from both the intra and inter-day repeatability tests were fallen within the acceptable range of % RSD value (14%) suggested in CAC/GL 71-2009 (Organization, 2014). The resultant results indicated that the developed immunosensor has the ability to produce a high precision detection for acrylamide determination.

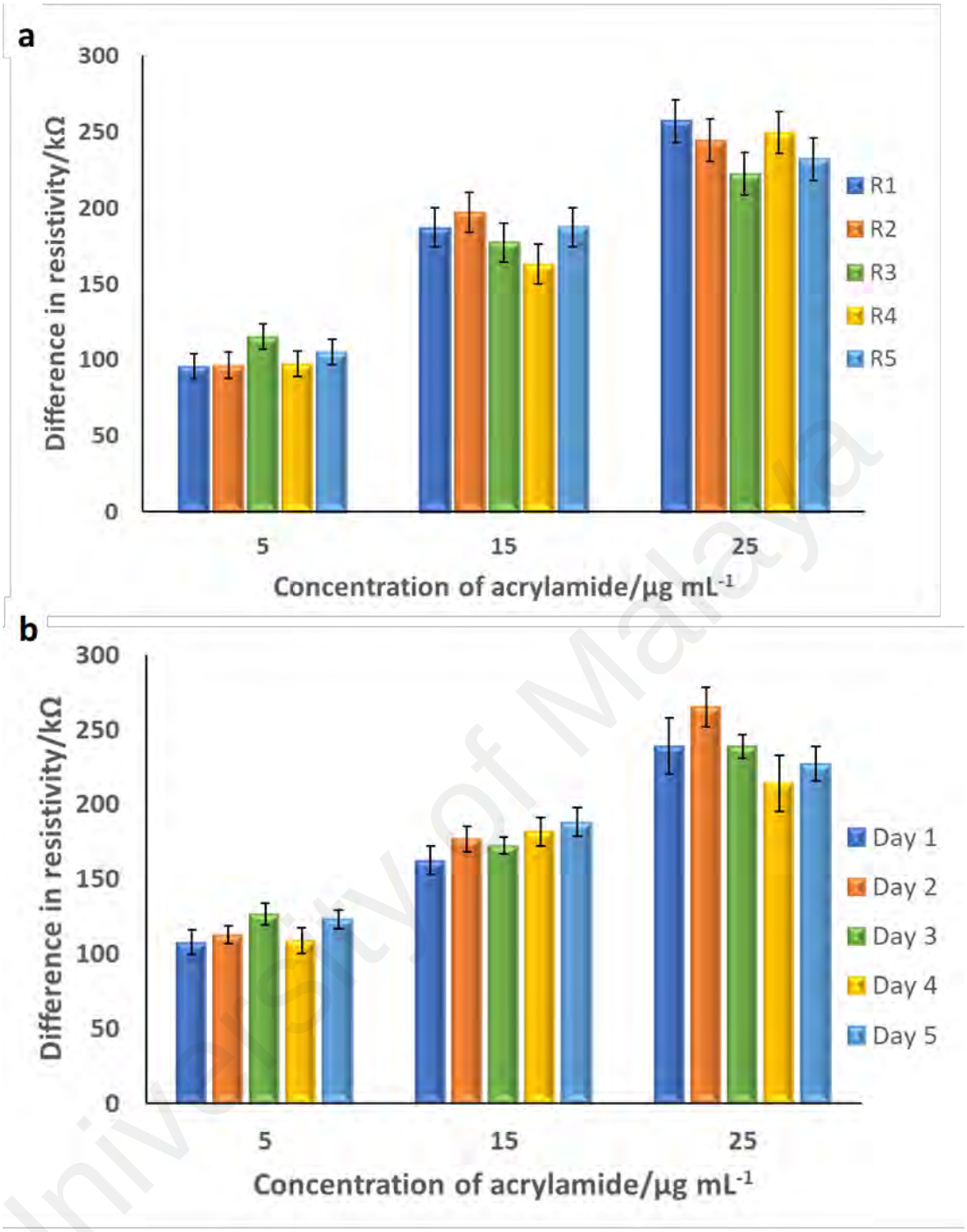

Figure 4.15: (a) Intra-day repeatability study of developed immunosensor surface for 5 µg mL^{-1}, 15 µg mL^{-1} and 25 µg mL^{-1} of acrylamide prepared in PBS at pH 7.4, (b) Inter-day repeatability study of developed immunosensor surface for 5 µg mL^{-1}, 15 µg mL^{-1} and 25 µg mL^{-1} of acrylamide prepared in PBS at pH 7.4 for consecutive 5 days.

4.6 Selectivity assessment on the developed immunosensor

The selectivity properties is one of the most important features for a practical detection to ensure the specificity of immunosensor towards acrylamide. To evaluate the specificity of immunosensor, small organic molecules including methacrylic acid, acrylic acid, N,N'-dimethylenebis(acrylamide) and propionic acid were tested with the fabricated electrode surface under optimized experimental conditions using the same concentration. These small molecules were selected as they have a similar chemical structure with acrylamide, where the chemical structure of each molecule as shown in Figure 4.16. Each small molecule was prepared in PBS at pH 7.4 and individually exposed to the fabricated immunosensor. After the displacement of surface bound antibody, the decrease in resistivity was presented in Figure 4.16. A significant difference in resistivity was obtained after the immunosensor surface was pulse in acrylamide solution with the aid of electro-pulsion. In contrast, the developed immunosensor did not show a sharp decrease in resistivity after tested in methacrylic acid, acrylic acid, N,N'-dimethylenebis(acrylamide) and propionic acid solutions. This showed the antibody dissociated form surface bound hapten only with the presence of acrylamide. Although the polyclonal antibody was used in the present study as currently only polyclonal acrylamide antibody was commercialized, however the resultant difference in resistivity for other small molecules did not show an obvious resistivity change. As shown in Figure 4.16, N,N'-dimethylenebis(acrylamide) displayed a higher resistivity change among the other tested small organic molecules. This might due to of N,N'-dimethylenebis(acrylamide) has a chemical structure highly similar to acrylamide. Nevertheless, the resistivity change in N,N'-dimethylenebis(acrylamide) showed only one tenth of acrylamide and furthermore, this molecule normally used as cross-linking agent for polymerization (Joshi et al., 2018; Sun et al., 2014) and thus has a relatively low possibility to presence in food samples. Hence, the results exhibited the high the

selectivity of the interfacial design to perform a significant change in resistivity toward acrylamide and indicating the specificity of established immunosensor.

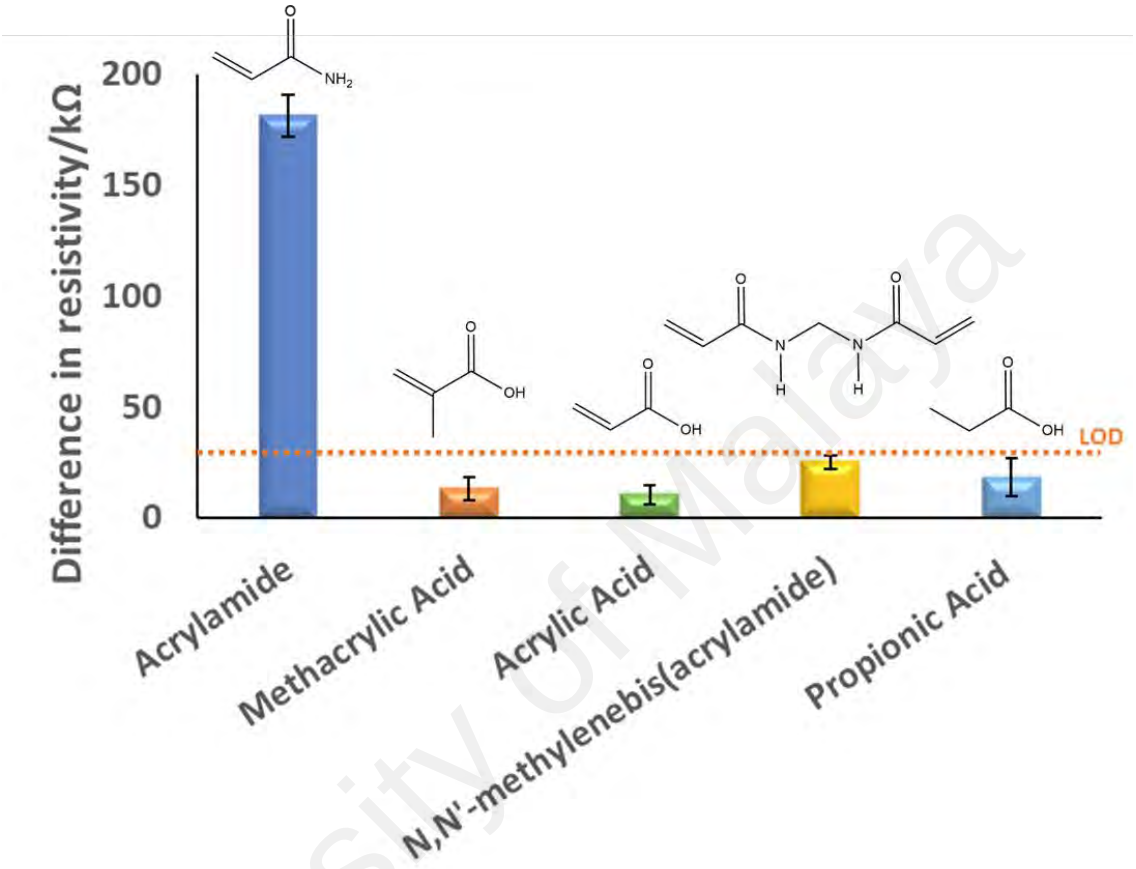

Figure 4.16: Selectivity assessment of the developed immunosensor surface with four different small organic molecule (e.g., methacrylic acid, acrylic acid, N,N'-dimethylenebis(acrylamide) and propionic acid).

4.7 Stability test on the developed acrylamide immunosensor

The long-term stability of fabricated layers was evaluated by storing the electrode in PBS at 4 °C and the detection ability was analysed. The immunosensor was later used for acrylamide detection after storing for 1, 2, 3, 4, 5, 7, 14, 21 and 28 days. Three different electrodes were prepared for each day of detection and the resistivity changes are illustrated in Figure 4.17. There was no significant loss in immunosensor detection ability can be observed after being stored for 28 days. The developed immunosensor retained its

detection ability for 98.69% after storage of 1 week, 83.60% for 2 weeks and 88.43% for 3 weeks. Furthermore, after 28 days of storage, the immunosensor surface has retained its detection ability as high as 90.96% of the initial respond. Hence, the developed immunosensor was suggested to be stable for 28 days when storing in PBS at 4 °C. The RSD of the developed immunosensor for stability test at 4 °C was determined to be 7.70% (< 14%). In addition, a two tailed t-test was performed to investigate the significance of the difference in resistivity after 28 days. Results taken on day 28 were compared to results taken on day 1, no significant difference was obtained with p-value of 0.318.

After a week, the developed immunosensor retained 88.31% of its detection capacity and retained 86.47% of its detection capacity after two weeks for room temperature stability test (25 °C). In addition, the RSD for room temperature stability testing was determined to be 5.20% and the t-test result for day 1 with day 14 was 0.03. The t-test showed significant difference in resistivity after 14 days of storage. Based on the stability tests at two different temperatures (25 °C and 4 °C), it was suggested that the immunosensor be stored at 4 ° C because the immunosensor developed retained a higher detectability after storage in this condition.

The electrode surface could exhibit a long-term stability because of the interface design demonstrated and as well as the fabrication technique (Darwish et al., 2016). The modification of aryl diazonium salt layer on the surface of the glassy carbon plate was performed by electrochemical reduction and formed a covalent binding with electrode surface (Liu et al., 2007). Moreover, the modification of anti-fouling agent and surface bound hapten on the immunosensor surface were mainly through the formation of an amide covalent bond. Thus, the strong binding of the fabricated layer on electrode surface has produced a stable immunosensor surface.

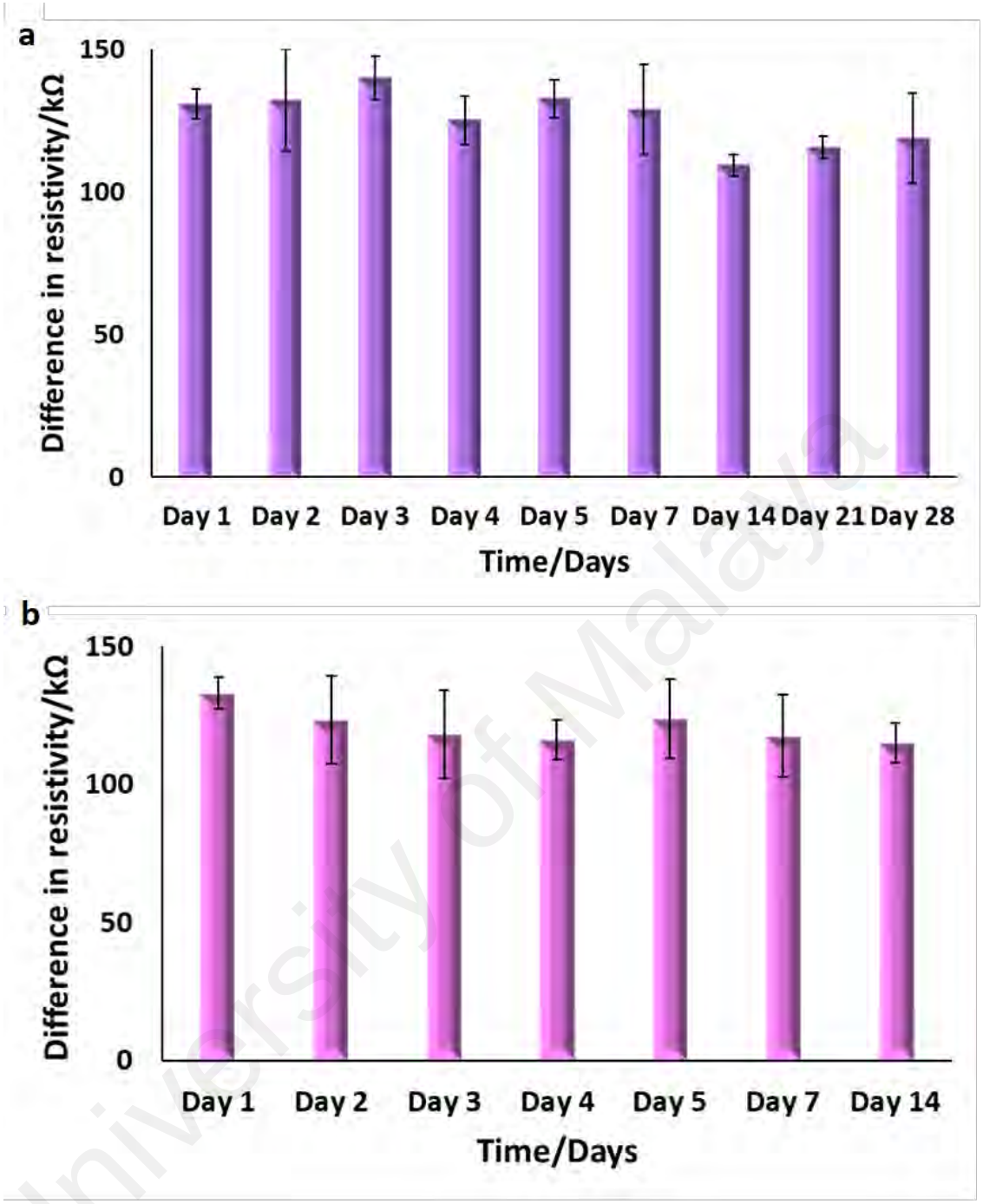

Figure 4.17: (a)The long-term stability assessment of the developed immunosensor for day 1 to day 28, after storage of immunosensor in PBS at temperature of 4 °C, (b) Long-term stability assessment of the developed immunosensor for day 1 to day 14, after storage of the immunosensor at 25 °C.

4.8 Real food sample analysis for direct detection of acrylamide by using the developed electrochemical immunosensor

The fabricated immunosensor surface was utilized for acrylamide quantitative measurement in food samples. For the electrochemical immunosensor quantification, no pre-treatment steps but only simple dissolvation or dilution step was involved in the sample preparation step. In order to avoid the interferences of food matrixes which might hindered the resultant signal, the standard addition was applied as the quantitative analysis method. By assuming the matrix effect was equally in all solutions, the standard addition method was commonly used to eliminate the matrix effect presented in the tested sample. In addition, with the aid of negative electro-pulsion and combinations of antibody properties which highly selective towards the target analyte, contributed to the highly sensitive and specific detection of developed immunosensor towards acrylamide.

Coffee, coco and prune juice were selected for real sample analysis, this is because coffee and coco are the commonly consumed beverages as part of breakfast or during tea-break. Besides, prune juice was suggested to treat the infants and toddlers (foods other than vegetables and pureed fruits) to relieved from constipation problem (Loening-Baucke, 2005). Hence, with the interest of promoting consumer health awareness, it is practicable and beneficial to evaluate the acrylamide concentration present in these selected liquid food samples. The quantification analysis of these food samples was carried out as described in Section 3.11. For solid foods containing acrylamide such as potato chips and French fries, the inclusion of fine-grained food in PBS has been evaluated. The mixture was vortex for 1 min and left for 1 hour, subsequently the precipitate was removed with filter paper. The collected solution (PBS), however, contained a coating of sticky oil, which could cause the reference electrode to be blocked. Consequently, direct measurement of the concentration of acrylamide in the solid sample was not possible.

The standard addition graphs obtained were plotted in Figure 4.18 and the unknown acrylamide concentration was determined when y = 0 or at x-intercept. The concentration obtained was compared with a standard method, GC-MS as shown in Table 4.7. In standard addition plot, a good correlation was obtained between the spiked acrylamide concentrations with the difference in resistivity with the evidence of $R^2 > 0.9$. As referred in Figure 4.18, R^2 for coffee, cocoa and prune juice was 0.967, 0.926 and 0.935 respectively. The amount of acrylamide found in coffee was 0.2849 ug g^{-1} by electrochemical immunosensor and 0.2967 ug g^{-1} by GC-MS; in cocoa was found to be 0.2017 ug g^{-1} by immunosensor and 0.2093 ug g^{-1} by GC-MS; and for prune juice was 1.2245 ug g^{-1} and 1.2162 ug g^{-1} by using electrochemical immunosensor and GC-MS, respectively. The acrylamide concentration present in the tested food samples has exceeded the recommended daily tolerable intake which was 0.0026 μg g^{-1} (to prevent cancer risk) (Tardiff et al., 2010). Prune juice contained higher acrylamide concentrations compared to coffee and coco beverages, primarily due to the presence of asparagine and sugar in the starting materials (plum) (Becalski et al., 2011). Additionally, it could be an interesting note typically for the coffee lover, the dark roasted coffee has a lower acrylamide concentration and might due to the degradation of acrylamide during the long roasting processing time (Granby & Fagt, 2004). However, the most effective way to prevent the over exposure of acrylamide is to reduce the consumption of coffee, coco and prune juice.

Besides that, the LOD and LOQ for each detected sample were hardly to be determined, since mean of blank was needed (referred equation 4.2 and 4.3 in Section 4.3). To obtain the value of LOB, it requires a blank sample without the presence of acrylamide. Nevertheless, acrylamide-free coffee, cocoa and prune juice samples are difficult to obtain, in other words, an ideal negative/blank food sample could not be obtained. Whereas the linear dynamic range for coffee and cocoa samples were between 0.03 to

0.13 μg mL^{-1} and the linear dynamic range for prune juice was determined as 0.33 to 1.33 μg mL^{-1}. In short, the linear dynamic ranges obtained in food samples were still within the range of linear dynamic range of the immunosensor conducted in PBS at pH 7.4 (Section 4.3).

The recovery test was conducted to validate the practical applicability and to analyse the accuracy of developed immunosensor for acrylamide detection in food samples. The real samples were spiked with different concentration of acrylamide. Coffee and cocoa were spiked at 40, 80 and 120 μg mL^{-1}, prune juice contained a higher initial concentration of analyte was spiked with 400, 800 and 1200 μg mL^{-1} of acrylamide. The recovery of each sample was defined as the following equation:

$$\% \text{ recovery} = \frac{C_{spiked} - C_{unspiked}}{C_{added}} \times 100 \quad (4.6)$$

where C_{spiked} is the determined concentration of spiked acrylamide in food sample

$C_{unspiked}$ is the concentration of unspiked food sample

C_{added} is the known concentration of acrylamide spiked into the food sample

And the "measured concentration" as shown in Table 4.8 was determined from $C_{spiked} - C_{unspiked}$.

The recovery range determined from the developed immunosensor was resulted from 90.33% to 99.23%, indicating this developed immunosensor has performed a satisfactory result in real sample analysis. The performed recovery testes have produced an acceptable recovery range (80 – 120%) and RSD obtained was < 20% (Table 4.8). This has demonstrated the matrix effect in food sample has no significant interference effect on the direct detection of acrylamide. Therefore, this present developed immunosensor surface could perform results which are comparable with GC-MS and at the same time exhibited a simpler and fast detection ability as compared to GC-MS.

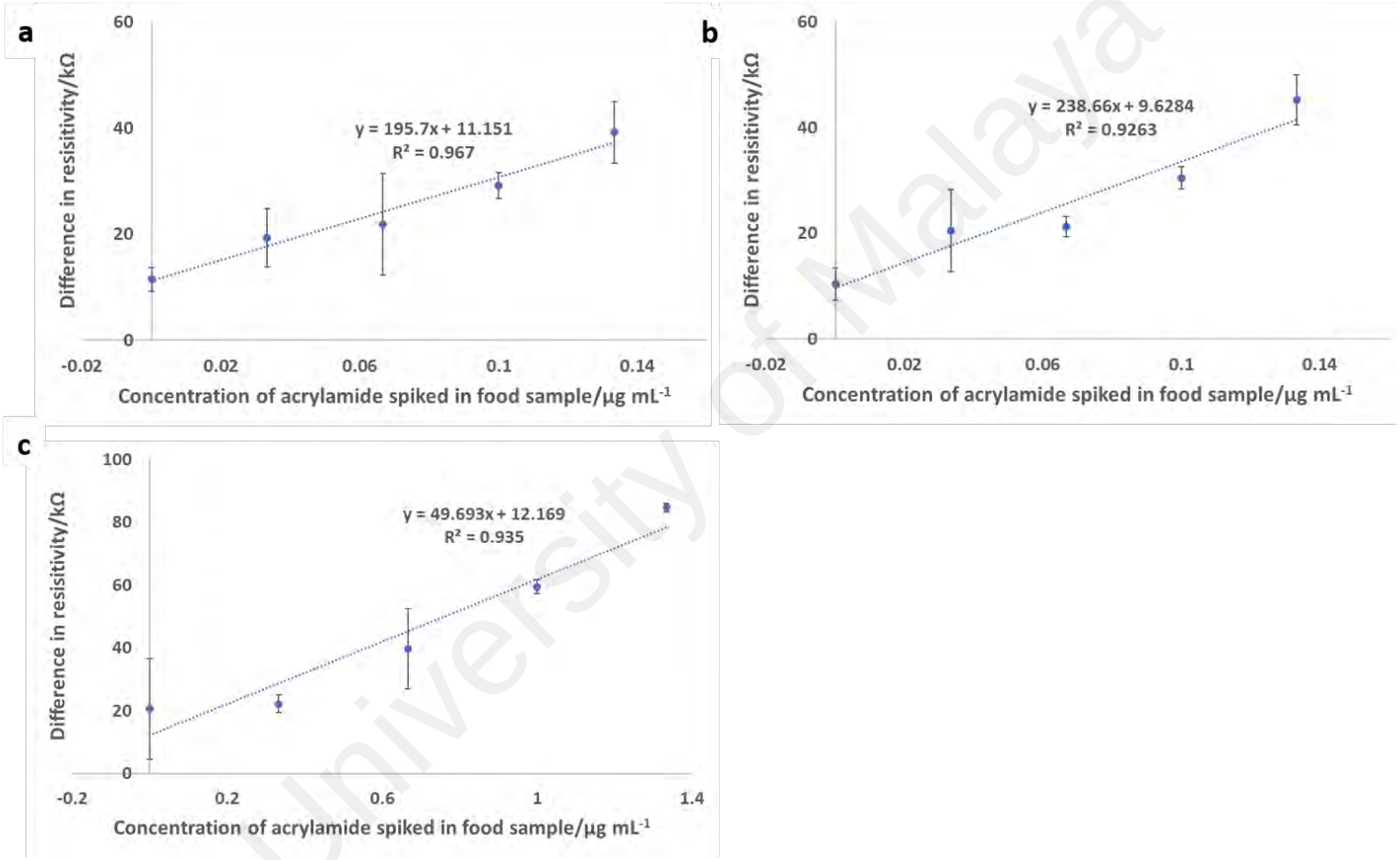

Figure 4.18: Acrylamide concentration quantification in food samples using developed immunosensor with the standard addition method. The standard addition plots for quantitative detection of acrylamide by using the fabricated interface in (a) coffee, (b) cocoa, and (c) prune juice samples.

Table 4.7: The comparison of acrylamide concentration in food samples between GC-MS determination with electrochemical immunosensor determination (performed with a standard addition method), and the advised daily tolerable intake of acrylamide.

Sample	GC-MS/μg g^{-1}	Electrochemical immunosensor/μg g^{-1}	Tolerable intake/ μg g^{-1} per day
Coffee	0.2967 ± 0.0178	0.2849 ± 0.0141	0.0026
Cocoa	0.2093 ± 0.0183	0.2017 ± 0.0190	0.0026
Prune juice	1.2162 ± 0.0243	1.2245 ± 0.1562	0.0026

Table 4.8: Recovery test of acrylamide determined using the developed electrochemical immunosensor.

Sample	Spiked concentration/ ng mL^{-1}	Measured concentration/ ng mL^{-1}	RSD/%	Recovery/%
Coffee	40	36.13	10.62	90.33
	80	79.29	4.50	99.11
	120	117.18	5.94	97.65
Cocoa	40	38.00	11.87	95.00
	80	75.46	8.55	94.33
	120	119.08	4.06	99.23
Prune juice	400	369.30	6.09	92.33
	800	737.90	7.22	92.24
	1200	1167.90	2.72	97.33

CHAPTER 5: CONCLUSION AND FUTURE PERSPECTIVES

An electrochemical immunosensor interface for direct detection of acrylamide has been developed via a displacement assay. The bottom up fabrication steps on the electrode surface was characterized and validated by using electrochemical method (CV and EIS), FT-IR and FESEM. The application of a displacement assay allows the developed immunosensor to perform a user intervention free detection without involving any sample pre-treatment step in real food sample analysis. The dissociation of surface bound antibody from hapten has been enhanced with the aid of electro-pulsion by pulsing the glassy carbon electrode with a negative potential. Conversely, the use of a positive electro-pulsion shows a higher absorption of antibody on the working electrode surface. Hence, this implies that the anti-acrylamide antibody utilized in present study carried a net negative charged under neutral condition at pH 7.4. Besides that, the displacement assay occurs at the electrode surface can be affected by pulsing duration, pulsing potential and the concentration of acrylamide. The impact of these three important factors on the dissociation of surface bound antibody was evaluated experimentally and theoretically. In the real experimental study, pulsing the electrode with -800 mV for 10 min was selected as the optimal conditions for the displacement assay in which the greatest decrease in resistivity was observed. While in a theoretical statistical study, the effect of three factors were optimized simultaneously to achieve the maximum difference in resistivity before and after a displacement assay. The Box-Behnken design has predicted a similar optimal displacement conditions as proven in experimental study. The presence of free acrylamide was the dominant factor for the dissociation of antibody from the surface bound hapten as exhibited from Box-Behnken design as well as in the real experimental study. No significant resistivity changes were obtained when acrylamide was absent. As such, electro-pulsion with negative potential at -800 mV for 10 min

pulsing duration was selected and applied for the occurrence of a displacement assay in acrylamide determination.

For quantitative analysis of acrylamide concentration under the optimized conditions, the developed immunosensor illustrates a good linearity between acrylamide concentration with respect to the difference in resistivity, resulting in a linear dynamic range in the range from 0.01 μg mL^{-1} to 35.00 μg mL^{-1} and LOD of 3.84 ng mL^{-1}. The developed immunosensor possesses a high reproducible with the RSD of 3.13% after evaluated with five different electrodes interface. In addition, with the RSD resulted in the range between 5.49% to 8.22% from the intra-day and inter-day repeatability assessment, this acrylamide immunosensor was proven to have the ability to generate a precision detection. Besides that, the selectivity of developed immunosensor towards acrylamide has been confirmed, as no significant in the difference of resistivity was obtained after exposure of methacrylic acid, acrylic acid, N,N'-dimethylenebis(acrylamide) and propionic acid solutions on the electrode surface. Without any obvious loss of detection ability, the developed immunosensor has retained its detection capability after being stored at 4 °C for 28 days. Therefore, the developed immunosensor surface in the present study exhibited a high reproducibility, repeatability, specificity, selectivity and long-term stability detection to acrylamide.

To evaluate the performance of this developed immunosensor in food samples, the standard addition method was implied to detect acrylamide level in coffee, cocoa and prune juice. The immunosensor was able to perform a quantitative detection of acrylamide as indicated by the decrease in resistivity with increasing acrylamide concentration. The acrylamide concentration in food samples was determined using the developed immunosensor showed a good correlation with the standard method, GC-MS. This demonstrated that the antibody-antigen specific affinity reaction with the aid of negative electro-pulsion allows the fabricated immunosensor to generate an accurate and

sensitive detection signals for acrylamide determination in real food samples. In addition, the developed immunosensor yielded the recovery from the range of 90.33% to 99.23% in real sample analysis. The resultant recoveries have validated that without the needed of sample pre-treatment steps, the immunosensor interface was able to perform a reliable result for the detection of acrylamide. The food matrixes effect was eliminated and no significant interference effect has hindered the detecting signal during acrylamide detection in the selected liquid food samples. Thus, the developed immunosensor is believed to be a promising route to generate a reliable, direct, rapid and quantitative analytical sensor device towards acrylamide. The target end-user of this developed immunosensor may be the food and beverage manufacturer. To ensure that the concentration of acrylamide falls within the tolerable intake range, the company should assess the concentration of acrylamide in its manufactured product before it is put on the market. This developed immunosensor could facilitate detection within a shorter time frame.

Herein, the developed electrochemical immunosensor exhibit the advantage of rapidity which able to perform a direct quantitative acrylamide detection without any sample pre-treatment step. However, this immunosensor interface detection is limited for liquid based samples with low content of fats; while acrylamide concentration in solid foods that contain oil and fats such as potato chip and fries are unable to be detected. This is mainly because the presence of fats can hinder the electron transfer between working electrode and electrolyte, therefore, hexane defatting step is normally practiced in electrochemical detection. However, the disadvantages of using hexane defatting method are it requires an additional reagent and it is time consuming, thus this has restricted the simplicity of electrochemical immunosensor detection. To overcome this limitation, the development of a Teflon filter cap is proposed as the future perspective. In the conventional electrochemical evaluating cell, Teflon cap is used to hold the reference and counter

electrode. An additional hole at the Teflon filter cap is proposed for the purpose of adding sample solution into the inner part of filter. The outer Teflon cap is printed by using a 3D printer with the Teflon resin. Then, the inner part of the Teflon filter cap is modified with three layers of filter as shown in Figure 5.1. For the three layers filter, the pore size on filter membrane should be getting smaller as the filtrate getting lower, for example filter layer 1 with 2 μm pore size, filter layer 2 with 0.45 μm and subsequently filter layer 3 with 0.22 μm pore size. For real food application, mix the grind potato chips or fries with phosphate buffer and after a period of time, transfer the buffer solution into the Teflon filter (since acrylamide can dissolve in buffer). These three filter layers can filter/separate out the undissolved fats contained in oil content food and the filtered sample solution can directly flow onto the working electrode (in Teflon evaluating cell). Consequently, perform the electrochemical detection of acrylamide after all of the filtered sample solution flow into the evaluating cell. Hence, the Teflon filter cap is replacing the hexane defatting method to allow electrochemical detection of acrylamide in oil and fats content food.

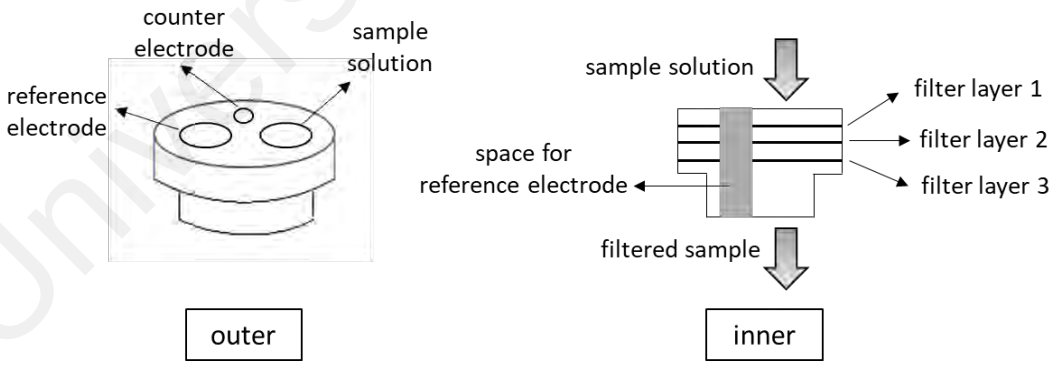

Figure 5.1: Proposed Teflon filter cap in future perspective: Teflon filter outer cap (left) and Teflon filter cap inner design (right).

The second future perspective is suggested to detect the epoxide of acrylamide, glycidamide. Typically, the acrylamide and glycidamide adduct can be detected in vitro/vivo and the sum of these two adducts indicate the total exposure of acrylamide in

human or rodents. Nevertheless, detecting of glycidamide concentration alone is seldom been evaluated. Although it is at low concentration, glycidamide can be found in food samples. The formation of glycidamide is resulted from a reaction between acrylamide and unsaturated fatty acid during the heating process. Besides, glycidamide also has been classified as a potential carcinogen beside showing higher reactivity than acrylamide. Thus, the electrochemical sensing that can simultaneously detect these two carcinogens should be developed. The displacement assay format can be utilized, but some modifications have to be made on the antibodies. Both of the detecting antibodies can be conjugated with different nano-metal particles. The selected nano-particles should exhibit a different reduction/oxidation peak, in order to differentiate the dissociation of each antibody. In addition, the specificity towards the analyte and cross reactivity analysis of sensor between these two analytes must be investigated as glycidamide and acrylamide have a relatively high similarity of molecular structure. The most challenging part is that the antibody of glycidamide has to be custom made, this is because the commercialized anti-glycidamide antibody is yet to be available in the market.

REFERENCES

Abouzari, M. R. S., Berkemeier, F., Schmitz, G., & Wilmer, D. (2009). On the physical interpretation of constant phase elements. *Solid State Ionics, 180*(14), 922-927.

Andrzejewski, D., Roach, J. A. G., Gay, M. L., & Musser, S. M. (2004). Analysis of coffee for the presence of acrylamide by LC-MS/MS. *Journal of Agricultural and Food Chemistry, 52*(7), 1996-2002.

Araujo, F. M., Santos, M. D. R., de Oliveira, M. A. L., Matos, R. C., & Matos, M. A. C. (2017). Box–behnken design applied to optimize the ultrasound-assisted extraction of petroleum biomarkers in river sediment samples using green analytical chemistry. *Analytical Methods, 9*(40), 5859-5867.

Asanov, A. N., Wilson, W. W., & Oldham, P. B. (1998). Regenerable biosensor platform: A total internal reflection fluorescence cell with electrochemical control. *Analytical Chemistry, 70*(6), 1156-1163.

Asnaashari, M., Esmaeilzadeh Kenari, R., Farahmandfar, R., Taghdisi, S. M., & Abnous, K. (2018). Fluorescence quenching biosensor for acrylamide detection in food products based on double-stranded DNA and gold nanoparticles. *Sensors and Actuators, B: Chemical, 265*, 339-345.

Asnaashari, M., Kenari, R. E., Farahmandfar, R., Abnous, K., & Taghdisi, S. M. (2019). An electrochemical biosensor based on hemoglobin-oligonucleotides-modified electrode for detection of acrylamide in potato fries. *Food Chemistry, 271*, 54-61.

Authority, E. F. S. (2012). Update on acrylamide levels in food from monitoring years 2007 to 2010. *EFSA Journal, 10*(10), 1-38.

Batra, B., Lata, S., Sharma, M., & Pundir, C. S. (2013). An acrylamide biosensor based on immobilization of hemoglobin onto multiwalled carbon nanotube/copper nanoparticles/polyaniline hybrid film. *Analytical Biochemistry, 433*(2), 210-217.

Beach, R. D., Conlan, R. W., Godwin, M. C., & Moussy, F. (2005). Towards a miniature implantable in vivo telemetry monitoring system dynamically configurable as a potentiostat or galvanostat for two- and three-electrode biosensors. *IEEE Transactions on Instrumentation and Measurement, 54*(1), 61-72.

Becalski, A., Brady, B., Feng, S., Gauthier, B. R., & Zhao, T. (2011). Formation of acrylamide at temperatures lower than 100°C: The case of prunes and a model study. *Food Additives & Contaminants: Part A, 28*(6), 726-730.

Belkhamssa, N., Justino, C. I. L., Santos, P. S. M., Cardoso, S., Lopes, I., Duarte, A. C., . . . Ksibi, M. (2016). Label-free disposable immunosensor for detection of atrazine. *Talanta, 146*, 430-434.

Bergmark, E. (1997). Hemoglobin adducts of acrylamide and acrylonitrile in laboratory workers, smokers and nonsmokers. *Chemical Research in Toxicology, 10*(1), 78-84.

Bezerra, M. A., Santelli, R. E., Oliveira, E. P., Villar, L. S., & Escaleira, L. A. (2008). Response surface methodology (RSM) as a tool for optimization in analytical chemistry. *Talanta, 76*(5), 965-977.

Bhardwaj, S. K., Sharma, A. L., Bhardwaj, N., Kukkar, M., Gill, A. A. S., Kim, K.-H., & Deep, A. (2017). TCNQ-doped Cu-metal organic framework as a novel conductometric immunosensing platform for the quantification of prostate cancer antigen. *Sensors and Actuators B: Chemical, 240*, 10-17.

Bianchi, F., Careri, M., Musci, M., & Mangia, A. (2007). Fish and food safety: Determination of formaldehyde in 12 fish species by SPME extraction and GC–MS analysis. *Food Chemistry, 100*(3), 1049-1053.

Bjellaas, T., Olesen, P. T., Frandsen, H., Haugen, M., Stølen, L. H., Paulsen, J. E., . . . Becher, G. (2007). Comparison of estimated dietary intake of acrylamide with hemoglobin adducts of acrylamide and glycidamide. *Toxicological Sciences, 98*(1), 110-117.

Brod, E., Nimri, S., Turner, B., & Sivan, U. (2008). Electrical control over antibody–antigen binding. *Sensors and Actuators B: Chemical, 128*(2), 560-565.

Bueno, M., Resconi, V. C., Campo, M. M., Ferreira, V., & Escudero, A. (2019). Development of a robust HS-SPME-GC-MS method for the analysis of solid food samples. Analysis of volatile compounds in fresh raw beef of differing lipid oxidation degrees. *Food Chemistry, 281*, 49-56.

Butterworth, A., Corrigan, D. K., & Ward, A. C. (2019). Electrochemical detection of oxacillin resistance with SimpleStat: A low cost integrated potentiostat and sensor platform. *Analytical Methods, 11*(14), 1958-1965.

Čadková, M., Metelka, R., Holubová, L., Horák, D., Dvořáková, V., Bílková, Z., & Korecká, L. (2015). Magnetic beads-based electrochemical immunosensor for monitoring allergenic food proteins. *Analytical Biochemistry, 484*(1), 4-8.

Capuano, E., & Fogliano, V. (2011). Acrylamide and 5-hydroxymethylfurfural (HMF): A review on metabolism, toxicity, occurrence in food and mitigation strategies. *LWT - Food Science and Technology, 44*(4), 793-810.

Darwish, N. T., Alrawi, A. H., Sekaran, S. D., Alias, Y., & Khor, S. M. (2016). Electrochemical immunosensor based on antibody-nanoparticle hybrid for specific detection of the dengue virus NS1 biomarker. *Journal of the Electrochemical Society, 163*(3), B19-B25.

Dávalos-Pantoja, L., Ortega-Vinuesa, J. L., Bastos-González, D., & Hidalgo-Álvarez, R. (2000). A comparative study between the adsorption of IgY and IgG on latex particles. *Journal of Biomaterials Science, Polymer Edition, 11*(6), 657-673.

Domínguez, I., Romero González, R., Arrebola Liébanas, F. J., Martínez Vidal, J. L., & Garrido Frenich, A. (2016). Automated and semi-automated extraction methods for GC–MS determination of pesticides in environmental samples. *Trends in Environmental Analytical Chemistry, 12*, 1-12.

EC08, A. A. N. (2011). Basic overview of the working principle of a potentiostat/galvanostat (PGSTAT)–Electrochemical cell setup. *Metrohm Autolab. BV*, 1-3.

Erkekoğlu, P., & Baydar, T. (2010). Toxicity of acrylamide and evaluation of its exposure in baby foods. *Nutrition Research Reviews, 23*(2), 323-333.

Erlandsen, S. L., Frethem, C., & Chen, Y. (2000). Field emission scanning electron microscopy (FESEM) entering the 21st century: Nanometer resolution and molecular topography of cell structure. *Journal of Histotechnology, 23*(3), 249-259.

Felix, F. S., & Angnes, L. (2018). Electrochemical immunosensors – A powerful tool for analytical applications. *Biosensors and Bioelectronics, 102*, 470-478.

Fernandes, J. O., & Soares, C. (2007). Application of matrix solid-phase dispersion in the determination of acrylamide in potato chips. *Journal of Chromatography A, 1175*(1), 1-6.

Ferreira, S. L. C., Bruns, R. E., Ferreira, H. S., Matos, G. D., David, J. M., Brandão, G. C., . . . dos Santos, W. N. L. (2007). Box-behnken design: An alternative for the optimization of analytical methods. *Analytica Chimica Acta, 597*(2), 179-186.

Friedman, M. (2003). Chemistry, biochemistry, and safety of acrylamide. A review. *Journal of Agricultural and Food Chemistry, 51*(16), 4504-4526.

Galuch, M. B., Magon, T. F. S., Silveira, R., Nicácio, A. E., Pizzo, J. S., Bonafe, E. G., . . . Visentainer, J. V. (2019). Determination of acrylamide in brewed coffee by dispersive liquid–liquid microextraction (DLLME) and ultra-performance liquid chromatography tandem mass spectrometry (UPLC-MS/MS). *Food Chemistry, 282*, 120-126.

Garabagiu, S., & Mihailescu, G. (2011). Simple hemoglobin-gold nanoparticles modified electrode for the amperometric detection of acrylamide. *Journal of Electroanalytical Chemistry, 659*(2), 196-200.

Gomes, S. V. F., Portugal, L. A., dos Anjos, J. P., de Jesus, O. N., de Oliveira, E. J., David, J. P., & David, J. M. (2017). Accelerated solvent extraction of phenolic compounds exploiting a Box-Behnken design and quantification of five flavonoids by HPLC-DAD in passiflora species. *Microchemical Journal, 132*, 28-35.

Gooding, J. J., Wasiowych, C., Barnett, D., Hibbert, D. B., Barisci, J. N., & Wallace, G. G. (2004). Electrochemical modulation of antigen-antibody binding. *Biosensors and Bioelectronics, 20*(2), 260-268.

Goud, K. Y., Sunil Kumar, V., Hayat, A., Vengatajalabathy Gobi, K., Song, H., Kim, K.-H., & Marty, J. L. (2019). A highly sensitive electrochemical immunosensor for zearalenone using screen-printed disposable electrodes. *Journal of Electroanalytical Chemistry, 832*, 336-342.

Granby, K., & Fagt, S. (2004). Analysis of acrylamide in coffee and dietary exposure to acrylamide from coffee. *Analytica Chimica Acta, 520*(1), 177-182.

Granvogl, M., Koehler, P., Latzer, L., & Schieberle, P. (2008). Development of a stable isotope dilution assay for the quantitation of glycidamide and its application to foods and model systems. *Journal of Agricultural and Food Chemistry, 56*(15), 6087-6092.

Hleli, S., Martelet, C., Abdelghani, A., Burais, N., & Jaffrezic-Renault, N. (2006). Atrazine analysis using an impedimetric immunosensor based on mixed biotinylated self-assembled monolayer. *Sensors and Actuators B: Chemical, 113*(2), 711-717.

Holford, T. R. J., Davis, F., & Higson, S. P. J. (2012). Recent trends in antibody based sensors. *Biosensors and Bioelectronics, 34*(1), 12-24.

Hu, Q., Xu, X., Fu, Y., & Li, Y. (2015). Rapid methods for detecting acrylamide in thermally processed foods: A review. *Food Control, 56*, 135-146.

Hu, Q., Xu, X., Li, Z., Zhang, Y., Wang, J., Fu, Y., & Li, Y. (2014). Detection of acrylamide in potato chips using a fluorescent sensing method based on acrylamide polymerization-induced distance increase between quantum dots. *Biosensors and Bioelectronics, 54*, 64-71.

Huang, S., Lu, S., Huang, C., Sheng, J., Zhang, L., Su, W., & Xiao, Q. (2016). An electrochemical biosensor based on single-stranded DNA modified gold electrode for acrylamide determination. *Sensors and Actuators, B: Chemical, 224*, 22-30.

Hussain, S. Z., & Maqbool, K. (2014). GC-MS: Principle, technique and its application in food science. *International Journal of Current Science, 13*, 116-126.

IARC. (1994). Acrylamide. IARC monographs on the evaluation of carcinogenic risks to humans, some industrial chemicals. Lyon, France.

Ignatov, O. V., Rogatcheva, S. M., Kozulin, S. V., & Khorkina, N. A. (1997). Acrylamide and acrylic acid determination using respiratory activity of microbial cells. *Biosensors and Bioelectronics, 12*(2), 105-111.

Ionescu, R. E., Gondran, C., Bouffier, L., Jaffrezic-Renault, N., Martelet, C., & Cosnier, S. (2010). Label-free impedimetric immunosensor for sensitive detection of atrazine. *Electrochimica Acta, 55*(21), 6228-6232.

Jin, W., Yang, G., Wu, L., Wang, Q., Shao, H., Qin, A., . . . Cai, B. (2011). Detecting 5-morpholino-3-amino-2-oxazolidone residue in food with label-free electrochemical impedimetric immunosensor. *Food Control, 22*(10), 1609-1616.

Joshi, A., Nandi, S., Chester, D., Brown, A. C., & Muller, M. (2018). Study of poly(N-isopropylacrylamide-co-acrylic acid) (pNIPAM) microgel particle induced deformations of tissue-mimicking phantom by ultrasound stimulation. *Langmuir, 34*(4), 1457-1465.

Kambham, B. S., Ram, V. V., & Raju, S. (2019). Investigation of laboratory and field aging of bituminous concrete with and without anti-aging additives using FESEM and FTIR. *Construction and Building Materials, 222*, 193-202.

Khoo, M. M., Rahim, Z., Darwish, N. T., Alias, Y., & Khor, S. M. (2016). Non-invasive control of protein-surface interactions for repeated electrochemical immunosensor use. *Sensors and Actuators, B: Chemical, 224*, 683-691.

Khor, S. M., Liu, G., Fairman, C., Iyengar, S. G., & Gooding, J. J. (2011). The importance of interfacial design for the sensitivity of a label-free electrochemical immuno-biosensor for small organic molecules. *Biosensors and Bioelectronics, 26*(5), 2038-2044.

Khor, S. M., Thordarson, P., & Gooding, J. J. (2013). The impact of antibody/epitope affinity strength on the sensitivity of electrochemical immunosensors for detecting small molecules. *Analytical and Bioanalytical Chemistry, 405*(11), 3889-3898.

Kim, C. T., Hwang, E.-S., & Lee, H. J. (2007). An improved LC-MS/MS method for the quantitation of acrylamide in processed foods. *Food Chemistry, 101*(1), 401-409.

Kovář, D., Farka, Z., & Skládal, P. (2014). Detection of aerosolized biological agents using the piezoelectric immunosensor. *Analytical Chemistry, 86*(17), 8680-8686.

Krajewska, A., Radecki, J., & Radecka, H. (2008). A voltammetric biosensor based on glassy carbon electrodes modified with single-walled carbon nanotubes/hemoglobin for detection of acrylamide in water extracts from potato crisps. *Sensors, 8*(9), 5832-5844.

Kumar, A., Prasad, B., & Mishra, I. M. (2008). Optimization of process parameters for acrylonitrile removal by a low-cost adsorbent using box–behnken design. *Journal of Hazardous Materials, 150*(1), 174-182.

Lau, P. Y., Ng, K. L., Azah, Y. N., Liu, G., Yatimah, A., & Khor, S. M. (2019). A sample pre-treatment-free electrochemical immunosensor with negative electro-pulsion for the quantitative detection of acrylamide in coffee, cocoa and prune juice. *Analytical Methods, 11*(33), 4299-4313.

Leung, A., Shankar, P. M., & Mutharasan, R. (2007). A review of fiber-optic biosensors. *Sensors and Actuators, B: Chemical, 125*(2), 688-703.

Li, N., Liu, X., Zhu, J., Zhou, B., Jing, J., Wang, A., . . . Guo, S. (2020). Simple and sensitive detection of acrylamide based on hemoglobin immobilization in carbon ionic liquid paste electrode. *Food Control, 109*, 106764.

Lin, J., & Ju, H. (2005). Electrochemical and chemiluminescent immunosensors for tumor markers. *Biosensors and Bioelectronics, 20*(8 SPEC. ISS.), 1461-1470.

Lipman, N. S., Jackson, L. R., Trudel, L. J., & Weis-Garcia, F. (2005). Monoclonal versus polyclonal antibodies: Distinguishing characteristics, applications, and information resources. *ILAR Journal, 46*(3), 258-267.

Liron, Z., Tender, L. M., Golden, J. P., & Ligler, F. S. (2002). Voltage-induced inhibition of antigen-antibody binding at conducting optical waveguides. *Biosensors and Bioelectronics, 17*(6-7), 489-494.

Lisdat, F., & Schäfer, D. (2008). The use of electrochemical impedance spectroscopy for biosensing. *Analytical and Bioanalytical Chemistry, 391*(5), 1555-1567.

Little, T. A. (2015). Method validation essentials, limit of blank, limit of detection, and limit of quantitation. *BioPharm International, 28*(4), 48-51.

Liu, C., Luo, F., Chen, D., Qiu, B., Tang, X., Ke, H., & Chen, X. (2014). Fluorescence determination of acrylamide in heat-processed foods. *Talanta, 123*, 95-100.

Liu, G., Böcking, T., & Gooding, J. J. (2007). Diazonium salts: Stable monolayers on gold electrodes for sensing applications. *Journal of Electroanalytical Chemistry, 600*(2), 335-344.

Liu, G., Khor, S. M., Iyengar, S. G., & Gooding, J. J. (2012). Development of an electrochemical immunosensor for the detection of HbA1c in serum. *Analyst, 137*(4), 829-832.

Liu, G., Luais, E., & Gooding, J. J. (2011). The fabrication of stable gold nanoparticle-modified interfaces for electrochemistry. *Langmuir, 27*(7), 4176-4183.

Liu, J., Zhao, G., Yuan, Y., Chen, F., & Hu, X. (2008). Quantitative analysis of acrylamide in tea by liquid chromatography coupled with electrospray ionization tandem mass spectrometry. *Food Chem, 108*(2), 760-767.

Liu, S., Dai, Z., Chen, H., & Ju, H. (2004). Immobilization of hemoglobin on zirconium dioxide nanoparticles for preparation of a novel hydrogen peroxide biosensor. *Biosensors and Bioelectronics, 19*(9), 963-969.

Liu, X., Yang, Z., Zhang, Y., & Yu, R. (2013). A novel electrochemical immunosensor for ochratoxin A with hapten immobilization on thionine/gold nanoparticle modified glassy carbon electrode. *Analytical Methods, 5*(6), 1481-1486.

Liu, Y., Qin, Z., Wu, X., & Jiang, H. (2006). Immune-biosensor for aflatoxin B1 based bio-electrocatalytic reaction on micro-comb electrode. *Biochemical Engineering Journal, 32*(3), 211-217.

Loening-Baucke, V. (2005). Prevalence, symptoms and outcome of constipation in infants and toddlers. *Journal of Pediatrics, 146*(3), 359-363.

Lvovich, V. F. (2012). *Impedance spectroscopy: Applications to electrochemical and dielectric phenomena*. Hoboken, NJ: John Wiley & Sons.

Ma, X., Liu, X., Xiao, H., & Li, G. (2005). Direct electrochemistry and electrocatalysis of hemoglobin in poly-3-hydroxybutyrate membrane. *Biosensors and Bioelectronics, 20*(9), 1836-1842.

Mani, V., Periasamy, A. P., & Chen, S.-M. (2012). Highly selective amperometric nitrite sensor based on chemically reduced graphene oxide modified electrode. *Electrochemistry Communications, 17*, 75-78.

Marín-Barroso, E., Messina, G. A., Bertolino, F. A., Raba, J., & Pereira, S. V. (2019). Electrochemical immunosensor modified with carbon nanofibers coupled to a paper platform for the determination of gliadins in food samples. *Analytical Methods, 11*(16), 2170-2178.

Mercer, C., Bennett, R., Conghaile, P. Ó., Rusling, J. F., & Leech, D. (2019). Glucose biosensor based on open-source wireless microfluidic potentiostat. *Sensors and Actuators B: Chemical, 290*, 616-624.

Mohamed, M. A., Jaafar, J., Ismail, A. F., Othman, M. H. D., & Rahman, M. A. (2017). Chapter 1 - Fourier transform infrared (FTIR) spectroscopy. In N. Hilal, A. F. Ismail, T. Matsuura & D. Oatley-Radcliffe (Eds.), *Membrane Characterization* (pp. 3-29): Elsevier.

Monošíka, R., Streďanskýb, M., Šturdík, E.,. (2012). Biosensors — classification, characterization and new trends. *Acta Chimica Slovaca, 5*(1), 109-120.

Mottram, D. S., Wedzicha, B. L., & Dodson, A. T. (2002). Food chemistry: Acrylamide is formed in the maillard reaction. *Nature, 419*(6906), 448-449.

Muhammad-Tahir, Z., & Alocilja, E. C. (2003). A conductometric biosensor for biosecurity. *Biosensors and Bioelectronics, 18*(5-6), 813-819.

Nguyen, T. N. H., Nolan, J. K., Park, H., Lam, S., Fattah, M., Page, J. C., . . . Lee, H. (2019). Facile fabrication of flexible glutamate biosensor using direct writing of platinum nanoparticle-based nanocomposite ink. *Biosensors and Bioelectronics, 131*, 257-266.

Omanovic, S., & Roscoe, S. G. (1999). Electrochemical studies of the adsorption behavior of bovine serum albumin on stainless steel. *Langmuir, 15*(23), 8315-8321.

Ono, H., Chuda, Y., Ohnishi-Kameyama, M., Yada, H., Ishizaka, M., Kobayashi, H., & Yoshida, M. (2003). Analysis of acrylamide by LC-MS/MS and GC-MS in processed Japanese foods. *Food Additives & Contaminants, 20*(3), 215-220.

Organization, F. A. A. O. W. H. (2014). Guidelines for the design and implementation of national regulatory food safety assurance program associated with the use of vaterinary drugs in food producing animals.

Pang, P., Teng, X., Chen, M., Zhang, Y., Wang, H., Yang, C., . . . Barrow, C. J. (2018). Ultrasensitive enzyme-free electrochemical immunosensor for microcystin-LR using molybdenum disulfide/gold nanoclusters nanocomposites as platform and Au@Pt core-shell nanoparticles as signal enhancer. *Sensors and Actuators B: Chemical, 266*, 400-407.

Pingarrón, J. M., Yáñez-Sedeño, P., & González-Cortés, A. (2008). Gold nanoparticle-based electrochemical biosensors. *Electrochimica Acta, 53*(19), 5848-5866.

Preston, A., Fodey, T., & Elliott, C. (2008). Development of a high-throughput enzyme-linked immunosorbent assay for the routine detection of the carcinogen acrylamide in food, via rapid derivatisation pre-analysis. *Analytica Chimica Acta, 608*(2), 178-185.

Prodromidis, M. I. (2010). Impedimetric immunosensors—A review. *Electrochimica Acta, 55*(14), 4227-4233.

Qin, L., Zhang, Y. Y., Xu, X. B., Wang, X. S., Liu, H. W., Zhou, D. Y., . . . Thornton, M. (2017). Isotope dilution HPLC-MS/MS for simultaneous quantification of acrylamide and 5-hydroxymethylfurfural (HMF) in thermally processed seafood. *Food Chemistry, 232*, 633-638.

Quan, Y., Chen, M., Zhan, Y., & Zhang, G. (2011). Development of an enhanced chemiluminescence ELISA for the rapid detection of acrylamide in food products. *Journal of Agricultural and Food Chemistry, 59*(13), 6895-6899.

Ragonese, R., Macka, M., Hughes, J., & Petocz, P. (2002). The use of the box–behnken experimental design in the optimisation and robustness testing of a capillary electrophoresis method for the analysis of ethambutol hydrochloride in a pharmaceutical formulation. *Journal of Pharmaceutical and Biomedical Analysis, 27*(6), 995-1007.

Ramírez-Hernández, A., Aguilar-Flores, C., & Aparicio-Saguilán, A. (2019). Fingerprint analysis of FTIR spectra of polymers containing vinyl acetate. *DYNA, 86*(209), 198-205.

Ricci, F., Volpe, G., Micheli, L., & Palleschi, G. (2007). A review on novel developments and applications of immunosensors in food analysis. *Analytica Chimica Acta, 605*(2), 111-129.

Senesac, L. R., Yi, D., Greve, A., Hales, J. H., Davis, Z. J., Nicholson, D. M., . . . Thundat, T. (2009). Micro-differential thermal analysis detection of adsorbed explosive molecules using microfabricated bridges. *Review of Scientific Instruments, 80*(3), 1-9.

Serafín, V., Torrente-Rodríguez, R. M., González-Cortés, A., García de Frutos, P., Sabaté, M., Campuzano, S., . . . Pingarrón, J. M. (2018). An electrochemical immunosensor for brain natriuretic peptide prepared with screen-printed carbon electrodes nanostructured with gold nanoparticles grafted through aryl diazonium salt chemistry. *Talanta, 179*, 131-138.

Sharma, P., Singh, L., & Dilbaghi, N. (2009). Optimization of process variables for decolorization of disperse yellow 211 by bacillus subtilis using box–behnken design. *Journal of Hazardous Materials, 164*(2), 1024-1029.

Sharma, S., Zapatero-Rodríguez, J., Saxena, R., O'Kennedy, R., & Srivastava, S. (2018). Ultrasensitive direct impedimetric immunosensor for detection of serum HER2. *Biosensors and Bioelectronics, 106*, 78-85.

Shein, J. B., Lai, L. M. H., Eggers, P. K., Paddon-Row, M. N., & Gooding, J. J. (2009). Formation of efficient electron transfer pathways by adsorbing gold nanoparticles to self-assembled monolayer modified electrodes. *Langmuir, 25*(18), 11121-11128.

Silva, N., Gil, D., Karmali, A., & Matos, M. (2009). Biosensor for acrylamide based on an ion-selective electrode using whole cells of Pseudomonas aeruginosa containing amidase activity. *Biocatalysis and Biotransformation, 27*(2), 143-151.

Silva, N. A. F., Matos, M. J., Karmali, A., & Rocha, M. M. (2011). An electrochemical biosensor for acrylamide determination: Merits and limitations. *Portugaliae Electrochimica Acta, 29*(5), 361-373.

Silva, N. F. D., Magalhães, J. M. C. S., Barroso, M. F., Oliva-Teles, T., Freire, C., & Delerue-Matos, C. (2019). In situ formation of gold nanoparticles in polymer inclusion membrane: Application as platform in a label-free potentiometric immunosensor for Salmonella typhimurium detection. *Talanta, 194*, 134-142.

Stan, H.-J. (2005). Chapter 6 GC-MS. I: Basic principles and technical aspects of GC-MS for pesticide residue analysis. *Comprehensive Analytical Chemistry* (Vol. 43, pp. 269-337): Elsevier.

Stobiecka, A., Radecka, H., & Radecki, J. (2007). Novel voltammetric biosensor for determining acrylamide in food samples. *Biosensors and Bioelectronics, 22*(9-10), 2165-2170.

Sun, A. L. (2018). A potentiometric immunosensor for enterovirus 71 based on bis-MPA-COOH dendrimer-doped AgCl nanospheres with a silver ion-selective electrode. *Analyst, 143*(2), 487-492.

Sun, Y.-n., Gao, G.-r., Du, G.-l., Cheng, Y.-j., & Fu, J. (2014). Super tough, ultrastretchable, and thermoresponsive hydrogels with functionalized triblock copolymer micelles as macro-cross-linkers. *ACS Macro Letters, 3*(5), 496-500.

Surma, M., Sadowska-Rociek, A., Cieślik, E., & Sznajder-Katarzyńska, K. (2017). Optimization of QuEChERS sample preparation method for acrylamide level determination in coffee and coffee substitutes. *Microchemical Journal, 131*, 98-102.

Tardiff, R. G., Gargas, M. L., Kirman, C. R., Leigh Carson, M., & Sweeney, L. M. (2010). Estimation of safe dietary intake levels of acrylamide for humans. *Food and Chemical Toxicology, 48*(2), 658-667.

Tareke, E., Rydberg, P., Karlsson, P., Eriksson, S., & Törnqvist, M. (2000). Acrylamide: A cooking carcinogen? *Chemical Research in Toxicology, 13*(6), 517-522.

Tareke, E., Rydberg, P., Karlsson, P., Eriksson, S., & Törnqvist, M. (2002). Analysis of acrylamide, a carcinogen formed in heated foodstuffs. *Journal of Agricultural and Food Chemistry, 50*(17), 4998-5006.

Thévenot, D. R., Toth, K., Durst, R. A., & Wilson, G. S. (2001). Electrochemical biosensors: Recommended definitions and classification. *Biosensors and Bioelectronics, 16*(1-2), 121-131.

Trivedi, U. B., Lakshminarayana, D., Kothari, I. L., Patel, N. G., Kapse, H. N., Makhija, K. K., . . . Panchal, C. J. (2009). Potentiometric biosensor for urea determination in milk. *Sensors and Actuators, B: Chemical, 140*(1), 260-266.

Varmira, K., Abdi, O., Gholivand, M. B., Goicoechea, H. C., & Jalalvand, A. R. (2018). Intellectual modifying a bare glassy carbon electrode to fabricate a novel and ultrasensitive electrochemical biosensor: Application to determination of acrylamide in food samples. *Talanta, 176*, 509-517.

Velasco-Garcia, M. N. (2009). Optical biosensors for probing at the cellular level: A review of recent progress and future prospects. *Seminars in Cell and Developmental Biology, 20*(1), 27-33.

Wang, H., & Ma, Z. (2018). A cascade reaction signal-amplified amperometric immunosensor platform for ultrasensitive detection of tumour marker. *Sensors and Actuators B: Chemical, 254*, 642-647.

Wang, S. F., Chen, T., Zhang, Z. L., Shen, X. C., Lu, Z. X., Pang, D. W., & Wong, K. Y. (2005). Direct electrochemistry and electrocatalysis of heme proteins entrapped in agarose hydrogel films in room-temperature ionic liquids. *Langmuir, 21*(20), 9260-9266.

Wang, W., Zhang, T. J., Zhang, D. W., Li, H. Y., Ma, Y. R., Qi, L. M., . . . Zhang, X. X. (2011). Amperometric hydrogen peroxide biosensor based on the immobilization of heme proteins on gold nanoparticles–bacteria cellulose nanofibers nanocomposite. *Talanta, 84*(1), 71-77.

Watzek, N., Böhm, N., Feld, J., Scherbl, D., Berger, F., Merz, K. H., . . . Eisenbrand, G. (2012). N7-glycidamide-guanine DNA adduct formation by orally ingested acrylamide in rats: A dose–response study encompassing human diet-related exposure levels. *Chemical Research in Toxicology, 25*(2), 381-390.

Weideborg, M., Källqvist, T., Ødegård, K. E., Sverdrup, L. E., & Vik, E. A. (2001). Environmental risk assessment of acrylamide and methylolacrylamide from a grouting agent used in the tunnel construction of romeriksporten, norway. *Water Research, 35*(11), 2645-2652.

Wen, W., Yan, X., Zhu, C., Du, D., & Lin, Y. (2017). Recent advances in electrochemical immunosensors. *Analytical Chemistry, 89*(1), 138-156.

WHO. (2017). Guidelines for drinking-water quality: Fourth edition incorporating the first addendum. Geneva.

Wijeyesekera, D. C., Ho, M. H., Bai, X., & Bakar, I. (2016). Strength and stiffness development in soft soils: A FESEM aided soil microstructure viewpoint. *IOP Conference Series: Materials Science and Engineering, 136*, 1-12.

Wilson, K. M., Vesper, H. W., Tocco, P., Sampson, L., Rosén, J., Hellenäs, K. E., . . . Willett, W. C. (2009). Validation of a food frequency questionnaire measurement of dietary acrylamide intake using hemoglobin adducts of acrylamide and glycidamide. *Cancer Causes and Control, 20*(3), 269-278.

Wu, J., Shen, Y. D., Lei, H. T., Sun, Y. M., Yang, J. Y., Xiao, Z. L., . . . Xu, Z. L. (2014). Hapten synthesis and development of a competitive indirect enzyme-linked immunosorbent assay for acrylamide in food samples. *Journal of Agricultural and Food Chemistry, 62*(29), 7078-7084.

Wu, M. F., Wang, Y., Li, S., Dong, X. X., Yang, J. Y., Shen, Y. D., . . . Xu, Z. L. (2019). Ultrasensitive immunosensor for acrylamide based on chitosan/SnO2-SiC hollow sphere nanochains/gold nanomaterial as signal amplification. *Analytica Chimica Acta, 1049*, 188-195.

Yadav, N., Chhillar, A. K., & Pundir, C. S. (2018a). Preparation, characterization and application of haemoglobin nanoparticles for detection of acrylamide in processed foods. *International Journal of Biological Macromolecules, 107*, 1000-1013.

Yadav, N., Narang, J., Chhillar, A. K., & Pundir, C. S. (2018b). Chapter Six - Preparation, characterization, and application of enzyme Nanoparticles. In C. V. Kumar (Ed.), *Methods in Enzymology* (Vol. 609, pp. 171-196): Academic Press.

Yan, Q., Cao, L., Dong, H., Tan, Z., Liu, Q., Zhang, W., . . . Dong, Y. (2019). Sensitive amperometric immunosensor with improved electrocatalytic Au@Pd urchin-shaped nanostructures for human epididymis specific protein 4 antigen detection. *Analytica Chimica Acta, 1069*, 117-125.

Zeiger, E., Recio, L., Fennell, T. R., Haseman, J. K., Snyder, R. W., & Friedman, M. (2008). Investigation of the low-dose response in the in vivo induction of micronuclei and adducts by acrylamide. *Toxicological Sciences, 107*(1), 247-257.

Zhang, Z., Dong, S., Ge, D., Zhu, N., Wang, K., Zhu, G., . . . Xu, H. (2018). An ultrasensitive competitive immunosensor using silica nanoparticles as an enzyme carrier for simultaneous impedimetric detection of tetrabromobisphenol A bis(2-hydroxyethyl) ether and tetrabromobisphenol A mono(hydroxyethyl) ether. *Biosensors and Bioelectronics, 105*, 77-80.

Zhao, G., Wang, H., Liu, G., & Wang, Z. (2016). Box–behnken response surface design for the optimization of electrochemical detection of cadmium by square wave anodic stripping voltammetry on bismuth film/glassy carbon electrode. *Sensors and Actuators B: Chemical, 235*, 67-73.

Zhou, S., Zhang, C., Wang, D., & Zhao, M. (2008). Antigen synthetic strategy and immunoassay development for detection of acrylamide in foods. *Analyst, 133*(7), 903-909.

LIST OF PUBLICATION AND PAPER PRESENTED

PUBLICATION

Lau, P. Y., Ng, K. L., Azah, Y. N., Liu, G., Yatimah, A., & Khor, S. M. (2019). A sample pre-treatment-free electrochemical immunosensor with negative electro-pulsion for the quantitative detection of acrylamide in coffee, cocoa and prune juice. *Analytical Methods*, *11(33)*, 4299-4313.

PAPER PRESENTED

Lau, P. Y., Yatimah, A., & Khor, S. M. (2019). *An electrochemical immunosensor for acrylamide detection via a displacement assay*. Paper presented at 6th International Conference on Bio-Sensing Technology, 16 – 19 June 2019, Kuala Lumpur, Malaysia.